

Copyright Warning & Restrictions

The copyright law of the United States (Title 17, United States Code) governs the making of photocopies or other reproductions of copyrighted material.

Under certain conditions specified in the law, libraries and archives are authorized to furnish a photocopy or other reproduction. One of these specified conditions is that the photocopy or reproduction is not to be “used for any purpose other than private study, scholarship, or research.” If a user makes a request for, or later uses, a photocopy or reproduction for purposes in excess of “fair use” that user may be liable for copyright infringement,

This institution reserves the right to refuse to accept a copying order if, in its judgment, fulfillment of the order would involve violation of copyright law.

Please Note: The author retains the copyright while the New Jersey Institute of Technology reserves the right to distribute this thesis or dissertation

Printing note: If you do not wish to print this page, then select “Pages from: first page # to: last page #” on the print dialog screen

The Van Houten library has removed some of the personal information and all signatures from the approval page and biographical sketches of theses and dissertations in order to protect the identity of NJIT graduates and faculty.

ABSTRACT

***IN SITU* ENHANCEMENT OF WELL RECOVERY BY PNEUMATIC MEDIA INJECTION**

by
Michael Thomas Galbraith

The objective of this thesis was to develop a new process for enhancing recovery wells at hazardous waste sites. The process, known as an extended radius well (ERW), involves injection of ceramic beads directly into groundwater plumes to create drainage paths for liquid contaminants. This is a variant of Pneumatic Fracturing, which is a patented *in situ* remediation process developed to increase permeability of soil and rock formations by injection of high pressure gas.

The research study comprised laboratory investigations, engineering scale tests, and a field pilot demonstration. The laboratory investigations examined the properties of several candidate media to determine their gradation, permeability, mechanical strength and flowability. Ultimately, ceramic beads were chosen for use in the field demonstration. Engineering scale injection tests were subsequently conducted in a 20 yd³ (15.3 m³) vessel filled with silty sand to establish system operating parameters.

A field pilot demonstration of the ERW process was performed at an industrial site underlain by silty fine sands containing a plume of petroleum hydrocarbons. Two ERWs were established and pumping tests performed over an 85 day period. The two ERWs displayed average increases in product recovery of 225% and 335%, respectively, compared with previous results from conventional recovery systems. Soil borings confirmed that discrete lenses extended outward from the ERWs, and model analyses attributed the observed enhancement to an increase in effective well diameter.

***IN SITU* ENHANCEMENT
OF WELL RECOVERY BY
PNEUMATIC MEDIA INJECTION**

by
Michael Thomas Galbraith

**A Thesis
Submitted to the Faculty of
New Jersey Institute of Technology
in Partial Fulfillment of the Requirements for the Degree of
Master of Science in Civil Engineering**

Department of Civil and Environmental Engineering

May 1999

Copyright © 1999 by Michael Thomas Galbraith

ALL RIGHTS RESERVED

APPROVAL PAGE

***IN SITU* ENHANCEMENT
OF WELL RECOVERY BY
PNEUMATIC MEDIA INJECTION**

Michael Thomas Galbraith

John R. Schuring, Thesis Advisor Date
Professor of Civil and Environmental Engineering, NJIT

Paul Chan, Committee Member Date
Professor of Civil and Environmental Engineering, NJIT

Edward G. Dauheimer, Committee Member Date
Professor of Civil and Environmental Engineering, NJIT

BIOGRAPHICAL SKETCH

Author: Michael Thomas Galbraith
Degree: Master of Science in Civil Engineering
Date: May 1999

Undergraduate and Graduate Education:

- Master of Science in Civil Engineering
New Jersey Institute of Technology
Newark, NJ, 1999
- Bachelor of Science in Environmental Science
Cook College, Rutgers University
New Brunswick, NJ, 1994

Major: Civil Engineering

This thesis is dedicated
to my parents, Janet and John R. Galbraith,
for their love, support and encouragement.

ACKNOWLEDGMENT

I would like to express my sincere gratitude to my advisor, Dr. John R. Schuring, for his guidance and encouragement throughout the research and writing of this thesis. His inspiration and tireless work ethic have been invaluable in developing my technical, leadership and writing skills.

I thank Dr. Chan and Prof. Dauenheimer for serving as committee members and for their careful review and thoughtful suggestions. In addition, I appreciate Dr. Chan's advice and guidance in preparing my application for the U.S. Department of Defense Environmental Fellowship Program.

Special thanks to my pneumatic fracturing colleagues and friends Tom Boland, Heather Hall, Brian Sielski, Jenny Lin and Janinna Alvarez. Thanks also to Sean McGonigal, of Louis Berger and Associates, for his help and involvement throughout the field demonstration, and to Frank Johansson, of Pumping Systems, Inc. for fabricating the 15-Port Helical Nozzle used for the field demonstration. I would also like to thank McLaren Hart Inc., for the generous use of their equipment and facilities for the engineering scale testing.

I am sincerely grateful to the U.S. Department of Defense for supporting my studies for the last two years under the Environmental Fellowship Program.

Finally, I wish to thank my family and close friends for their love and encouragement throughout the pursuit of this degree.

TABLE OF CONTENTS

Chapter	Page
1 INTRODUCTION.....	1
1.1 General.....	1
1.2 Objectives and Scope.....	3
2 BACKGROUND AND THEORY.....	5
2.1 Pneumatic Fracturing.....	5
2.1.1 Technology Overview.....	5
2.1.2 Process Description.....	6
2.2 Overview of Dry Media Injection.....	7
2.3 Grain Size Effects on Soil Permeability.....	10
2.4 Well Analysis Methods.....	12
3 LABORATORY APPROACH.....	16
3.1 Concept of Extended Radius Wells (ERWs).....	16
3.2 Laboratory Procedures.....	19
3.2.1 Characterization of Site Soils.....	19
3.2.2 Evaluation of Injection Media.....	20
3.2.3 Media Flow Testing and Strength Testing.....	21
3.2.4 Media Permeability Testing.....	22
3.2.5 Injection Testing.....	23
3.2.5.1 Process Description.....	23
3.2.5.2 Nozzle Descriptions.....	23
3.2.5.3 Description of Injections.....	25

TABLE OF CONTENTS
(Continued)

Chapter	Page
3.2.5.4 Sieve Analysis of Media	26
3.3 Engineering Scale Procedures.....	26
3.3.1 Soil Excavations.....	27
4 TEST RESULTS AND PROTOTYPE DESIGN	30
4.1 Laboratory Results	30
4.1.1 Properties of Site Soils	30
4.1.2 Media Flow and Strength Testing Results.....	33
4.1.3 Media Selection and Design.....	34
4.1.4 Media Permeability Testing Results.....	36
4.1.5 Injection Testing and Degradability	40
4.2 Engineering Scale Results.....	43
4.3 Prototype Design.....	49
4.3.1 Fifteen Port Helical Nozzle	50
4.3.2 Movable Nozzle	50
5 FIELD DEMONSTRATION	52
5.1 Site Geology and Hydrogeology	52
5.2 Test Setup and Operations	53
5.2.1 Overview of Field Activities	53
5.2.2 Injection Nozzle Installation Procedure	55
5.2.2.1 Fifteen Port Helical Nozzle.....	55
5.2.2.2 Movable Nozzle	56

TABLE OF CONTENTS
(Continued)

Chapter	Page
5.2.3 Media Injections	56
5.2.3.1 Fifteen Port Helical Nozzle.....	56
5.2.3.2 Movable Nozzle	59
5.2.4 Recovery Well Installation	63
5.2.4.1 Installation of Recovery Well 08-WL-70.....	63
5.2.4.2 Installation of Recovery Well 08-WL-69.....	63
5.3 Field Demonstration Results.....	63
5.3.1 Results for Recovery Well 08-WL-70 (Helical Nozzle Setting)	64
5.3.2 Results for Recovery Well 08-WL-69 (Movable Nozzle Setting)	64
5.3.3 Geoprobe Soil Sampling	66
5.3.3.1 Geoprobe Boring Description and Locations.....	66
5.3.3.2 Geoprobe Boring Results	69
5.3.4 Cost Analysis of ERWs at Field Pilot Test Site	75
6 CONCLUSIONS AND RECOMMENDATIONS	82
6.1 Bench and Engineering Scale Conclusions.....	82
6.2 Field Demonstration Conclusions.....	84
6.3 Recommendations for Future ERWs	86
APPENDIX A EXTENDED RADIUS WELL VS. CONVENTIONAL 4 IN. RECOVERY WELL ENHANCEMENT CALCULATIONS.....	88
APPENDIX B PERMEABILITY CALCULATIONS OF NATIVE SOIL	91
APPENDIX C FLOW AND STRENGTH TEST DATA.....	92

TABLE OF CONTENTS
(Continued)

Chapter	Page
APPENDIX D MEDIA SIZE CALCULATION	104
APPENDIX E HYDRAULIC CONDUCTIVITY CALCULATIONS FOR CERAMIC BEADS	105
APPENDIX F WELL LOGS	115
APPENDIX G SOIL BORING LOGS.....	118
REFERENCES	149

LIST OF TABLES

Table	Page
3.1 Groundwater flow enhancement calculations	19
3.2 List of media selected for use as a conductive lens	21
4.1 Head Space Analysis.....	31
4.2 Hydraulic Conductivity testing results of native soil	33
4.3 Flow and Strength test data of various media	34
4.4 Summary of laboratory injection tests	41
4.5 Engineering scale injection data	43
5.1 Summary of field activities.....	55
5.2 Fifteen Port Helical Nozzle Injection Data	58
5.3 Movable Nozzle Injection Data	61
5.4 Economic Cost Analysis of ERWs vs. conventional recovery wells.....	81
C.1 Flow Testing Data for various Media	93
C.2 Strength Test Data for various Media.....	100

LIST OF FIGURES

Figure	Page
2.1 Pneumatic Fracturing Concept.....	8
2.2 Applicability of Pneumatic Fracturing.....	9
3.1 Conventional Well vs. Extended Radius Well (ERW).....	18
3.2 Schematic Diagram of Laboratory Media Injection System.....	24
3.3 Engineering Scale Injection Test Setup.....	28
3.4 Dry Media Injection System Schematic.....	29
4.1 Grain Size Analysis Soil Boring SE (9 to 15 ft).....	32
4.2 Summary of Grain Size Testing CarboCeramics Proppant.....	35
4.3 Summary of Hydraulic Conductivity Results using CarboCeramics Proppant.....	38
4.4 Summary of Hydraulic Conductivity Results using 16/30 CarboProp and native soil.....	39
4.5 Bench Scale Injections Sieve Analysis Summary.....	42
4.6 Engineering Scale Excavation, Injection #2, Section View.....	45
4.7 Engineering Scale Excavation, Injection #2, Plan View.....	46
4.8 Engineering Scale Excavation, Injection #3, Section View.....	47
4.9 Engineering Scale Excavation, Injection #3, Plan View.....	48
5.1 Site Plan of Field Demonstration.....	54
5.2 Free Product Recovery at 08-WL-69, 08-WL-70 and 08-WL-65.....	65
5.3 Geoprobe Boring Locations Around Recovery Well 08-WL-70 (Helical Nozzle).....	67

**LIST OF FIGURES
(Continued)**

Figure	Page
5.4 Geoprobe Boring Locations Around Recovery Well 08-WL-69 (Movable Nozzle).....	68
5.5 Helical Nozzle Geoprobe Borings (recovery well 08-WL-70), North/South subsurface section	71
5.6 Helical Nozzle Geoprobe Borings (recovery well 08-WL-70), East/West subsurface section	72
5.7 Helical Nozzle Geoprobe Borings (recovery well 08-WL-70), Southwest/Northeast subsurface section	73
5.8 Helical Nozzle Geoprobe Borings (recovery well 08-WL-70), Southeast/Northwest subsurface section	74
5.9 Movable Nozzle Geoprobe Borings (recovery well 08-WL-69), North/South subsurface section	76
5.10 Movable Nozzle Geoprobe Borings (recovery well 08-WL-69), East/West subsurface section	77
5.11 Helical Nozzle Geoprobe Borings (recovery well 08-WL-69), Southwest/Northeast subsurface section	78
5.12 Helical Nozzle Geoprobe Borings (recovery well 08-WL-69), Southeast/Northwest subsurface section	79

CHAPTER 1

INTRODUCTION

1.1 General

Decades of poor storage and disposal practices by industry and government facilities have resulted in widespread release of hazardous waste. These waste releases have contaminated the environment both above and below the ground surface. Since the 1970's, a shift in environmental awareness and attitudes has led to new legislation to prevent future misuse and remediate areas presently impacted. The principal legislative actions have included the Resource Conservation and Recovery Act (RCRA 1976), and the Comprehensive Environmental Response, Compensation, and Liability Act (CERCLA 1980). These laws, combined with newer legislation and regulation, have forced responsible parties to identify and remediate contaminants at impacted areas.

In an effort to address the problem of subsurface contamination, a new field of environmental engineering has spawned: the remediation of hazardous chemicals trapped in the subsurface. Contamination in the form of volatile organic compounds (VOCs), semi volatile organic compounds (SVOCs), heavy metals such as mercury and arsenic, and free product in the form of gasoline and heating oil are examples that are prevalent. Treatment approaches are generally categorized as either above ground (*ex situ*) or below the ground (*in situ*). *In situ* treatment technologies are usually more desirable because of lower costs and reduced site disruption.

In situ technologies have been developed to treat both soil and groundwater. A limiting factor of the effectiveness of any *in situ* technology is the natural permeability of the geologic formation being treated because it limits the transport of pore fluids. Formations underlain by fine-grained soils and tight bedrock are classified as having low permeability, and these formations pose special challenges for recovery or treatment of contaminants. Cleanup times may be lengthy and costs high, if cleanup is feasible at all.

In response to these difficult geologic conditions, a process known as Pneumatic Fracturing (PF) was developed at New Jersey Institute of Technology (NJIT) at the Center for Environmental Engineering and Science (CEES). PF is an enhancement technology that increases soil permeability in low permeable formations. In addition to permeability enhancement, PF can improve homogeneity, and access pockets of contaminants previously unattainable. PF has been used to enhance pump and treat, free product recovery, soil vapor extraction, dual phase extraction, *in situ* bioremediation, and air sparging. The PF enhancement process can significantly reduce remediation time and costs.

In addition to the original process, several variants of PF have been developed. The PF injection system can be used to emplace media beneath the ground to a zone of interest. Injection of media may be desirable for a variety of applications including bioremediation, *in situ* vitrification, and reductive dechlorination. PF has already been successfully applied to delivery bioremediation microbes, graphite/glass frit and iron filings at separate sites.

1.2 Objectives and Scope

The overall objective of this study is to extend the PF process to enhance free product recovery in formations with moderate permeability. Such formations include silts, fine sands, and silty sands. One difficulty in remediating these formations is the permeability is too low to allow efficient recovery of free product. Another difficulty is that these soils do not exhibit enough cohesion to benefit from the traditional pneumatic fracturing process.

In order to improve recovery of free product in cohesionless soils of moderate permeability, a new variant of the PF process is developed known as an extended radius well (ERW). This involves injection of coarse-grained media into the native soil to form highly permeable, conductive pathways for the collection of free product.

The development of the ERW requires the performance of laboratory studies, permeability enhancement modeling and bench and engineering scale injection tests. In addition, the concept is field tested at an industrial site in southern New Jersey.

The objectives and scope of this investigation are therefore to:

1. Identify a suitable solid media for injection by the PF process to create ERWs in formations of moderate permeability
2. Conduct laboratory tests on the mechanical properties of the selected media.
3. Quantify the effect of the injected media on aquifer permeability using laboratory tests as well as mathematical modeling.
4. Modify the design of the current PF nozzle system to accommodate the new media and to adapt to the cohesionless soil conditions.

5. Conduct bench scale and engineering scale tests of the new system.
6. Design and execute a field pilot test of the new ERW system and evaluate the results.
7. Develop recommendations for field application and future improvement of the new system.

This thesis will begin with an overview of the PF history and process description including an overview of dry media injection. Well analysis methods and the effects of soil grain size on soil permeability will also be reviewed (Chapter 2). This will be followed by a discussion of the laboratory tests and prototype design (Chapters 3, 4, respectively). Next, the setup and results of the field demonstration are presented (Chapter 5). Finally, conclusions and recommendations for future application of ERWs are presented (Chapter 6).

CHAPTER 2

BACKGROUND AND THEORY

2.1 Pneumatic Fracturing

2.1.1 Technology Overview

Pneumatic Fracturing (PF) is a patented technology developed at New Jersey Institute of Technology (NJIT) at the Center for Environmental Engineering and Science (CEES). Development of Pneumatic Fracturing first began in 1988 with initial bench experiments to study the effect of PF on soil vapor extraction (SVE). A contaminated soil mixture (at a known concentration) was packed into Plexiglass soil tanks. SVE testing was applied prior to, and again after PF. The results of this study indicated that PF enhanced the rate of removal by 170% to 360% (Papanicolau, 1989; Shah, 1991).

Bench scale tests also focused on integration of bioremediation with PF through the injection of microorganisms into the subsurface (Fitzgerald, 1993). The use of surfactants and time release nutrients with PF was also studied (Rahman, 1994). In addition, studies were conducted on the integration of the PF process with *in situ* vitrification (ISV) (McGonigal, 1995). This particular study involved the injection of a glass/graphite frit mixture as a starter path for the ISV process, and it was the first time PF was used to inject dry media. More recent research at CEES has emphasized the injection of various iron powders to dechlorinate trichloroethylene (TCE).

A number of field demonstrations of the PF technology have been conducted since 1989. The first PF field test at an industrial site was conducted for AT&T in

Richmond, Virginia (Schuring *et al.*, 1991). This was followed by two U.S. EPA SITE demonstrations: one at a site in Hillsborough, NJ to enhance mass removal rates of SVE (U.S. EPA, 1993), and the other at an oil refinery in Southeast Pennsylvania to enhance *in situ* bioremediation through the delivery of nutrients and buffer solutions (U.S. EPA, 1995). These demonstrations provided key engineering data that allowed the technology to transition from the research stage to the commercial market.

The PF process was patented in July 1991 (U.S. Patent # 5,032,042). Recent research includes dry media injection, and mathematical modeling (Puppala, 1998). Also a computer application program called PF-Model, has been developed to screen sites for PF applications and generate site specific preliminary design data (Sielski, 1999). Other research includes fracture longevity in swelling clays (Hall, in progress) and PF coupled with ultrasound to enhance VOC removal (Fernandez, 1997, Lin 1999).

PF is currently offered commercially by ARS Technologies, Inc. of Highland Park, NJ and McLaren Hart, Inc. of Warren, NJ. To date, the technology has been applied at over 40 sites throughout the United States and Canada.

2.1.2 Process Description

The PF process consists of injecting large volumes of gas at high pressures and high flow rates into a well or borehole in a geologic formation. The gas is introduced to an isolated interval for a short period of time, usually less than one minute. As long as the injection pressure exceeds the natural *in situ* stresses of the formation, and the flow rate exceeds the natural permeability of the formation, fractures are propagated outward from the point of injection.

Normally, the interval is isolated by two packers arranged in a “straddle” configuration. Depending upon applications, the interval can vary from two feet to five feet in length. The sources of the injected gas include gas cylinders, a tube trailer, or a nitrogen tanker truck. The injected gas is carefully regulated and transported to the zone of interest via high pressure hose and rigid steel pipe. The injected gas is directed laterally into the formation by a “HQ Injector”, which focuses the gas to a discrete interval. The induced fractures can increase both air permeability (vadose zone) and hydraulic conductivity (saturated zone) within the geologic formation. Figure 2.1 illustrates the permeability enhancement effects of the PF process in fine-grained soils and sedimentary rock formations (HSMRC *et al.*, 1994).

There are two principal advantages of applying PF to contaminated sites with low permeable soil conditions. First, the mass transfer rates are improved so that overall remediation time can be significantly reduced. Second, the spacing of the treatment wells can be increased thereby reducing the number of wells that must be drilled. The end result is cost savings in both the installation and operation phase of the clean-up project.

2.2 Overview of Dry Media Injection

In addition to using PF for enhancing *in situ* permeability, it can also be used as a delivery tool to introduce various media into the geologic zone of interest. Figure 2.2 summarizes the various uses of PF which include the injection of liquid and solid amendments. Such media include microorganisms, nutrients, iron powder, graphite and ceramic beads. Solid media are introduced into the subsurface with a Dry Media Injection System developed at NJIT. This system has been used successfully to inject a

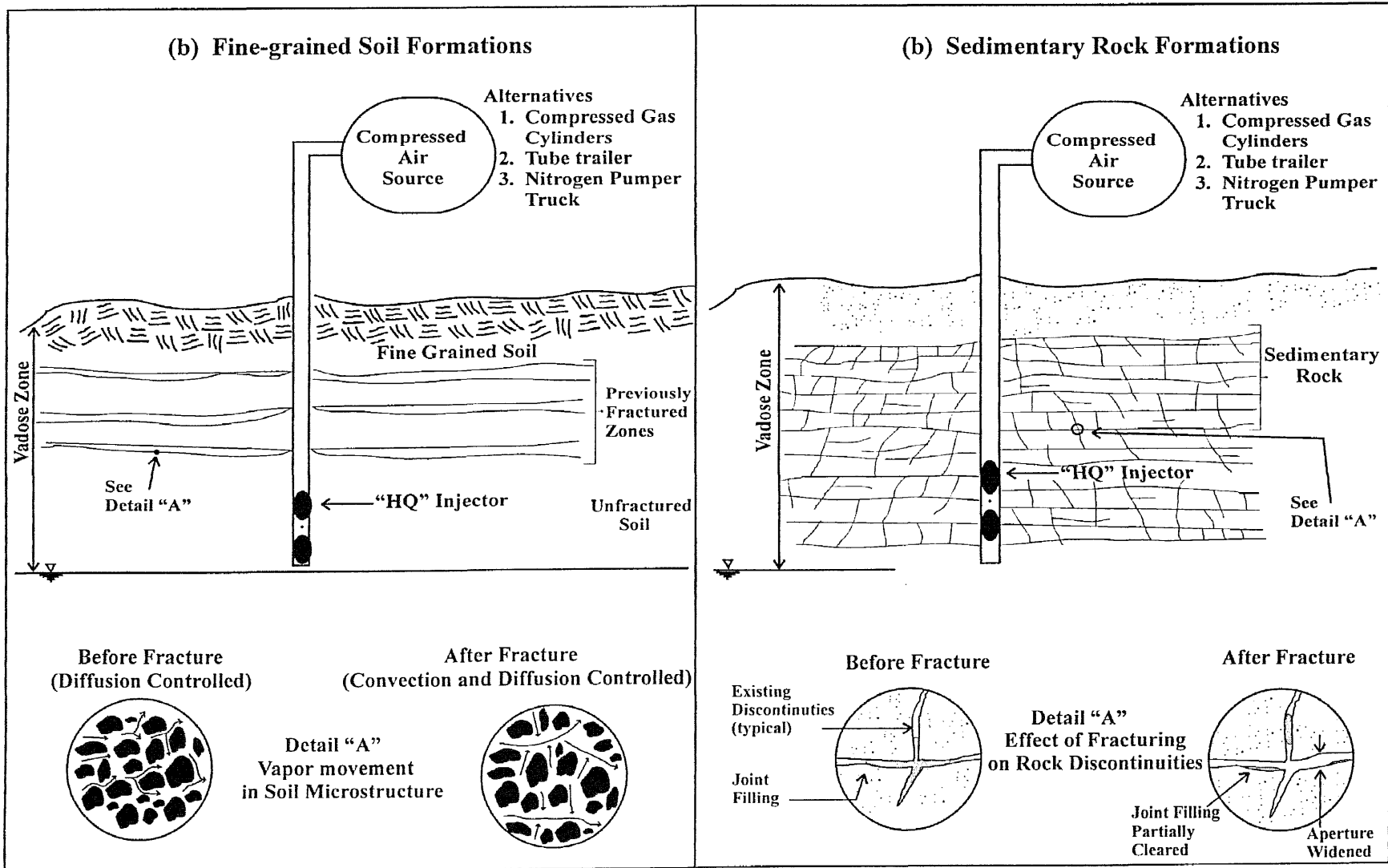


Figure 2.1 Pneumatic Fracturing Concept (Schuring and Chan, 1992)

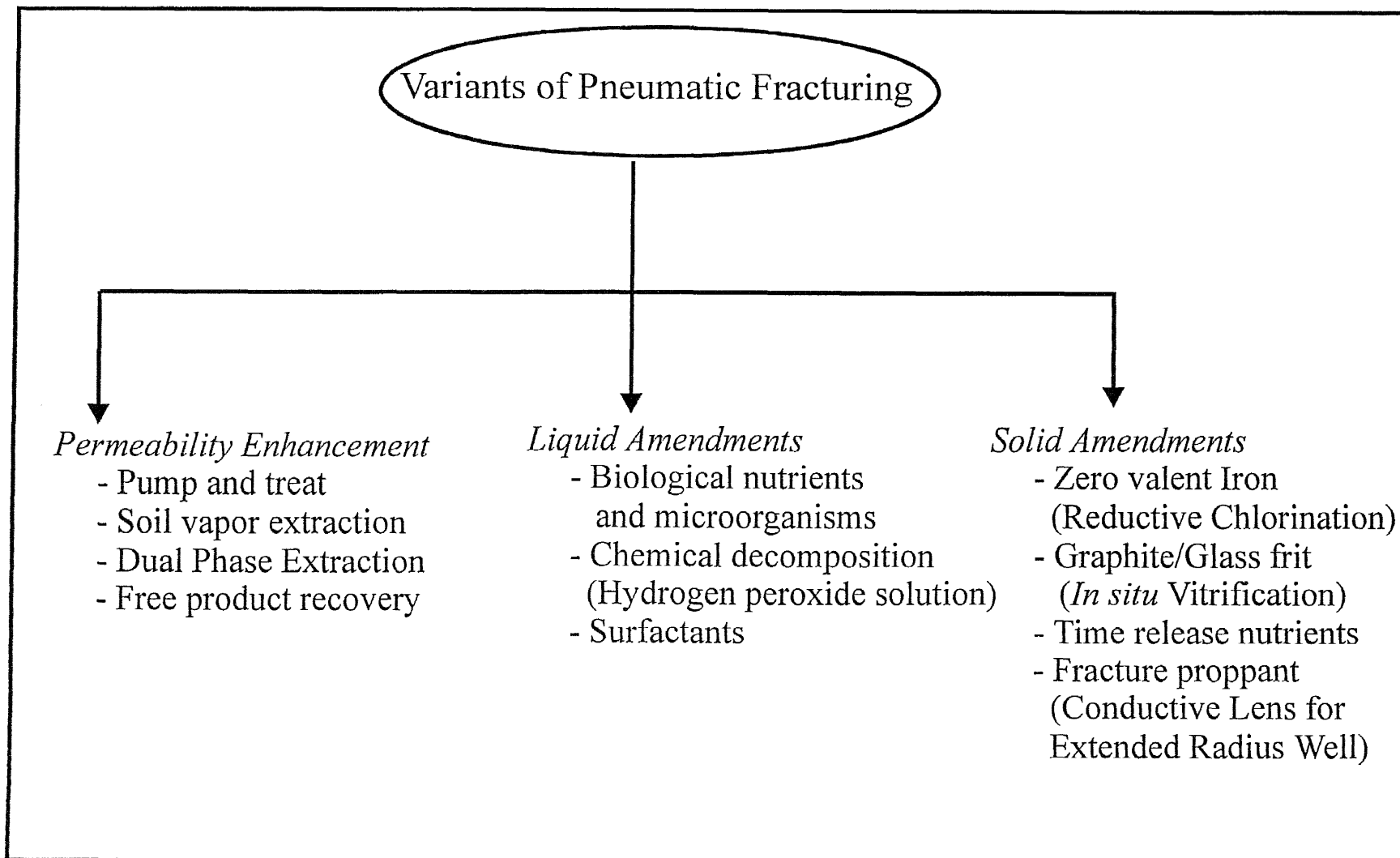


Figure 2.2 Applicability of Pneumatic Fracturing

graphite/glass frit mixture at the Hanford site to induce *in-situ* Vitrification. The Dry Media Injection System was also used to treat a plume of trichloroethylene in Kansas City, Kansas by injection iron filings. The present research involves the injection of ceramic beads into a fine sand formation impacted with fuel oil.

2.3 Grain Size Effects on Soil Permeability

Permeability may be defined as the ease which a fluid will move through a porous medium (Driscoll, 1986). Hydraulic conductivity, or K , may be defined as a coefficient of proportionality describing the rate at which water moves through a porous medium, and it is governed by the size and shape of the pores and interconnection between the pores (Fetter, 1994). The larger the grain size of the material through which the fluid flows, the higher the hydraulic conductivity value. Soil exhibits a tremendous range of hydraulic conductivity and can vary over 15 orders of magnitude. The hydraulic conductivity of fine to coarse gravel may be as high as 10^2 cm/sec while the hydraulic conductivity of clay may be as low as 10^{-11} cm/sec.

Various empirical relationships have been developed for determining hydraulic conductivity. Allen Hazen (1892) developed a formula for determining hydraulic conductivity of filter sands. The formula is expressed as:

$$K = 100d_{10}^2 \quad (2.1)$$

where;

K = hydraulic conductivity (L/T)

d_{10} = the 10 percent grain size expressed as percent passing, also known as Hazen's effective size, d_e (L)

These studies were based upon sands with an effective grain diameter (d_e) ranging from 0.1 and 3.0 mm (0.004 to 0.12 in.). The coefficient value of 100 represents an average of many tests; individual values ranged from 41 to 146, but most of the values were between 81 and 117. Although this method was developed for filter sands, it is widely applied for rough estimates of permeability (Taylor, 1948).

Other studies, such as those performed by Slichter (1898), focused on determining hydraulic conductivity of soils with effective grain size diameters from 0.01 to 5.0 mm (0.0004 to 0.2 in.). A basic form of the Slichter formula often encountered in literature is:

$$K = \frac{\gamma}{\mu} \cdot 10.0219 \cdot n^{3.287} \cdot d_{10}^2 \quad (2.2)$$

where:

- γ = specific weight (M/L^2T^2)
- μ = absolute viscosity (M/LT)
- n = porosity (dimensionless)

Another empirical relationship was developed by Kozeny (1953) for determining the hydraulic conductivity of coarse sands (i.e. 0.7 – 2.0 mm). The dimensionally homogeneous form of the Kozeny formula is usually expressed as:

$$K = \frac{g}{\nu} \cdot C_K \cdot \frac{n^3}{(1-n)^2} \cdot d_e^2 \quad (2.3)$$

where:

- g = acceleration due to gravity (L/T^2)

- ν = kinematic viscosity (L^2/T)
- C_K = constant value of 8.83×10^{-3} (dimensionless)
- d_e = effective grain diameter, (L)

The preceding equations are just a few of the available methods which relate hydraulic conductivity to soil grain-size. Other methods have been developed for estimating the hydraulic conductivity of fine grained soils such as silts and clays as well as rock. For a more thorough review of empirical relationships, the reader is referred to Vukovic and Soro (1992). It is noted that all empirical methods provide only an estimate at best, and the most accurate way to determine hydraulic conductivity is to measure it *in situ*.

2.4 Well Analysis Methods

Wells are used for a variety of purposes. A principal use of wells is to access productive groundwater aquifers for potable water. For example, approximately 40% of the drinking water in the United States is supplied by groundwater wells. Wells are also used for farm irrigation in climates that are not normally suited for crop cultivation. Wells can also be drilled to access natural resources such as oil and natural gas. In addition, wells serve as the principal tool for *in situ* remediation technologies such as free product recovery, pump and treat, and soil vapor extraction. They are also used as monitor wells for obtaining samples of groundwater and soil gas. In other instances, wells are used for the reinjection of treated groundwater back into the aquifer.

When water is pumped from a well, a cone of depression develops in the aquifer around the well that is known as drawdown. An interactive relationship exists between

well drawdown, pumping rate, and aquifer permeability, which can be determined by well analysis. All well analysis methods are based upon Darcy's Law which is the fundamental equation that describes groundwater flow through porous media. The equation was originally developed by Henry Darcy in 1856 involving the design of cylindrical sand filters. The statement of Darcy's Law begins with the darcy flux velocity, V_{Df} , as:

$$V_{Df} = K \frac{(h_1 - h_2)}{L} \quad (2.4)$$

where;

$(h_1 - h_2) =$ difference in hydraulic head (L)

L = distance along the flowpath between h_1 and h_2 (L)

K = hydraulic conductivity (L/T)

It is convenient to define the gradient, I, as:

$$I = \frac{h_1 - h_2}{L} \quad (2.5)$$

This leads to the most often used form of Darcy's Law which relates the quantity of groundwater flow, Q (L^3/T), per unit area of aquifer, A (L^2).

$$Q = KIA \quad (2.6)$$

It is noted that Darcy's Law applies to laminar flow conditions only. Numerous extensions of Darcy's Law have been developed to quantify groundwater yields from wells.

In some geologic formations, the water bearing aquifer may be bounded above and below by material such as clay, which is significantly less permeable. This is known as a confined aquifer, or a pressure aquifer, since the water pressure in the aquifer exceeds normal hydrostatic pressure. Confined aquifers under steady flow condition are analyzed using a variant of Darcy's Law known as the Theim Equation (*e.g.* Fetter, 1962). This equation is written as:

$$Q = 2\pi KB \frac{h_2 - h_1}{\ln\left(\frac{r_2}{r_1}\right)} \quad (2.7)$$

where:

Q	=	constant pumping rate (L ³ /T)
K	=	hydraulic conductivity (L/T)
B	=	aquifer thickness (L)
h ₁ , h ₂	=	hydraulic heads at radii r ₁ and r ₂ , respectively (L)
r ₁ , r ₂	=	selected radii for observation of heads (L)

At other sites an unconfined condition may exist where the aquifer has no upper confining layer and is therefore open to the atmosphere. This is known as an unconfined aquifer and it is a common condition at many contaminated sites. Unconfined aquifers under steady flow conditions are analyzed by yet another variant of Darcy's Law known as the Dupuit-Forscheimer equation (*e.g.*, Leonards, 1962):

$$Q = \pi K \frac{h_2^2 - h_1^2}{\ln\left(\frac{r_2}{r_1}\right)} \quad (2.8)$$

where the terms are as defined previously.

The formulas just described are just two of the numerous methods available for analyzing groundwater flow into wells. The equations are based upon several assumptions including;

- (1) homogeneous, isotropic aquifer condition;
- (2) steady flow;
- (3) fully penetrating well;
- (4) 100% efficiency;
- (5) laminar groundwater flow, and;
- (6) a level potentiometric surface is present.

Although these equations assume somewhat ideal conditions, they are still extremely important in well design. When properly used, these equations can be utilized to estimate groundwater pumping rates, contaminant recovery, and well radius. For further study of well analysis and design, the reader is referred to Driscoll (1986).

CHAPTER 3

LABORATORY APPROACH

This chapter discusses the approach and methods utilized for the laboratory studies. These laboratory studies formed the basis for the eventual field demonstration. The chapter begins with an introduction to the concept of an extended radius well (ERW), which was the focus of the present study (Section 3.1). Next, the tests used to evaluate the various types of media for the conductive lens are discussed (Section 3.2). Finally, a series of engineering scale injection tests performed with selected media are described (Section 3.3).

3.1 Concept of Extended Radius Wells (ERWs)

The traditional PF technology creates fractures in cohesive soils such as clay and also in rocks (shale, mudstone, etc.). Such geologic formations exhibit “self-propping” behavior, which means that the asperities present on the fracture surface are appreciable, and fluid flow is maintained through the openings. This is due in part to the fact that the entire fracture event is quite rapid, typically 10 to 15 seconds, which causes formations to respond brittlely (King, 1993). However, in fine sands, silty sands, or silts, which do not possess cohesion, self-propping is minimal. As a result the conventional PF approach will not create fractures that induce fracture longevity.

In order to improve hydraulic conductivity of fine-textured cohesionless soils, NJIT has developed the concept of an ERW. An ERW is created by injecting

supplemental media into the subsurface at a specified depth, which then creates conductive lenses radiating outward from the well. These conductive lenses have a permeability which is significantly greater than that of the native soil, thus increasing recovery of liquids and vapors from the formation. The media are injected into the formation through the use of an injection nozzle, which is capable of creating conductive lenses in various directions and at multiple elevations.

The concept of an ERW is depicted in Figure 3.1, which also compares it with a standard recovery well. Traditional wells possess high permeability zones only adjacent to the well as part of the sand pack. In contrast, the ERW has high permeability lenses which extend outward from the sand pack into the formation, which greatly increases the effective diameter of the well. The lateral extent of the ERW will, of course, depend of site specific soil properties as well as injection flow rates and pressures.

In order to demonstrate the potential permeability enhancement of an ERW, the Dupuit-Forscheimer equation for unconfined aquifers is utilized (previously presented as Eqn 2.4);

$$Q = 2\pi K \frac{h_2^2 - h_1^2}{\ln\left(\frac{r_2}{r_1}\right)} \quad (2.4)$$

A theoretical comparison between a conventional well and an ERW can be made using the above expression by assuming;

- Identical hydrogeology, i.e., K is constant,
- Choose h_1 , at the well, holding it constant,
- Choose r_2 and h_2 at the point of maximum influence, holding both constant, and,
- Vary r_1 for various sizes of ERWs.

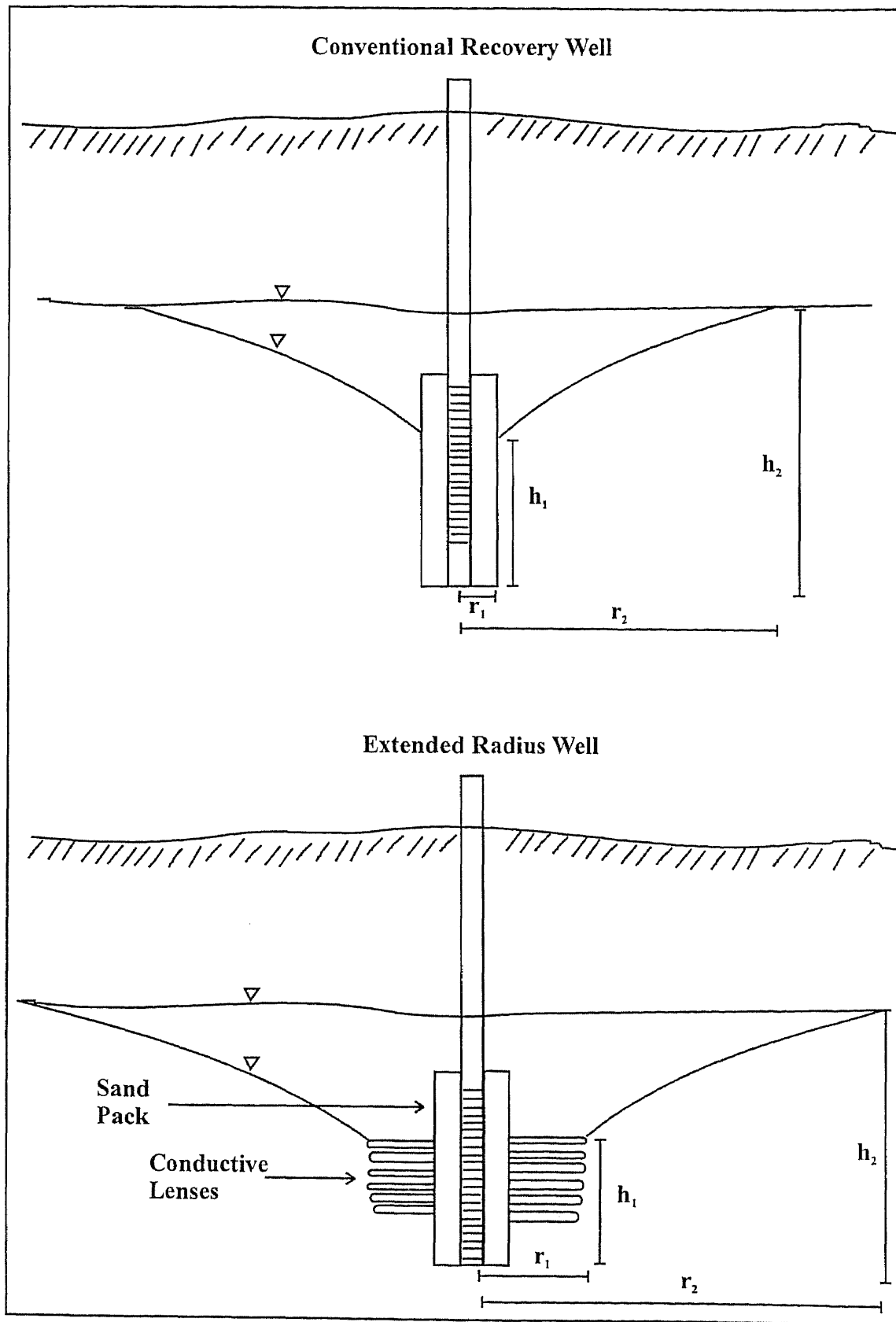


Figure 3.1 Conventional Well vs. Extended Radius Well (ERW)

The computational results of this comparison are summarized in Table 3.1, and the supporting calculations appear in Appendix A.

Table 3.1 Groundwater flow enhancement calculations

Recovery Well	Q at $r_2 = 12$ ft (cm^3/sec)	Increase in Well Flow (%)*
4 in. conventional well	2.44	0%
2 ft ERW	4.89	100%
3 ft ERW	6.32	158%
4 ft ERW	7.97	226%
5 ft ERW	10.00	309%

*compared with 4 in. conventional well

As indicated, the ERWs display increased recovery rates. As expected, the longer the length of the conductive lenses, the greater the enhancement. For example, the theoretical improvement in fluid recovery for a 5 ft (1.5 m) ERW would be 309%.

It is emphasized that the use of propping media is not universally recommended for all PF applications, but is only suggested for the present study since the soils are non-cohesive, *e.g.*, fine sands, silty sands, and silts. The fluid flow advantages of open, self-propping formations have been thoroughly documented elsewhere (Nautiyal, 1994, Hall, 1995) and are recommended for a majority of PF applications.

3.1 Laboratory Procedures

3.2.1 Characterization of Site Soils

In order to demonstrate the permeability enhancing effects of the ERW concept, a site in southern New Jersey was secured for a field demonstration. Four test borings (designated NE, NW, SE and SW) were drilled at the site during the design phase to recover soil

samples at depths ranging from 8 to 16 ft (2.4 to 4.9 m) below ground surface (bgs) at the site. The samples were returned to the NJIT laboratory for further analysis to determine their physical and chemical properties. A principal objective of the characterization tests was to match the grain size of the site soils with the appropriate media size.

A head space analysis was first performed using a photoionization detector (PID) on the soil samples in order to determine the extent and concentration of contaminants in the formation. Three grain size analyses were then performed on samples from soil boring SE using both sieve and hydrometer methods. Finally, falling head permeability testing was performed on a composite mixture from all four soil borings. The grain size analysis and permeability testing was performed in accordance with standards methods of the American Society for Testing and Materials (ASTM).

3.2.2 Evaluation of Injection Media

In order to select a specific media that could function effectively as a conductive lens in an ERW, several criteria were established. First, the material must have a permeability significantly higher than that of the soil into which it is injected. Second, the media must exhibit good flowability to assure efficient transport through hosing and pipe fittings during injection. Finally, the material must be strong enough to withstand the destructive effects of the injection process.

Candidate materials were researched by contacting vendors and requesting information on physical properties, product availability and pricing. It is noted that spherical media were preferred to optimize flowability and also to maximize the size of

pore spaces between the particles (porosity). Other desirable characteristics included modest cost and low reactivity.

Dozens of materials were evaluated including ceramics, glass, sand, plastic resins and organic materials. Materials that seemed to best meet the established criteria were obtained for subsequent testing. Eventually, 19 different products from nine different vendors were chosen for evaluative tests as listed in Table 3.2.

Table 3.2 List of Media selected for use as a conductive lens.

Supplier	Product Name	Available Sizes (mm)
CarboCeramics Inc.	CarboHSP** CarboProp** CarboLite** CarboEconoProp**	0.25 – 3.35
Fine Industrial Supply Co.	Hardball** Glass Beads	0.60 – 2.36 0.045 – 1.70
Union Process	Glass Beads	3.0 – 5.0
Agasco Corp.	Quartz	1.18 – 1.70
DuPont de Nemours, Inc.	Rynite 530 Resin [†] Derlin 500 Resin [†]	3.175
KLK, Inc.	Concrete Sand (ASTM C-33)* 00 Sand Blasting Sand* Mason Sand (ASTM C-144)*	4.75 – .075 0.03 – 0.06 4.75 – .075
Harrison Supply Co.	Concrete Sand (ASTM C-33)*	4.75 – .075
Unimin, Inc.	Industrial Sand	0.30 – 254.0
Esco, Inc.	Walnut Shell Corn Cob Aluminum Oxide Stainless Steel Shot	1.70 – 2.36 0.25 – 2.36 .038 – 0.85 0.05 – 2.00

*Uniform Size Only

**Ceramic Beads

[†]Plastic Resins

3.2.3 Media Flow Testing and Strength Testing

In order to evaluate the flowability of the selected media, flow testing was performed on all of the media listed in Table 3.2. The flow tests were performed using a modification of ASTM B 213 – 90, “*Standard Test Method for Flow Rate of Metal Powders*”. The

funnel recommended in the standard was not utilized due to its small orifice (0.10 in.). Instead, three funnels were selected: (1) glass funnel, 0.5 in. dia. (12.7 mm); (2) plastic funnel, 0.375 in. dia. (9.5 mm); and (3) glass funnel, 0.25 in. dia. (6.35 mm).

The flow tests were performed by carefully placing 50 ml of media into a funnel while covering the discharge orifice. The orifice was then opened and the elapsed time for the media to travel out of the funnel was determined with a stop watch. This procedure was repeated three times and an average flow time for the media was recorded.

In order to evaluate degradational effects of the injection process, strength testing was also performed. The objective of this test was to evaluate the crushing strength of individual particles of each media. To perform the tests, a particle of the selected media was placed onto a glass plate. A second identical plate was then placed above the particle. Downward pressure was applied in an increasing manner until the particle was crushed. A qualitative value was then assigned ranging from 1 to 5. For example, a value of 1 meant that the particle crushed easily, while a value of 5 indicated that the particle could not be crushed.

3.2.4 Media Permeability Testing

In order to help evaluate potential contaminant recovery using the extended well radius approach, permeability testing of the various sizes of selected media was performed. Testing was conducted with an ELE SoilTest[®] model K-605A combination permeameter. Permeability values were obtained using the constant head method, in accordance with ASTM standard 2434-68. The test procedure was repeated three times for each sample to

improve statistical confidence. Five increments in height (head) were used in order to examine a range of hydraulic gradients.

3.2.5 Injection Testing

3.2.5.1 Process Description: Selected media were subjected to injection testing in order to evaluate potential mechanical degradation. A schematic of the laboratory media injection system is shown in Figure 3.2. A Lindsay 100[®] mobile sandblaster was used for the injection testing. Compressed air was supplied from a gas supply tank via a 0.5 inch (1.27 cm) diameter high pressure hose connected to the sandblaster. A control valve located on the sandblaster regulated the flow of media exiting the sandblaster. A retaining line was installed on the valve to ensure it was opened identically for each injection. The air/media mixture exited the sandblaster through a flexible one-inch diameter high pressure hose connected to one of four different nozzles (See section 3.2.5.2 for more discussion on nozzle types.). Finally, the air/media mixture traveled through a 2.75 in. (6.99 cm) diameter clear plastic pipe where the media were collected into a 100 micron filter sock. Pressure readings were recorded on the supply tank before injections and on the sandblaster both before and during injections. Air flow measurements were made with an electronic flow meter.

3.2.5.2 Nozzle Descriptions: Test injections were made with four different nozzles to evaluate influence of material and nozzle geometry on particle degradation. All nozzles were constructed using one inch diameter pipe. The first nozzle consisted of a 90-degree galvanized threaded elbow. The second nozzle consisted of two-45-degree galvanized

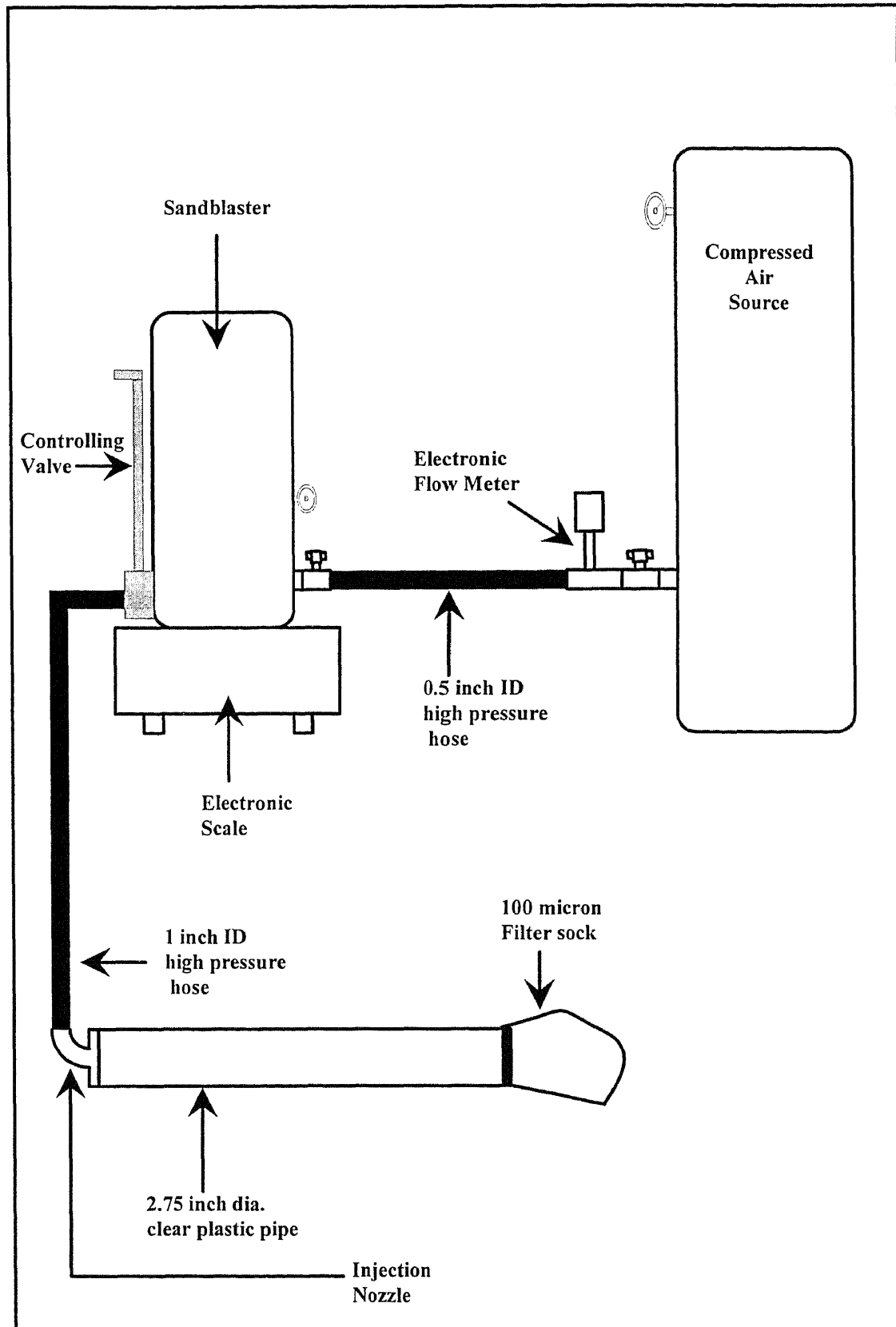


Figure 3.2 Schematic Diagram of Laboratory Media Injection System

threaded elbows with a shoulder nipple between them. The remaining two nozzles were fabricated from sweated copper fittings including a 90-degree elbow (third nozzle) and two-45-degree elbows (fourth nozzle).

The principal reason for the different materials (galvanized vs. copper) was to evaluate any degradation effects caused by the transition between the rougher threaded fittings and the smoother sweated copper fittings. The different fittings (90 vs. two-45-degree) were used to study the influence of nozzle geometry on degradation.

3.2.5.3 Description of Injections: Pressures were initially set between 95 and 98 psi (6.7 and 6.9 kg/cm²) at the air supply tank and the sandblaster tank. At the start of the injection, the sandblaster valve was partially opened for a period of thirty seconds to allow air to purge the system of any media. After this purge period, the controlling valve was completely opened, and the air/media mixture was injected for a duration of 10 seconds. During the injection, pressures, flow rates and visual observations of the media travelling through the clear pipe were recorded.

During all injections, the sandblaster was placed on an electronic scale. Prior to each injection, media was added to the sandblaster to bring the total weight of the sandblaster and ceramic beads to 87.5 lbs. (39.7 kg). The tare weight of the sandblaster was 68.1 lbs. (30.9 kg), leaving 19.4 lbs. (8.8 kg) of media in the sandblaster tank prior to each injection. After the injection, the weight of the sandblaster and ceramic beads were again recorded, thereby determining the weight of media injected. Flow rates were recorded using a Kurz[®] model 565-9-TA-AT Mass Flowmeter equipped with a digital display.

3.2.5.4 Sieve Analysis of Media: The purpose of performing a sieve analysis of the media was to evaluate any degradational effects of the different nozzle designs. Prior to injections, two baseline sieve analyses for each media were performed. These analyses were performed in the same manner as a standard soil sieve analysis (ASTM D 422). After each injection (section 3.2.5.3), the media was carefully removed from the 100 micron sock and placed into soil sieves and analyzed. The resulting grain size curve was then compared to that of the baseline curve to determine the degree of degradation for each nozzle design.

3.3 Engineering Scale Procedures

To bridge the gap between the bench scale research and the field demonstration, engineering scale studies were performed in a 15 yd³ (11.5 m³) dumpster which served as a containment vessel. The test procedure began by positioning a 1.25 in. (3.18 cm) injection nozzle at the front end of the containment vessel. Fine sand was then placed into the containment vessel using a small front end loader and compacted with hand tampers to a density of approximately 100 pounds per cubic foot (1600 kg/m³) in 10 to 12 in. (25 to 30.5 cm) lifts. Care was taken to ensure the soil was compacted properly around the injection nozzle in order to reduce any short circuiting around the edges of the delivery tube. The injection port was positioned at a depth of 30 in. (76.2 cm) from the top of the compacted soil, or six inches from the bottom of the containment vessel. For each injection air was first injected into the compacted soil creating fractures, then an air/media mixture was introduced.

The equipment configuration for the engineering scale injection tests is depicted in Figure 3.3 which consisted of the containment vessel, injection nozzle, compressed air source (8 air cylinders manifolded together), and dry media injection system. A detailed schematic of the dry media system is provided as Figure 3.4, which consisted of two 30 gallon storage tanks, air actuated ball valves, regulators, and pipe fittings. The function of the dry media injection system was to carefully energize and transport the media into the pneumatically created fractures. A total of six injections were performed for the engineering scale tests.

3.3.1 Soil Excavations

Soil excavations were made after each injection in order to examine the pattern of the media lenses in the soil. Excavation was initiated at the end of the containment vessel and continued towards the injection port. The compacted soil was excavated using shovels in a shearing manner from the soil surface to the base of the containment vessel. This process was continued until beads were encountered within the soil. Observations of the bead dispersal were then made as excavation progressed towards the nozzle. Of particular interest were radius of influence of air and media, daylighting and subsurface air voids. The dimensions and spatial locations of each of these features were recorded in a field notebook.

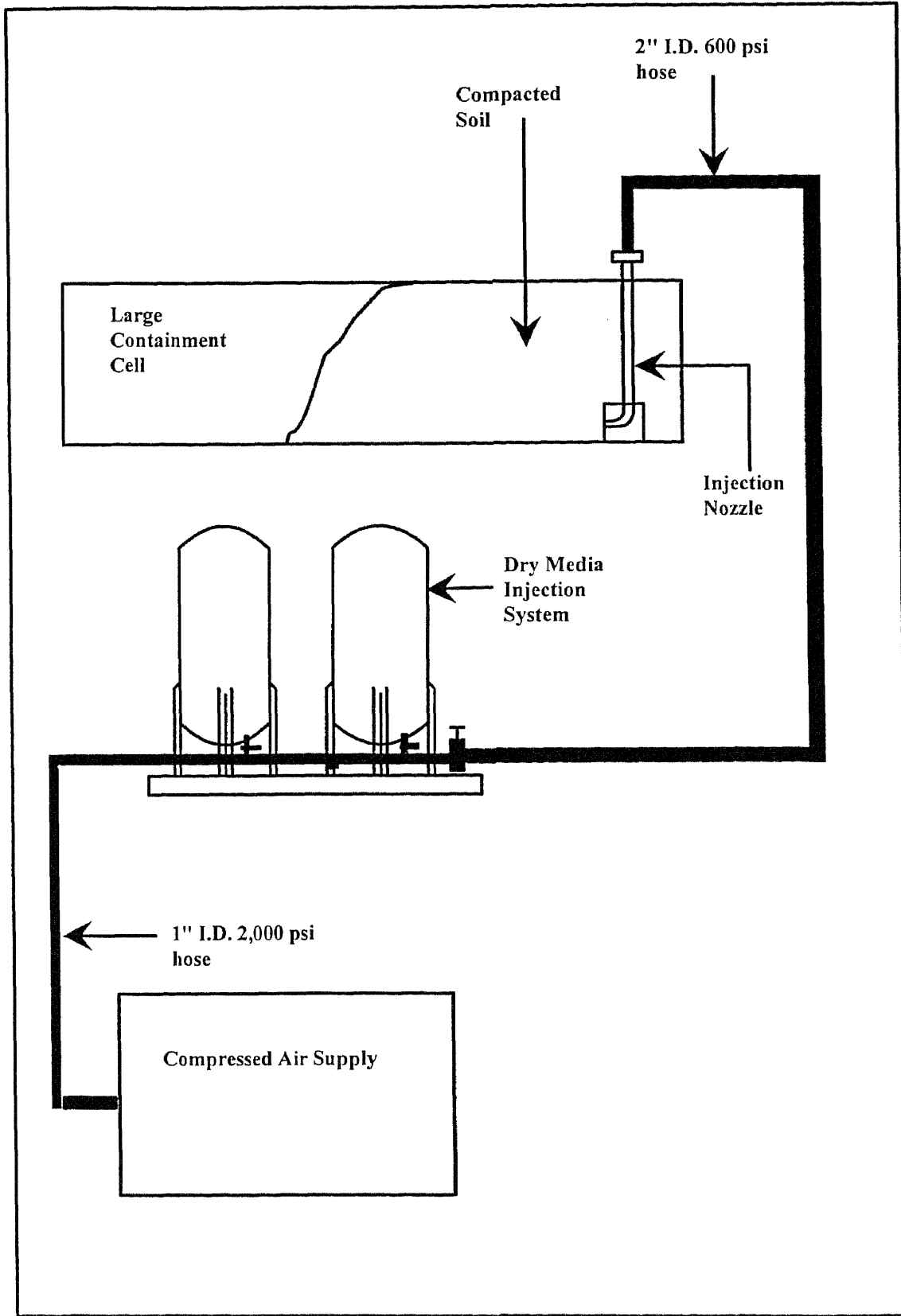


Figure 3.3 Engineering Scale Injection Test Setup

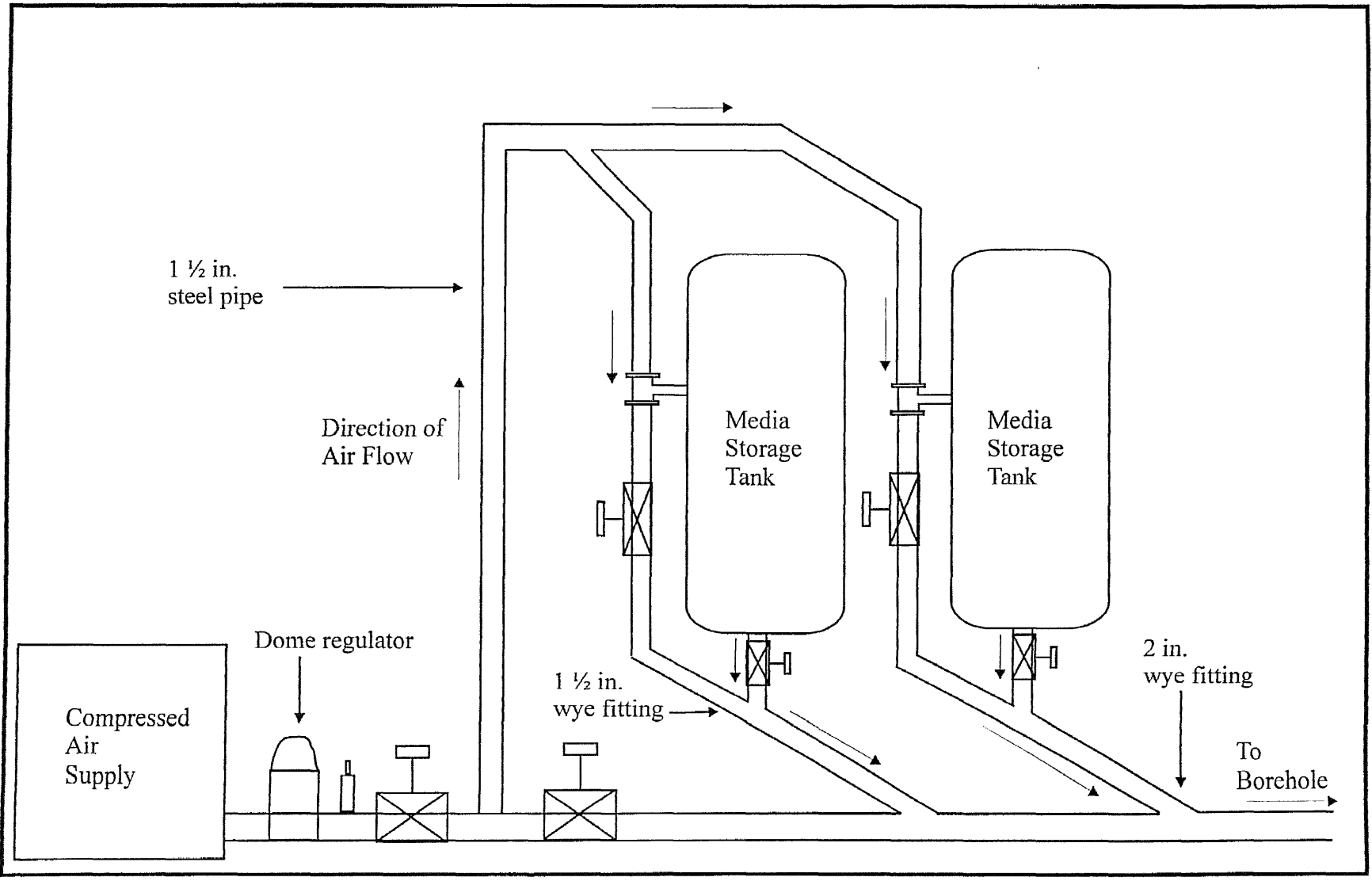


Figure 3.4 Dry Media Injection System schematic

CHAPTER 4

TEST RESULTS AND PROTOTYPE DESIGN

This chapter presents the results of the laboratory and engineering scale tests. The chapter also describes the design of the prototype injection nozzles. The results of the laboratory tests are first discussed including soil property analyses, media selection testing, permeability testing and injection testing (Section 4.1). Next, a summary of the engineering scale investigation is presented (Section 4.2). Finally, the prototype design for the injection nozzles used for the field demonstration are introduced (Section 4.3).

4.1 Laboratory Results

4.1.1 Properties of Site Soils

As previously discussed, soil borings were drilled at a site in southern New Jersey in preparation for the field pilot demonstration. A series of laboratory tests were conducted on the recovered samples including a head space analysis, grain size analysis, and permeability testing.

The purpose of the head space analysis was to aid in determining the depth at which contaminants are present beneath the site. The results of the head space analysis are presented in Table 4.1. A review of the data indicates that the highest VOC concentrations occurred in the range between 9 to 13 ft (2.7 to 4.0 m) below ground surface (bgs). This corresponds with the depth of the free product layer identified in

previous investigations, so the depth range selected for the ERW injections was 9 to 13 ft (2.7 to 4.0 m) bgs.

Table 4.1 Head Space Analysis

Soil Boring	Depth from Surface (ft)	Concentration (ppm)
SE	9 – 11 top, bottom	1388, 1562
	11 – 13 top, bottom	1812, 226
	13 – 15 top, bottom	61.0, 59.8
SW	8 – 10 top, bottom	227, 11.6
	10 – 12 top, bottom	23.8, 16.0
	12 – 14 top, bottom	12.9, 18.1
NE	9 – 11 top, bottom	447, 1797
	11 – 13 top, bottom	487, 668
	13 – 15 top, bottom	105, 13.0
NW	8 – 10 bottom	1951
	10 – 12 top, bottom	2476, >2500
	12 – 14 top	1571
	14 – 16 middle, bottom	80.4, 48.7

Three grain size analyses were conducted on soil boring SE at depths ranging from 9 to 15 ft (2.7 to 4.6 m) bgs using a mechanical sieve and hydrometer. The results of these analyses are depicted in Figure 4.1. The soil grain size in this depth zone is classified as silty fine SAND, or SM, under the Unified Soil Classification System (USCS).

Permeability tests were conducted on a composite sample of native soil as previously described in section 3.2.1. The results of the permeability testing are summarized in Table 4.2, and the supporting calculations are provided in Appendix B. The hydraulic conductivity values for the three tests were similar with an average of 4.22×10^{-5} cm/sec (1.38×10^{-6} ft/sec). This hydraulic conductivity is consistent with typical

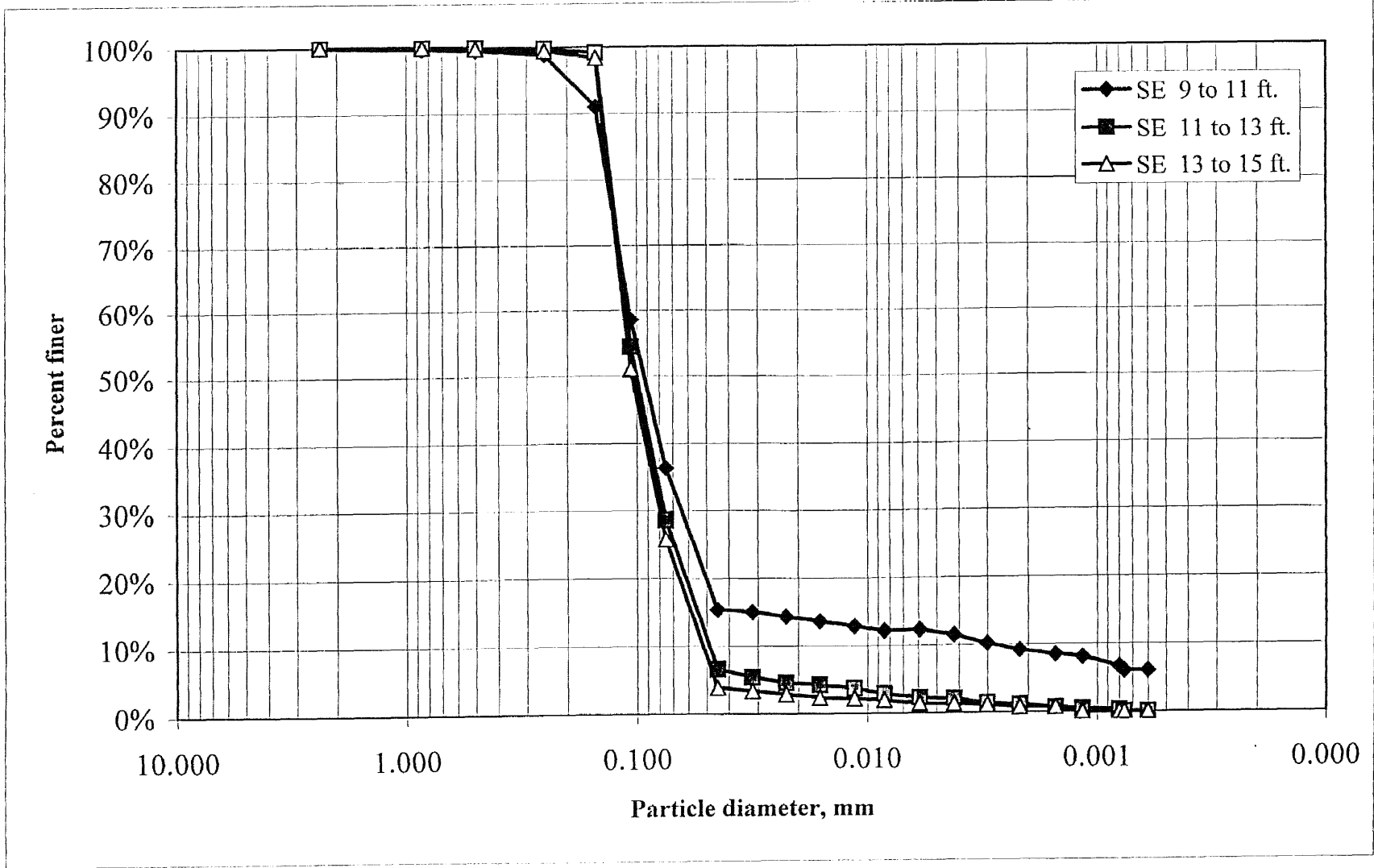


Figure 4.1 Grain Size Analysis Soil Boring SE (9 to 15 ft)

published values for silty fine sand which typically range from 10^{-3} to 10^{-6} cm/sec (Spitz and Moreno, 1996).

Table 4.2 Hydraulic Conductivity Testing results of native soil

Test #	Permeability (K)
1	4.08×10^{-5} cm/sec
2	4.27×10^{-5} cm/sec
3	4.30×10^{-5} cm/sec
Avg.	4.22×10^{-5} cm/sec

4.1.2 Media Flow and Strength Testing Results

Flow testing of the media was accomplished using three funnels, each with a different discharge orifice (section 3.2.3). Overall, the tests showed that small media with a uniform diameter flowed best. In contrast, well graded media such as concrete sand tended to clog the discharge orifice. The average elapsed time for various media using funnel #2 (9.5 mm orifice) is provided in Table 4.3. A complete listing of flow times and comments for all the media tests is provided in Appendix C.

Strength testing of the media was also performed to evaluate its potential degradability. As indicated in Table 4.3, media demonstrating the highest strength values were the ceramic beads, plastic resins, and walnut shells. The quartz media and the sand exhibited the lowest strength of the materials tested, probably on account of their brittle mineral structure. A complete listing of the strength test data can be found in Appendix C.

Table 4.3 Flow and Strength Test data of various media

Media	Avg. time through funnel #2 (sec)	Strength Rating (1-5)	Media	Avg. time through funnel #2 (sec)	Strength Rating (1-5)
CarboCeramics <i>CarboProp</i> , 16/30 sieve	3.00	4	KLK, Inc. <i>Sand Blasting Sand</i> size 00	4.88	1
Fine Industrial Supply <i>Glass Beads</i> Size 20/30 sieve	2.94	2.5	Esco, Inc. <i>Walnut Shell</i> 8/12 sieve	3.80	4
Agasco, Corp. <i>Quartz</i> #16F	3.37	1	Esco, Inc. <i>Corn Cob</i> 14/20 sieve	4.08	3
Dupont de Nemours <i>Delrin 500 resin</i> 0.125 in.	3.92	5	Esco, Inc. <i>Aluminum Oxide</i> 30 grit	3.73	3

4.1.3 Media Selection and Design

Based upon the results of the strength and the flow testing, the CarboProp ceramic beads manufactured by CarboCeramics were chosen for the conductive lens in the ERWs. It is interesting to note that this media is specifically designed to act as a proppant to sustain artificially created hydraulic fractures in the petroleum industry. The ceramic beads are spherical in shape, which allows them to flow smoothly. They also exhibit high strength characteristics (Table 4.3). Another advantage of this media is that it is available in a wide range of grain sizes, thus enabling its use in a variety of geologic formations. A grain size analysis (ASTM D 422) for all sizes of the ceramic beads was performed and is presented in Figure 4.2.

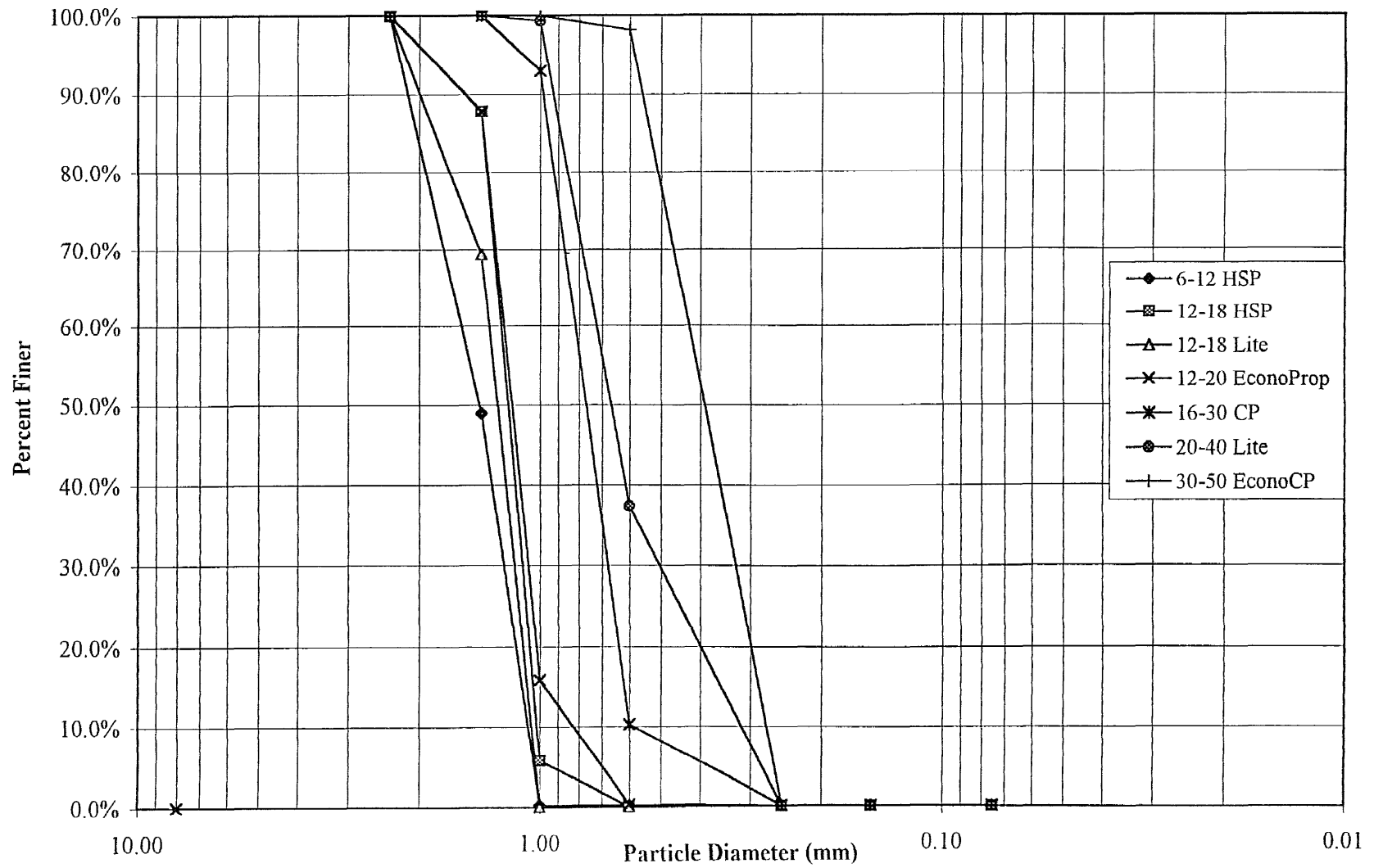


Figure 4.2 Summary of Grain Size Testing CarboCeramics Proppant

Final selection of the bead size for the conductive lenses was based upon filter pack design procedures (*e.g.*, Driscoll, 1986). This procedure may be outlined as follows:

- 1) Perform a sieve analysis of the native soil and plot the results as grain size (x-axis, logarithmic scale) vs. % passing (y-axis linear scale).
- 2) Multiply the D_{30} of the native soil by a factor between 4 and 10 and set this equal to the D_{70} of the filter media.
- 3) Check the uniformity coefficient (C_u) of the filter media using the Hazen Formula, where $C_u = D_{60}/D_{10}$.
- 4) Choose a filter media with a D_{70} in this range.

It is noted that the multiplier value (step 2, above) was chosen high in the present study to assure that maximum permeability for the conductive lenses. The filter calculation for the media selection is contained in Appendix D. The size of ceramic beads finally selected for the ERW was 16/30 (1.18 to 0.60 mm)

4.1.4 Media Permeability Testing Results

Permeability testing was performed on several sizes of ceramic beads in order to assess potential enhancement by the ERWs. Five increments in hydraulic head were used for each test specimen for statistical confidence. Hydraulic conductivity of the media was calculated using the following relation:

$$K = \frac{Q \cdot L}{A \cdot t \cdot h} \quad (4.1)$$

where;

K = hydraulic conductivity, L/T

Q = discharge flow of water from permeameter, L³/T

L = length of sample in permeameter, L

A = cross sectional area of permeameter, L²

t = time of discharge, T

h = vertical distance between water surface in funnel and discharge point on permeameter, L

The results of the permeability tests for the ceramic beads are summarized in Figure 4.3. As Figure 4.3 illustrates, hydraulic conductivity ranges within one order of magnitude and is roughly proportional to grain size. The 6/12 product size exhibited the highest hydraulic conductivity with a value of 0.320 cm/sec (0.01 ft/sec), while the 30/60 was the lowest at 0.048 cm/sec (0.002 ft/sec). All four products of 20/40 size exhibited similar hydraulic conductivity values, even though they had different densities. The hydraulic conductivity calculations for the tested media appear in Appendix E.

Permeability testing using various mixtures of the native soil and the beads were also conducted to assess potential recovery enhancements in the event that the media does not form discrete lenses. The results of these tests are presented in Figure 4.4. It is clear from the figure that when the native soil is mixed uniformly with the beads, the hydraulic conductivity is dominated by the native soil. An increase in conductivity is not observed until there is at least 70% media in the mixture.

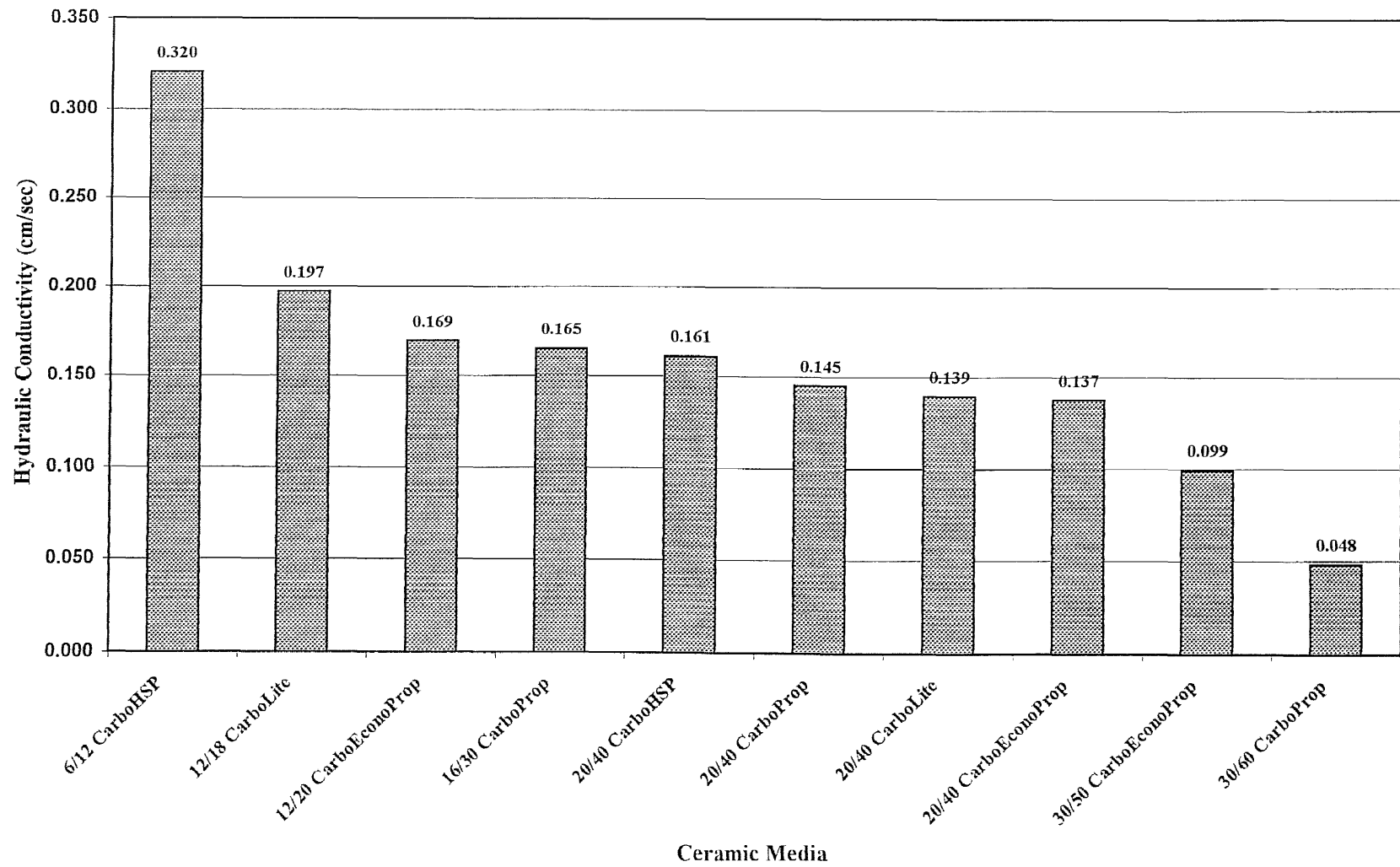


Figure 4.3 Summary of Hydraulic Conductivity Results Using CarboCeramics Proppant

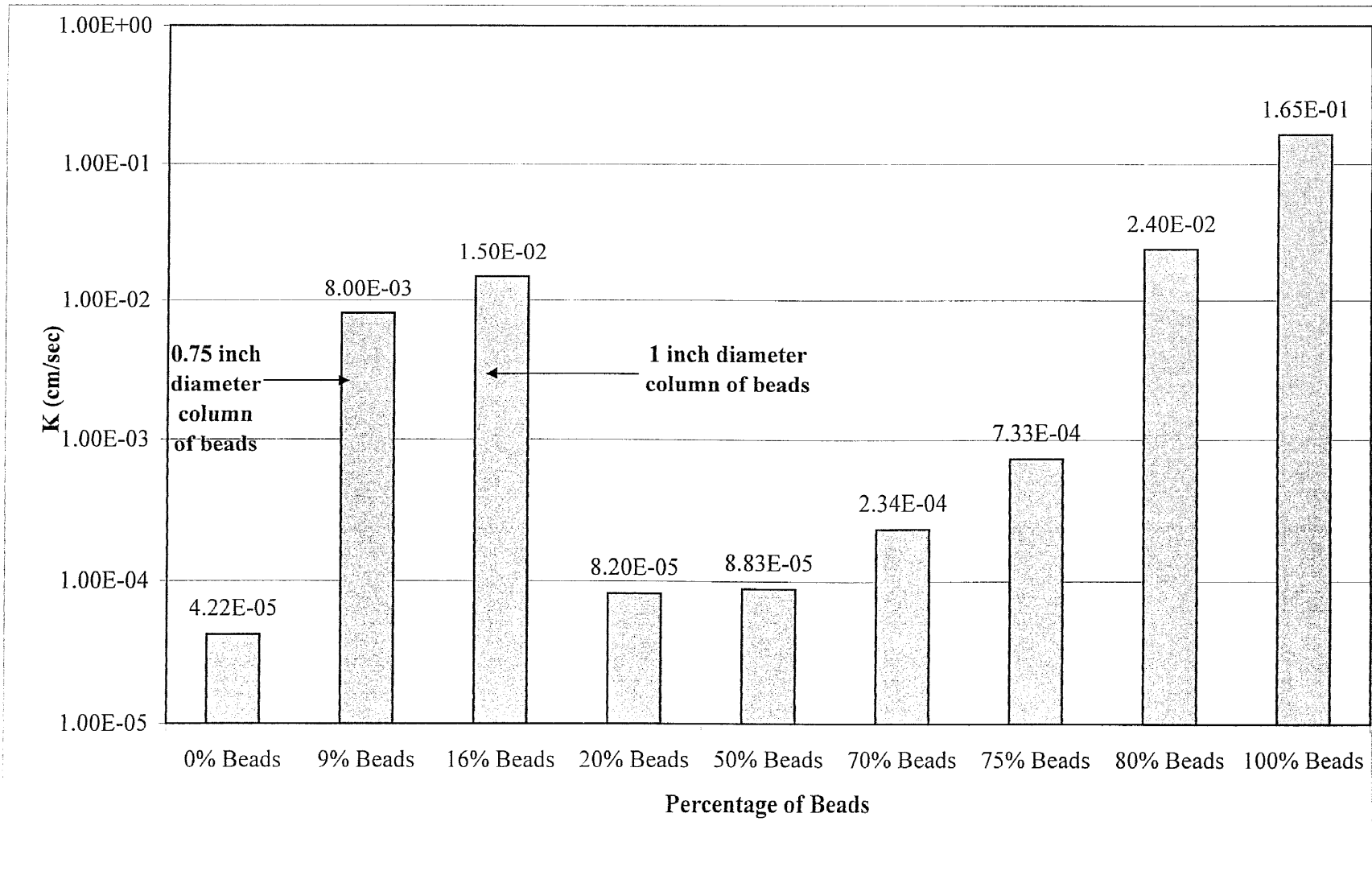


Figure 4.4 Summary of Hydraulic Conductivity Results using 16/30 CarboProp and native soil

Additional permeability tests were performed to examine the effects of conductive lenses in the native soil. Cylindrical columns of beads were placed in the center of the permeameter and the native soil (silty fine sand) was packed around the beads. Bead columns of two different diameters were investigated: 0.75 and 1.0 in (1.91 and 2.54 cm.). These yielded hydraulic conductivity values of 8.0×10^{-3} and 1.5×10^{-2} cm/sec (2.62×10^{-4} and 4.92×10^{-4} ft/sec), respectively. This testing further confirmed that discrete seams of media with little or no native soil particles between the beads will provide the best enhancement to free product recovery.

4.1.5 Injection Testing and Degradability

Once ceramic beads were selected for the conductive lens, bench scale injection testing was performed using this media with various nozzle types. Following injection, the beads were sieved, and a grain size analysis performed to evaluate changes in particle size as a result of the injection process. Four different nozzle designs were tested, and six injections were performed with each nozzle design. The operational parameters for the bead injection tests are summarized in Table 4.4. Every effort was made to keep the air flow rates relatively constant. Also, the weight of injected media and air supply pressures were held at comparable levels. The injections are identified by the date they were performed, followed by the injection number. CarboCeramics 16/30 CarboProp was utilized for all injections.

Table 4.4 Summary of Laboratory Injection Tests

Injection #	Injection Description	Air Flow During Media Injection (SCFM)	Weight of Beads Injected (lbs.)
010798#1	One inch 90 degree	72	0.8
010798#2	Galv. nozzle	56	2.9
010798#3	Series #1	60	1.4
012698#1	One inch 90 degree	58	2.1
012698#2	Galv. nozzle	56	2.2
012698#3	Series #2	56	2.2
011298#1	One inch 90 degree	65	1.4
011298#2	Copper nozzle	56	2.1
011298#3	Series #1	63	1.6
012798#1	One inch 90 degree	56	2.8
012798#2	Copper nozzle	58	2.2
012798#3	Series #2	58	2.0
010898#1	Two – one inch	56	2.7
010898#2	45 degree	62	1.6
010898#3	Galv. nozzle Series #1	62	2.1
012098#1	Two – one inch	55	2.2
012098#2	45 degree	56	2.2
012098#3	Galv. nozzle Series #2	56	1.9
011698#1	Two – one inch	56	2.0
011698#2	45 degree	59	1.9
011698#3	Copper nozzle Series #1	57	2.3
012298#1	Two – one inch	56	2.2
012298#2	45 degree	57	2.0
012298#3	Copper nozzle Series #2	58	2.0

Prior to performing the injections, the preinjection grain size distribution was determined to provide a baseline. Six injections were completed with each nozzle design, and the results averaged. The recovered beads were sieved and grain size curves established. A summary of the average grain size distributions for the nozzle designs are depicted in Figure 4.5. As Figure 4.5 indicates, there was measurable degradation of the media for both 90 degree nozzle designs (galvanized and copper). However, there was little, if any, degradation with either of the 45 degree nozzle designs. The results of the

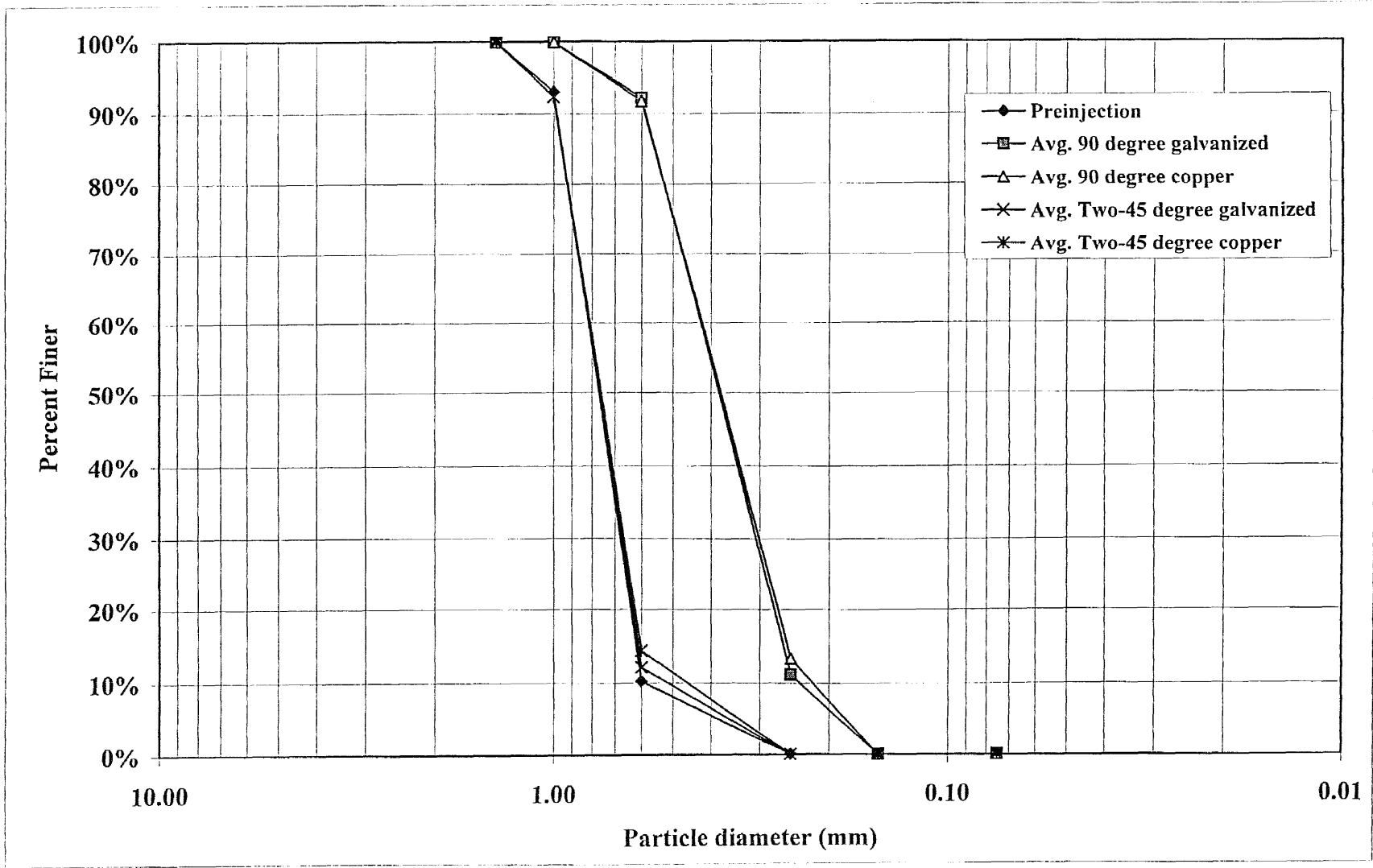


Figure 4.5 Bench Scale Injection Sieve Analysis Summary

injection tests strongly suggest that the nozzle geometry is more important than nozzle material (i.e. galvanized vs. copper).

4.2 Engineering Scale Results

Prior to the field demonstration (section 5), engineering scale studies were performed in a large containment vessel using sand that was representative of the native soil at the field site. A total of six injections were performed within the containment vessel. The operational parameters monitored for each injection are summarized in Table 4.5.

Table 4.5 Engineering Scale Injection Data

Injection #	Injection Time (sec.)	Weight Media Injected (lbs.)	Air Flow Rate (SCFM)
1	33	43	338
2*	10	18	673
3*	12	31	856
4	15	36	407
5	15	28	593
6	10	32	1180

*soil excavations performed

As the data in Table 4.5 indicate, large quantities of media were successfully injected into the containment vessel over a short injection period. These flow rates were comparable to those eventually used for the field demonstration. Thus, the engineering scale tests provided a valuable opportunity to optimize operational control of the system.

To better understand the formation of beads lenses (*i.e.* conductive lenses) for the ERWs, exploratory soil excavations were made for injections #2, and #3. Scaled drawings were prepared for these excavations detailing the pathways of the media and air within the containment vessel. The results of the excavations for injections #2 and #3 are

presented in Figures 4.6 through 4.9. Both a section view and a plan view are depicted for each injection, and include where the conductive lenses were formed, as well as any air voids which may have also formed.

The results of injection #2 shown in Figures 4.6 and 4.7 indicate that daylighting (air only) was observed in a radial pattern 24 to 30 in. (60.1 to 76.2 cm) from the injection point. Discrete seams of beads 1/8 to 1/4 in. (0.32 cm to 0.64 cm) in thickness were observed in a irregular radial pattern approximately 30 in. (76.2 cm) from the injection point, just beneath the soil surface. Within this lens, the beads were packed thicker at some locations (up to 1 in.). Short lenses of beads were also observed closer to the injection point from 0.8 to 1.5 ft (0.24 to 0.46 m.) below grade. Injection #2 also formed two large air voids within the soil. The first air void was located at the injection nozzle, and rectangular in shape approximately 6 in. X in. 6 in. X 10 in (15 cm X 15 cm X 15 cm). A larger rectangular air void approximately 8 in. X in. 5 in. X 17 in. (20.3 cm X 12.7 cm X 43.2 cm) was located 12 in. (30.5 cm) from the surface, 6 in. (15.2 cm) from the injection point. At the bottom of both of these air voids, beads and sand were well mixed together and loosely packed. Loose sand was observed between the two air voids.

Figures 4.8 and 4.9 also indicate that daylighting occurred for injection #3, approximately 22 to 30 in. (55.9 to 76.2 cm) from the injection point. On the surface of the soil beads were exposed and ejected from the daylighting fractures. The beads formed preferential pathways, and as a result, a large cell of beads approximately 15 in. X 12 in. X 3 in. (38.1 cm X 30.5 cm X 7.6 cm) was formed behind the injection nozzle against the containment vessel door. Beads were also observed along the delivery tube to approximately 8 in. (20.3 cm) below grade. A lens of beads was observed 19 in. (48.3

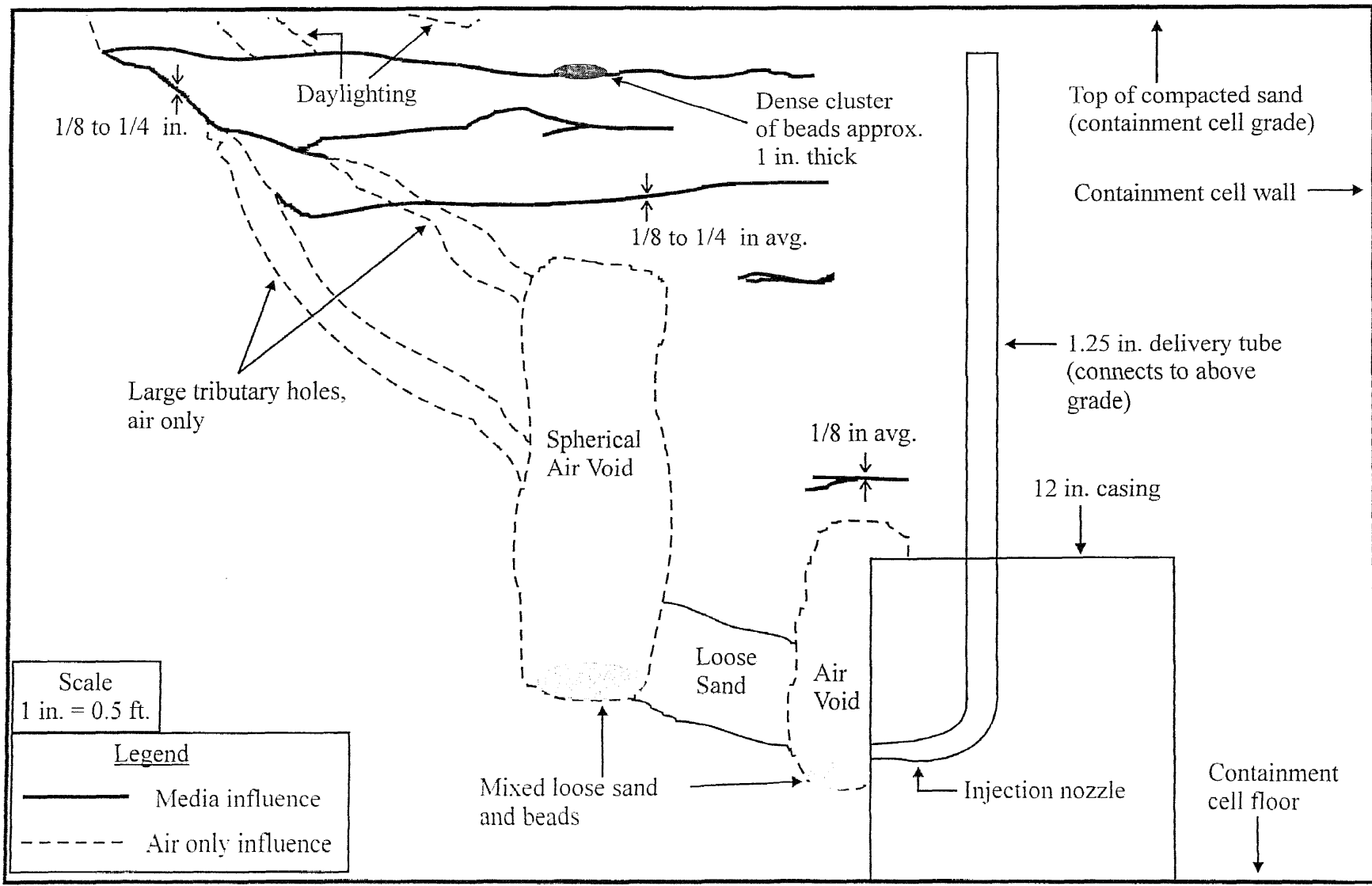


Figure 4.6 Engineering Scale Excavation, Injection #2, Section View

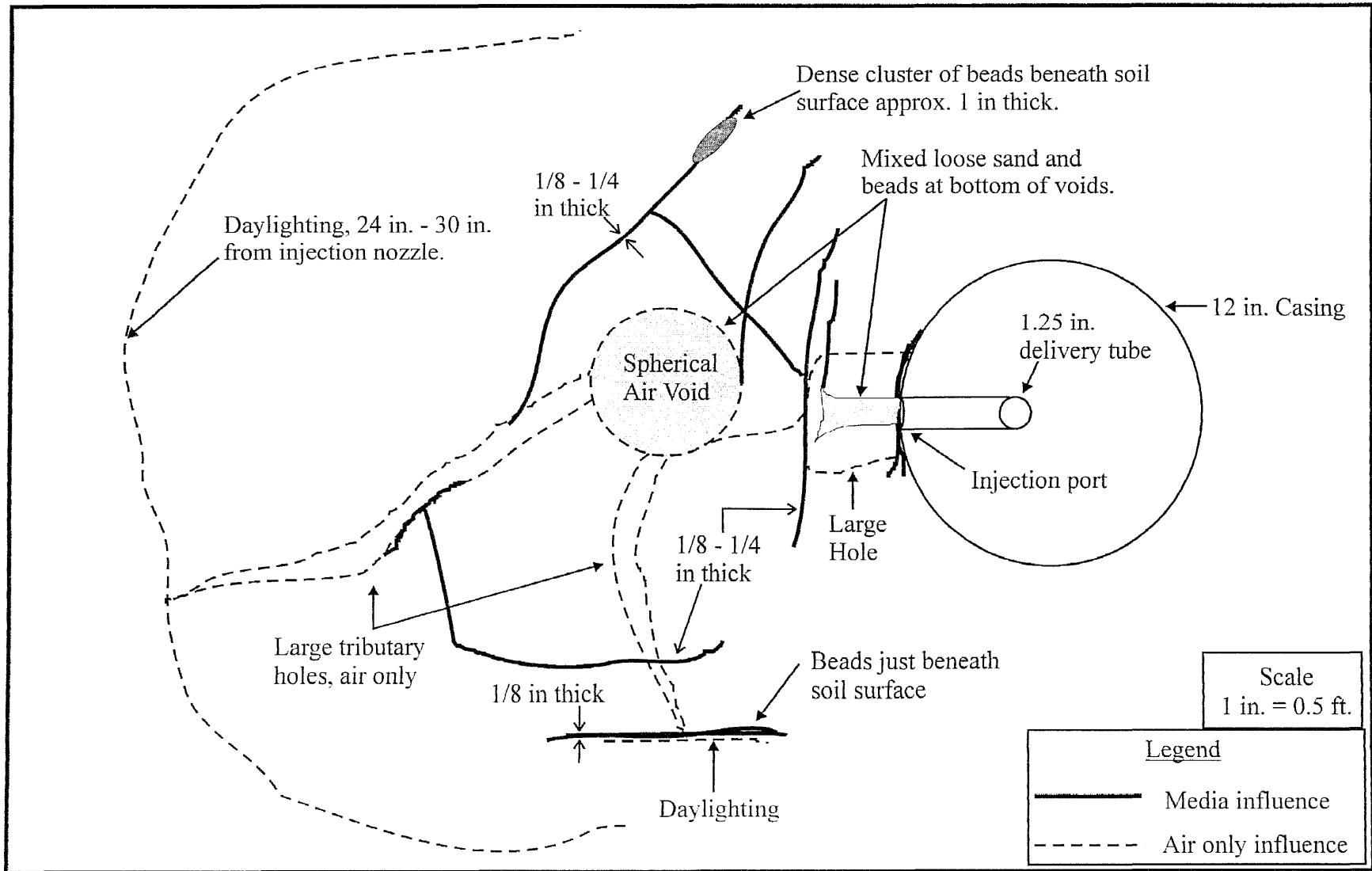


Figure 4.7 Engineering Scale Excavation, Injection #2. Plan View

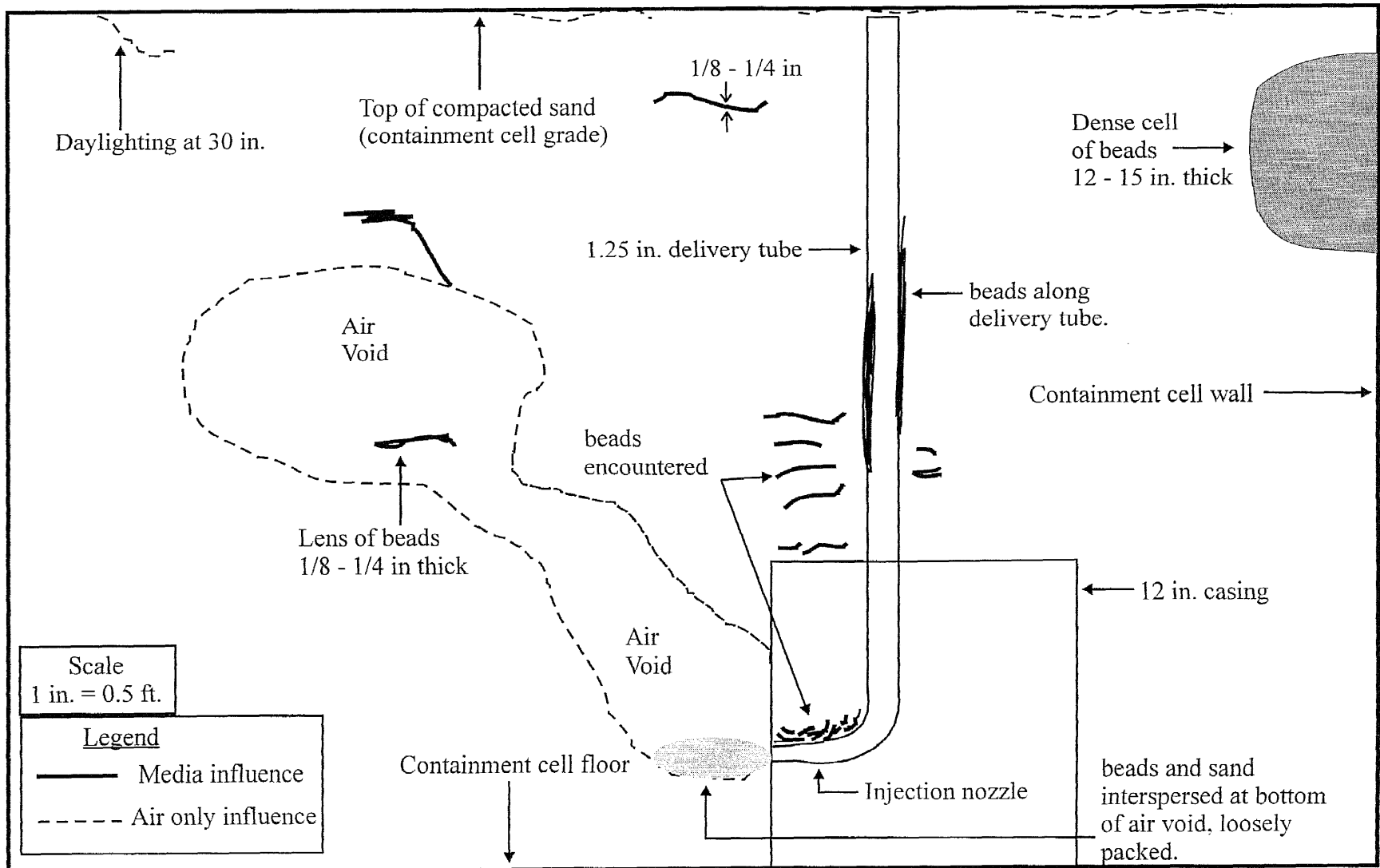


Figure 4.8 Engineering Scale Excavation, Injection #3, Section View

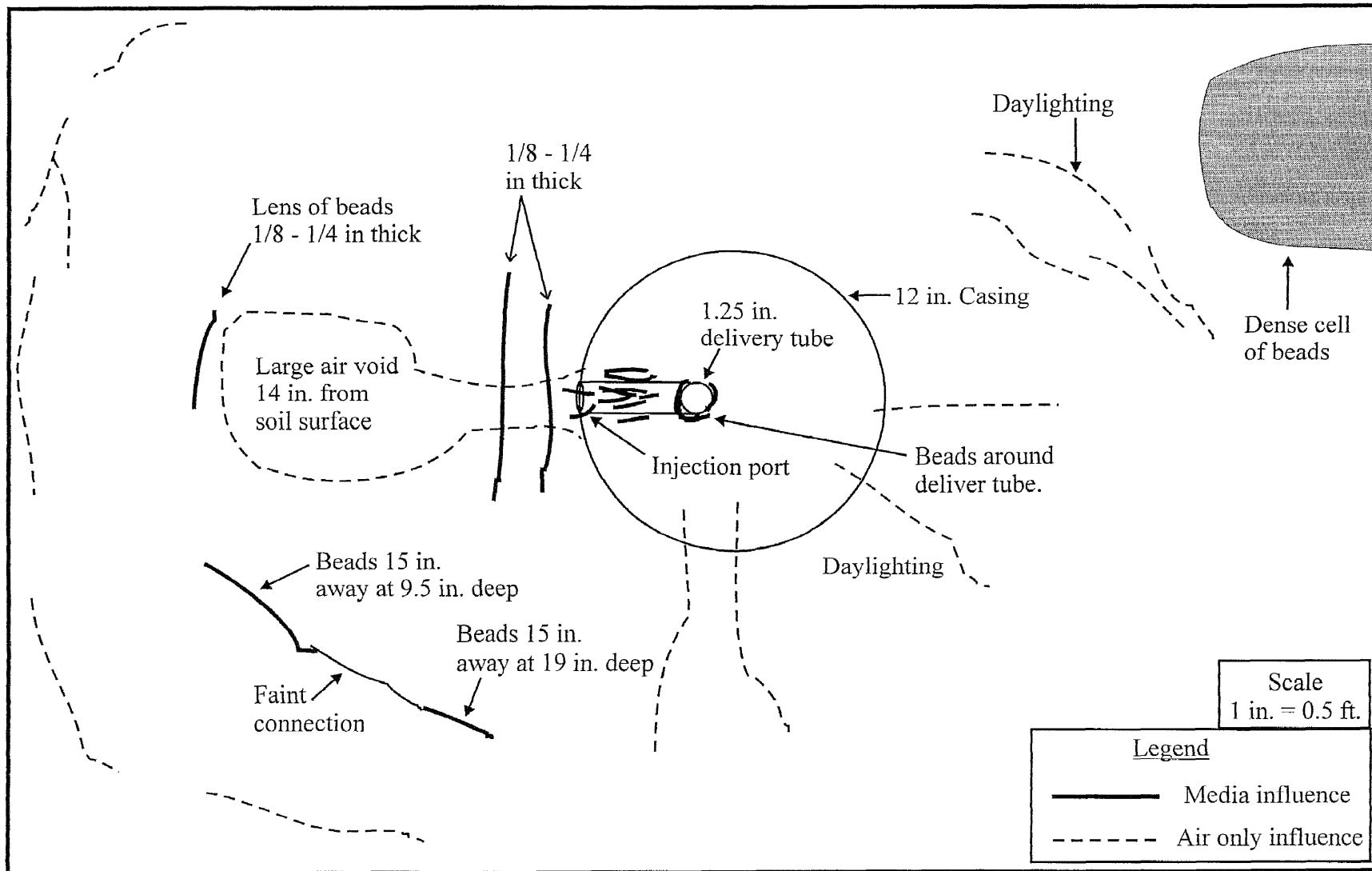


Figure 4.9 Engineering Scale Excavation, Injection #3, Plan View

cm) northwest of the injection point, 9.5 to 19 in. (24.1 to 48.3 cm) below grade. Beads were also observed in the vicinity of the injection nozzle. In addition to the creation of conductive lenses, a large spherical air void approximately 12 in. (30.5 cm) diameter was observed at a depth of 14 in. (35.6 cm) below grade, 10 in. (25.4 cm) from the nozzle port. This air void could be traced back to the injection nozzle (Figure 4.8). Beads and loose sand were interspersed at the bottom of the air void below the injection nozzle.

The engineering scale excavations demonstrated that discrete conductive lenses could indeed be formed in silty sand by pneumatic injection. They also proved that quantities of media could be successfully introduced into a geologic formation over a short time period. The beads flowed through the injection apparatus properly, and did not clog the hosing or the injection system. However, since the soil was underconsolidated, and only compacted to approximately 100 lbs/ft³ (1600 kg/m³), large air voids were formed in the sand by the injections. As a result, the ERW concept was not fully realized in this portion of the study since the conductive lenses were not continuous from the point of injection.

4.3 Prototype Design

To create high permeability conductive lenses in the field, two separate injection nozzles were utilized. One nozzle was designed to be an in-place nozzle with individual, fixed injection ports arranged in a helical pattern (15 Port Helical Nozzle). The other nozzle had a single injection port, and was designed to be adjusted within the formation (Movable Nozzle). Both of these nozzles are proprietary, although a general description is given in the following sections.

4.3.1 Fifteen Port Helical Nozzle

The 15 Port Helical Nozzle was designed to be stationary throughout the entire injection process. It is comprised of fifteen individual injection ports, each with 1.25 in. (3.18 cm) diameter delivery tubes. The entire matrix of piping is contained within a 12 in. (30.5 cm) diameter steel casing. Media is injected through each port in succession to create conductive lenses in the subsurface. In order to transfer the flow of beads flowing vertically down the delivery tube, and horizontally into the formation, long radius, 90-degree elbows were utilized. Long radius fittings were used to provide a more gradual transition than conventional 90-degree elbows, thereby reducing media degradation during injection.

The nozzle was designed to create high permeability, conductive lenses over an interval of three feet (0.9 m.). There were five injections per one foot interval, or a total of 15 injections over the entire recovery zone. Each injection port was spaced approximately 72 degrees apart, resulting in a helical, or screw-type pattern of injection ports emitting from the outer 12 in. (30.5 cm) casing.

4.3.2 Movable Nozzle

In addition to the 15-Port Helical Nozzle described in the preceding section, a Movable Nozzle was also used to create ERWs at a second location. The riser portion of the nozzle consisted of 3 in. (7.6 cm) outer diameter, NW casing. This type of casing is flush jointed so that friction is minimized during advancement and withdrawal. A 1.5 in. (3.8 cm) delivery tube was positioned inside of the NW casing and threaded to the movable injection nozzle attached to the top of the casing.

The injection nozzle was constructed of stainless steel and was machined to a conical point. The movable nozzle had male NW threading to accept the NW casing, and female 1.5 in. (3.8 cm) pipe threading to connect with the delivery tube. The exit port was machined so that the opening made a 90-degree transition from vertical to horizontal. The exit port was rectangular, measuring approximately 2.5 in. long X 0.75 in. wide (6.4 X 1.9 cm).

CHAPTER 5

FIELD DEMONSTRATION

The final phase of the research study was to demonstrate the concept of the ERW at a field pilot scale. This chapter begins with a description of the geology and hydrogeology of the site selected for the field demonstration (Section 5.1). The field demonstration setup and operations are next discussed (Section 5.2). Finally, the results of the field demonstration are presented (Section 5.3).

The selected site was ideal for the first ERW field demonstration for these reasons:

- The soils at the site had a moderate to low permeability, in the range of 10^{-3} to 10^{-6} cm/sec;
- In addition to low permeability, the soil was non-cohesive, so that media proppant was required to sustain the fractures; and
- Extensive pumping tests were made before and after creation of the ERW in order to evaluate flow enhancement.

5.1 Site Geology and Hydrogeology

The site is located in Southern New Jersey within the Coastal Plain Physiographic Province. The sediments in the Coastal Plain were formed during the Cretaceous and Miocene Periods and they are estimated to range in age from 135 to 5.3 million years. The particular formation underlying the site is the Kirkwood which generally consists of

unconsolidated sediments (*e.g.*, silty fine sand). The topography of the region is generally flat with gentle sloping *cuestas*. Glacial activity over the last two million years has created extensive wetlands throughout the Coastal Plain Province. It is noted the Coastal Plain contains a number of productive ground water aquifers that supply potable water to many communities in Southern New Jersey.

A number of active above ground storage tanks (AST's) are located on the test site. Past site operations led to the release of several hundred thousand gallons of petroleum hydrocarbons into the subsurface. Over the past thirty years, a large plume of free product has developed, which is slowly migrating off site. The soils underlying the site are predominately silty fine sands with a hydraulic conductivity of approximately 4.0×10^{-5} cm/sec (1.3×10^{-6} ft/sec). Several attempts have been made to recover the plume including free product recovery, bioventing, and vacuum enhanced free-product recovery (bioslurping). Two recovery trenches 50 foot and 100 foot long (15.2 m and 30.5 m), respectively were also installed in an attempt to increase the recovery of free product. On account of the marginal permeability of the site soils, product recovery rates with all the technologies attempted have been relatively low.

5.2 Test Setup and Operations

5.2.1 Overview of Field Activities

The objective of this field demonstration was to install two ERWs to enhance free product recovery. A plan of the site is depicted in Figure 5.1 which includes well locations and estimated product thicknesses.

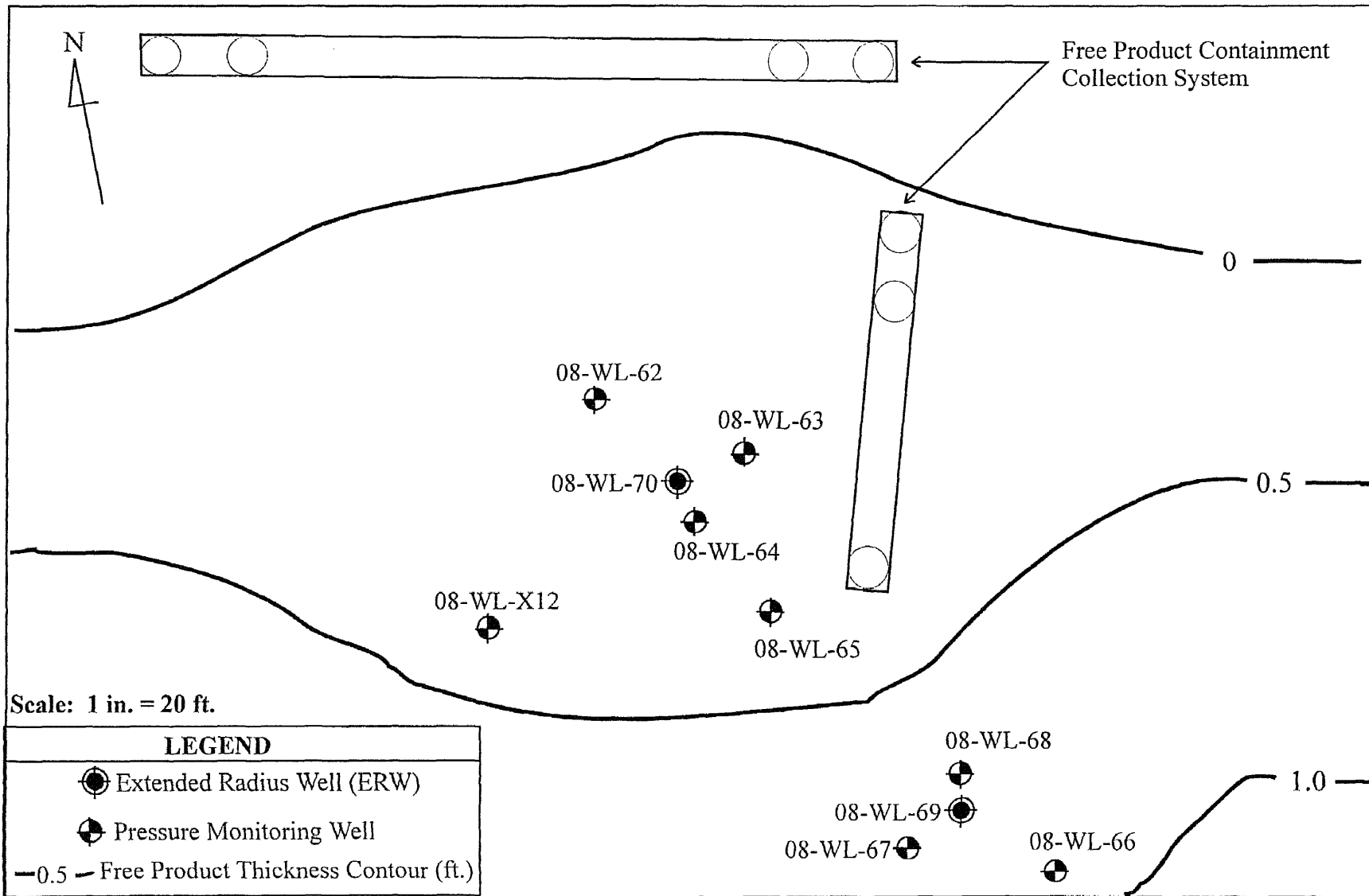


Figure 5.1 Site Plan of Field Demonstration

The installation of the ERWs is an integrated process involving several field activities including drilling, media injections, and well installation. In addition, monitoring wells were also installed around each ERW to monitor air pressures during the media injections. Upon completion of the ERWs, extended pumping tests were performed on each recovery well to evaluate their respective enhancements. Finally, geoprobe samples were taken to delineate the thickness and extent of the conductive lenses. A summary of the field activities is presented in Table 5.1.

Table 5.1 Summary of Field Activities

Date	Description of Field Activity
3/24/98	Installation of 15 Port Helical Nozzle
3/25/98	Installation of Movable Nozzle
3/25 – 3/26/98	Installation of monitor points
4/25 – 4/27/98	15 Port Helical Nozzle Injections
4/27 – 4/28/98	Movable Nozzle Injections
4/28/98	Installation of Recovery Well 08-WL-69 at Movable Nozzle location
4/29/98	Installation of Recovery Well 08-WL-70 at 15 Port Helical Nozzle location
5/27/98 – 8/19/98	Free Product Recovery Testing Movable Nozzle ERW (Recovery Well 08-WL-69)
7/8/98 – 8/19/98	Free Product Recovery Testing 15 Port Helical Nozzle ERW (Recovery Well 08-WL-70)
7/23, 7/24, 7/27/98	Geoprobe Soil Sampling

5.2.2 Injection Nozzle Installation Procedure

5.2.2.1 Fifteen Port Helical Nozzle: The 15 Port Helical Nozzle was designed to be stationary throughout the entire injection process. Installation began by boring a 8.25 in. (20.96 cm) I.D. hollow stem auger (HSA) to a depth of 22 ft (6.7 m), creating a 12 in.

(30.5 cm) O.D. hole. Before removing the auger, the center was flushed with water to remove any soil that accumulated in the stem. The nozzle was then lowered into the hole to a depth of approximately 13 ft (4.0 m) below ground surface (bgs), and pushed hydraulically to a final depth of 16.75 ft (5.10 m) bgs. The 2.8 ft (0.85 m) injection zone of the helical nozzle was positioned in the depth range from 10.1 to 12.9 ft (3.08 – 3.93 m) bgs. In order to provide a pressure seal, the nozzle was grouted from a depth of approximately 4 ft (1.2 m) bgs to the soil surface.

5.2.2.2 Movable Nozzle: To install the movable nozzle system, the nozzle and piping were pre-assembled prior to drilling. Installation began with augering a 2.25 in. (5.72 cm) HSA to approximately 4 ft (1.2 m) bgs. A 4 in. (10.2 cm) O.D. X 4.0 ft (1.2 m) long casing was then installed in the hole to prevent surface collapse during nozzle installation. The movable nozzle was then pushed to a depth of 13 ft (4.0 m) using a drill rig, with the exit port facing north for the first injection. Following each injection, the nozzle was rotated 90 degrees clockwise for the next injection. Upon completion of four injections at the same depth (N, E, S, W), the nozzle was then raised one foot and the process repeated for the next injection level.

5.2.3 Media Injections

5.2.3.1 Fifteen Port Helical Nozzle: Media injections were first conducted through the 15 Port Helical Nozzle. As discussed previously (section 4.3.1), there were three depth intervals of one foot each, with five injection ports per interval zone. Injections began with the deepest interval, and progressed to the shallowest interval. Operational

parameters for each injection were recorded including the time duration, flow rate, surface heave and pressure influence to surrounding monitor points. A complete listing of the injection data for the 15 Port Helical Nozzle is provided as Table 5.2.

On account of clogging, injections were not performed through two injection ports (positioned 12.5 ft (3.8 m) and 12.1 ft (3.7 m) bgs., respectively). Therefore, thirteen media injections were performed instead of fifteen. The air flow rates for the injections ranged from 208 to 892 ft³/min. (1.6 to 7.0 liters/min.). The flow rate of the beads was more consistent, varying between 96 and 178 lbs./min (43.5 and 80.7 kg/min.). The weight of the media injected per port varied between 58 lbs. (26.3 kg) and 91 lbs. (41.3 kg), with an average weight per injection of 78 lbs. (35.4 kg). The total weight of media injected into the formation through the 15 Port Helical Nozzle was approximately 1,000 lbs (454 kg). It is noted that air volumes for the injections performed on 4/25/98 are not available since a regulator had not yet been installed on the compressed air source.

Pressure influence at the surrounding monitor wells was recorded after each injection. The wells were equipped with maximum indicating gauges which recorded the peak pneumatic pressure observed during the injection. As the data in Table 5.2 indicate, once pressure influence was established with well 08-WL-64 during the first injection and pneumatic connection was subsequently observed for all the other injections, regardless of the direction of the injection port. The maximum observed pressure at the well was 7.4 psi (0.52 kg/cm²) (first injection) while the average pressure was 3.3 psi (0.23 kg/cm²). It is noted that pressure influence was not observed at any of the other three monitoring points during any of the injections which ranged from 5 to 31 ft (1.5 to 9.4 m) from the injection well.

Table 5.2 15 Port Helical Nozzle Injection Data

Injection Data								Surface Heave Measurements						Pressure Influence			
Inj. Port	Depth from Surf. (ft)	Time of Inj.	Length of Inj. (sec.)	Ft ³ Air Used	Flow Rate Air (CFM)	Flow Rate Beads (lbs/min)	Weight Beads Injected (lbs.)	Transit #1		Transit #2		Transit #3		08WL62	08WL63	08WL64	08WLY12
								Max. Surf. Heave (in.)	Resid. Surf. Heave (in.)	Max. Surf. Heave (in.)	Resid. Surf. Heave (in.)	Max. Surf. Heave (in.)	Resid. Surf. Heave (in.)				
4/25/98																	
C4	12.7	NA	NA	NA	NA	NA	85	16/16	10/16	1 4/16	4/16	16/16	8/16	0	0	7.4	NA
C2	12.3	17:08	35	NA	NA	127	74	10/16	3/16	10/16	3/16	7/16	1/16	0	0	1.8	NA
B4	11.7	17:45	45	NA	NA	104	78	9/16	2/16	6/16	8/16	7/16	1/16	0	0	5.0	NA
B3	11.5	18:05	34	NA	NA	161	91	5/16	1/16	5/16	1/16	3/16	0	1	0	3.6	NA
B2	11.3	18:15	28	NA	NA	184	86	8/16	2/16	6/16	1/16	6/16	0	0	0	3.3	NA
B1	11.1	18:21	30	NA	NA	128	64	12/16	2/16	12/16	2/16	1 4/16	2/16	0	0	4.4	NA
A5	10.9	18:30	NA	NA	NA	NA	89	8/16	2/16	9/16	1/16	8/16	0	0	0	3.0	0
A2	10.3	19:05	30	NA	NA	148	74	10/16	1/16	9/16	2/16	8/16	3/16	0	0	3.4	0
A1	10.1	19:13	25	NA	NA	194	81	4/16	1/16	4/16	1/16	7/16	0	0	0	2.2	0
4/27/98																	
C5	12.9	10:29	25	278	666	178	74	4/16	0	7/16	3/16	4/16	2/16	0	0	2.5	0
B5	11.9	11:48	42	624	892	96	67	11/16	6/16	13/16	8/16	9/16	2/16	0	0	3.2	0
A4	10.7	11:55	40	139	208	135	90	0	0	0	0	0	0	0	0	1.7	0
A3	10.5	13:15	35	208	357	99	58	2/16	0	2/16	0	3/16	0	0	0	3.4	0

Surface heave data were recorded at three points with engineering levels. Level #1 was positioned to monitor the casing of the injection nozzle. Level #2 was moved for each injection to monitor the ground surface at a horizontal distance of 2.0 ft (0.61 m) from the respective injection port. Level #3 monitored the ground surface at a fixed point, 3.8 ft (1.16 m) due north of the nozzle. During each injection the maximum surface heave was recorded, as well as the residual surface created by the injection of the media into the formation.

A maximum heave of 1.0 in. (2.54 cm) was observed on the casing (Level #1) as a result of the first injection, followed by a residual surface heave of 0.63 in. (1.6 cm). Overall, the average maximum and residual heaves recorded on the casing were approximately 0.48 in. and 0.14 in. (1.22 and 0.36 cm), respectively. The total cumulative heave for the casing as a result of all the injections was approximately 1.8 in. (4.6 cm). The maximum heave recorded at the monitoring point located 46 in. (116.8 cm) north of the casing (Level #3) was 1.25 in (3.2 cm). Average maximum and residual heaves recorded at this point were 0.45 in. and 0.09 in. (1.14 and 0.23 cm), respectively, and the total cumulative residual surface heave was approximately 1.1 in. (2.79 cm). It is noted that the total cumulative heave was estimated by adding the net residual surface heave from each injection.

5.2.3.2 Movable Nozzle: Once the conductive lenses were created with the 15 Port Helical Nozzle, injections were performed with the movable nozzle. The procedure was similar, except the injections were completed more rapidly, since connections to individual delivery tubes were not required. As described in section 5.2.2.2, the movable

nozzle was initially pushed into the formation to a depth of 12 ft (3.7 m) bgs. Once injections were completed at this level, the nozzle was raised approximately one foot (0.3 m). This process was continued until all of the injections were completed. Four injections were performed per level for the lowest three intervals, in the direction of north, east, south, and west. At the shallowest interval (8.9 ft, or 2.7 m), two injections were performed in the direction of southeast and southwest. A total of 14 injections were completed using the movable nozzle.

At the deepest interval (12 ft bgs) (3.7 m), the injection flow rates were similar to that of the 15 Port Helical Nozzle. However, for next three intervals, it was decided to inject the media at higher flow rates to determine if longer conductive lenses would be created. At these three intervals, the air flow rates were approximately 1,100 to 1,560 ft³/min. (8.7 to 12.3 liters/min.). During these injections, the weight of beads delivered into the formation were comparable to that of the 15 Port Helical Nozzle. Approximately 935 lbs. (424.5 kg) of media were injected into the formation through the movable nozzle with an average weight per injection of 67 lbs. (30.4 kg). Details for each injection are provided in Table 5.3.

During the media injections with the movable nozzle, pressure influence was recorded at monitor points 08-WL-66, 08-WL-67 and 08-WL-68 using maximum indicating pressure gauges. Monitor point 08-WL-66 was located approximately 15 ft (4.6 m) southeast from the injection nozzle, well 08-WL-67 was approximately 10 ft (4.5 m) southwest, and well 08-WL-68 was 5 ft (2.27 m) north. Pneumatic connection was observed at 08-WL-67 and 08-WL-68 during all the injections. Pneumatic connection was observed at 08-WL-66 for 12 of the 14 injections. The maximum pressure recorded

Table 5.3 Movable Nozzle Injection Data

Injection Data							Surface Heave Measurements						Pressure Influence		
Inj. Depth and Direct.	Time of Inj.	Length of Inj. (sec.)	Ft3 Air Use	Flow Rate Air (CFM)	Flow Rate Beads lbs/min	Weight Beads njecte (lbs.)	Transit #1		Transit #2		Transit #3		08WL67	08WL66	08WL68
							Max. Surf. Heave (in.)	Resid. Surf. Heave (in.)	Max. Surf. Heave (in.)	Resid. Surf. Heave (in.)	Max. Surf. Heave (in.)	Resid. Surf. Heave (in.)			
4/27/98															
12' W	15:56	32	405	759	152	81	10/16	3/16	10/16	4/16	10/16	3/16	5.5	6.3	7
12' N	16:15	30	278	555	172	86	NA	NA	9/16	3/16	9/16	3/16	7	5	9
12' E	16:27	25	197	472	168	70	NA	NA	4/16	1/16	5/16	0	5.8	4.5	6.5
12' S	16:32	20	150	451	159	53	NA	NA	1/16	0	2/16	0	3.8	0	6
4/28/98															
0' 11.5"	9:45	NA	694	NA	NA	80	NA	NA	8/16	1/16	8/16	3/16	6.5	5.4	7.8
0' 11.5"	9:50	23	353	920	183	70	8/16	-2/16	7/16	0	5/16	0	6.8	4	6
0' 11.5"	9:58	NA	590	NA	NA	81	NA	NA	9/16	1/16	7/16	1/16	6.5	3.5	6.5
10' 11" E	10:20	20	173	520	192	64	NA	NA	1/16	0	1/16	0	6.5	0.6	6.5
9' 11" E	11:30	25	468	1124	137	57	NA	NA	9/16	1/16	7/16	1/16	4.2	0.5	4
9' 11" S	11:35	33	694	1262	115	63	NA	NA	12/16	0	8/16	0	5	2	3.8
9' 11" W	11:40	28	590	1264	156	73	NA	NA	15/16	3/16	10/16	1/16	4.5	1.8	4
9' 11" N	11:45	38	746	1178	95	60	NA	NA	10/16	1/16	10/16	0	4	2	4.8
8' 11" SE	11:55	34	781	1378	109	62	NA	NA	9/16	1/16	8/16	0	3.2	1	3.4
8' 11" SW	12:05	30	781	1561	70	35	NA	NA	10/16	0	8/16	0	1.8	0	1.2

at 08-WL-66 was 6.3 psi (0.4 kg/cm²) which occurred as a result of the first injection, while the average pressure influence at this monitor point was 2.6 psi (0.18 kg/cm²). The maximum pressure recorded at 08-WL-67 was 7.0 psi (0.49 kg/cm²), and the average pressure influence was 5.1 psi (0.36 kg/cm²). The maximum pressure recorded at 08-WL-68 was 9.0 psi (0.63 kg/cm²), and the average pressure influence was 5.5 psi (0.39 kg/cm²).

Surface heave data were also recorded for the movable nozzle with three engineering levels. Level #1 was positioned to monitor the casing during the injection process. Level #2 monitored the ground surface 4.85 ft (1.48 m) west of the injection nozzle, while Level #3 monitored the ground surface 7.3 ft (2.2 m) east of the injection nozzle. Surface heave data were recorded for all the injections at Levels #2 and #3. It is noted that surface heave data for Level #1 is available for two of the injections.

The maximum surface heave recorded at Level #2 (4.85 ft west of the injection nozzle) was 0.94 in. (2.39 cm), while the average maximum surface heave for all the injections was 0.51 in (1.30 cm). The cumulative residual surface heave at this location was approximately 1.0 in. (2.54 cm). It is noted that during the injections residual surface heave was not always detectable if it was less than 0.06 inches (0.15 cm). For Level #3 (7.3 ft east of the injection nozzle), the maximum surface heave varied between 0.06 to 0.6 in. (0.15 to 1.5 cm), and the average for all the injections was 0.44 in. (1.11 cm). The total cumulative residual surface heave was 0.75 in. (1.91 cm) at this location.

5.2.4 Recovery Well Installation

5.2.4.1 Installation of Recovery Well 08-WL-70: Once the media were injected and high permeability conductive lenses were created, the 15 port helical injection nozzle was removed and a recovery well installed in its place. Recovery well 08-WL-70 was constructed removing the 15-Port Helical Nozzle from the formation and simultaneously filling the hole with revert and water to prevent collapse. A pre-assembled four inch PVC recovery well with 7.2 ft (2.19 m) long screen of 0.020 slot was placed into the hole, and #0 sand was packed around the well. The sand pack established connection between the well and the surrounding conductive lenses. A 1.34 ft (0.41 m) bentonite seal was installed above the sand pack, then the well was grouted to the surface. A construction log of recovery well 08-WL-70 is contained in Appendix F.

5.2.4.2 Installation of Recovery Well 08-WL-69: In order to complete recovery well 08-WL-69, the Movable Nozzle was removed with a drill rig and the hole was enlarged using a 8.25 in. I.D. (10 in. O.D.) HSA. A pre-assembled four inch PVC recovery well with 7 ft (2.1 m) long screen of 0.020 slot was installed in this hole, and the annular space was filled with #0 sand pack. A 1.0 ft (0.30 m) bentonite seal was placed in the upper casing and then grouted to the surface. Appendix F provides a construction log for recovery well 08-WL-70.

5.3 Field Demonstration Results

Once ERWs were converted to recovery wells, long term pumping tests to recover free product were performed by the site consultant. The free product recovery system

consisted of a skimmer pump, controller with battery, electronic timer, 55 gallon collection drum, and infrared tank sensor. The skimming pumps were ADJ 1000 Smart Skimmer pumps manufactured by Xitech Instruments. The pumps are equipped with hydrophobic membranes which prevent the capture of any groundwater and permit only free product to be recovered.

In order to evaluate the enhancement by ERWs, the pump test results were compared to a standard recovery well. Well 08-WL-65, which is located within the free product plume, was chosen as the baseline well. Pump tests on this well yielded a product recovery rate of approximately 0.4 gallons per day (gpd) (1.5 liters/day), which was comparable to previous testing of other recovery wells in the plume. It is noted that the average thickness of the plume at this well was 0.5 ft (0.17 m.).

5.3.1 Results for Recovery Well 08-WL-70 (Helical Nozzle Setting)

The pump test results for recovery well 08-WL-70 are presented in Figure 5.2. Over a 42 day period, a total of 55 gallons (208 liters) of free product were collected. Initial recovery rates averaged 1.3 gpd (4.92 liters/day) for the first 19 days, then tapered off to approximately 1.0 gpd (3.79 liters/day) for the remaining 23 days of the test . On average, this ERW demonstrated a 225% enhancement compared with the baseline recovery well 08-WL-65 (1.3 vs. 0.4 gpd).

5.3.2 Results for Recovery Well 08-WL-69 (Movable Nozzle Setting)

The pump test results for recovery well 08-WL-69 are presented in Figure 5.2 Over the 85 day test, a total of 147 gallons (556.4 liters) of free product were collected. On

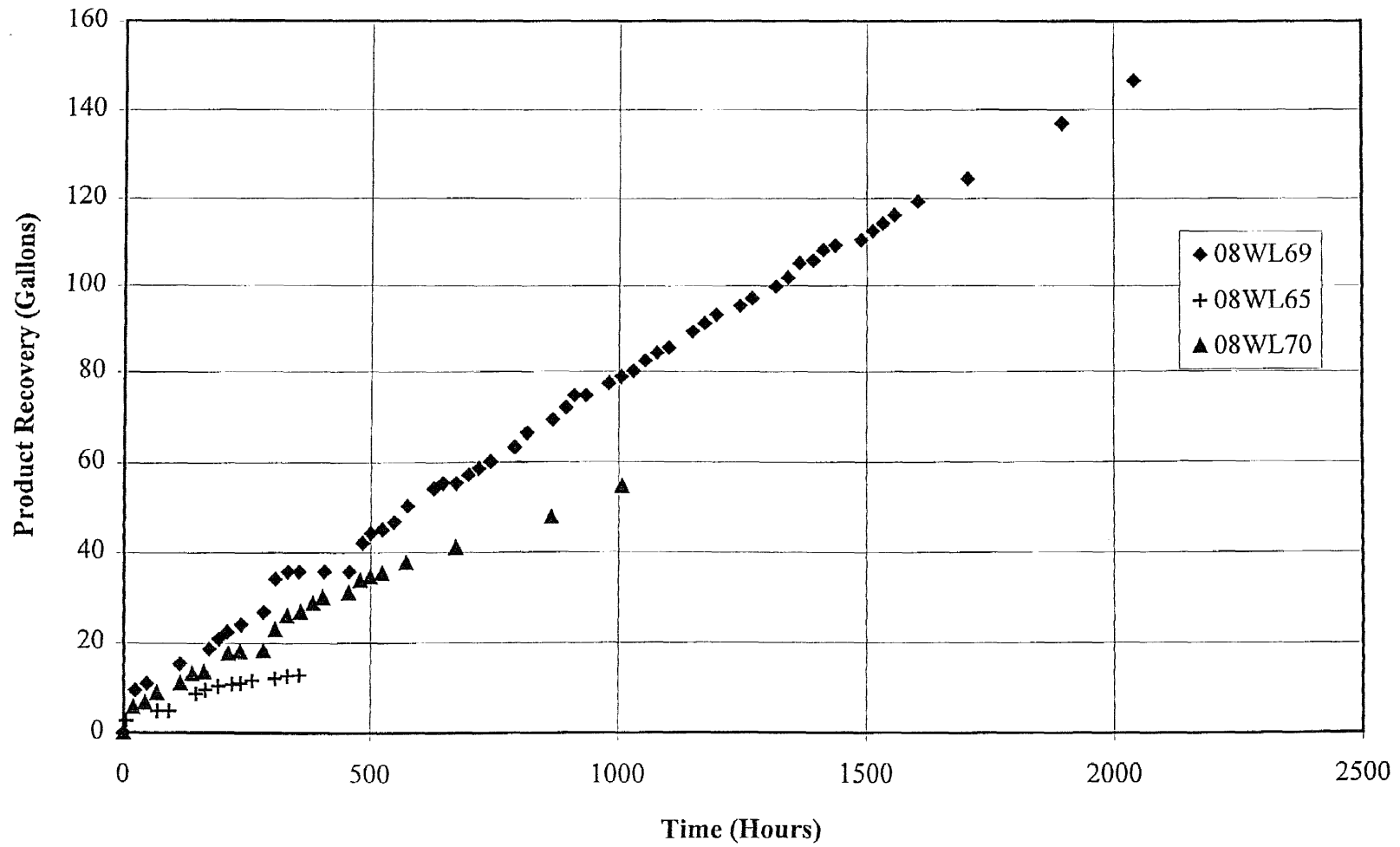


Figure 5.2 Free Product Recovery at 08-WL-69, 08-WL-70 and 08-WL-65

average, this ERW demonstrated a recovery rate of 1.7 gpd (6.5 liters/day) for this period, or a 325% enhancement compared with the baseline recovery well 08-WL-65. This higher enhancement of this well as compared to the other ERW (recovery well 08-WL-70) is primarily attributed to its location, since it is located closer to the source area.

5.3.3 Geoprobe Soil Sampling

5.3.3.1 Geoprobe Boring Description and Locations: In order to more effectively define the radius of influence of the conductive lenses for each ERW, soil samples were collected using a Geoprobe around recovery wells 08-WL-69 and 08-WL-70. Geoprobe sampling was performed with a retractable boring tip equipped with 1.5 inch (3.8 cm) diameter by 4.0 ft (1.2 m) long acetate sleeve and a sand catcher. This configuration assured that samples were collected at discrete intervals and also minimized loss of soil and media. Once the geoprobe pushed the sampling sleeve to the top of the sample interval, a long metal rod was advanced to the retractable tip. The rod unthreaded the tip, allowing it to push up through the acetate sleeve during the sampling process.

Geoprobe sampling was conducted during the period July 23 through July 27, 1998. A total of 28 geoprobe borings were accomplished, 14 around each of the injection wells. Sampling depths varied between 1 and 15 ft (0.3 and 4.6 m) below grade. The labeling convention for the borings was GP (for Geoprobe) followed by H or M (for Helical or Movable Nozzle), and finally 1 through 31 representing the particular probe number. The probings were at a radii varying between 14 and 96 inches (35.6 and 243.8 cm) measured from the center of the recovery well. A location plan for the geoprobe borings is depicted in Figures 5.3 and 5.4. After the samples were collected, they were

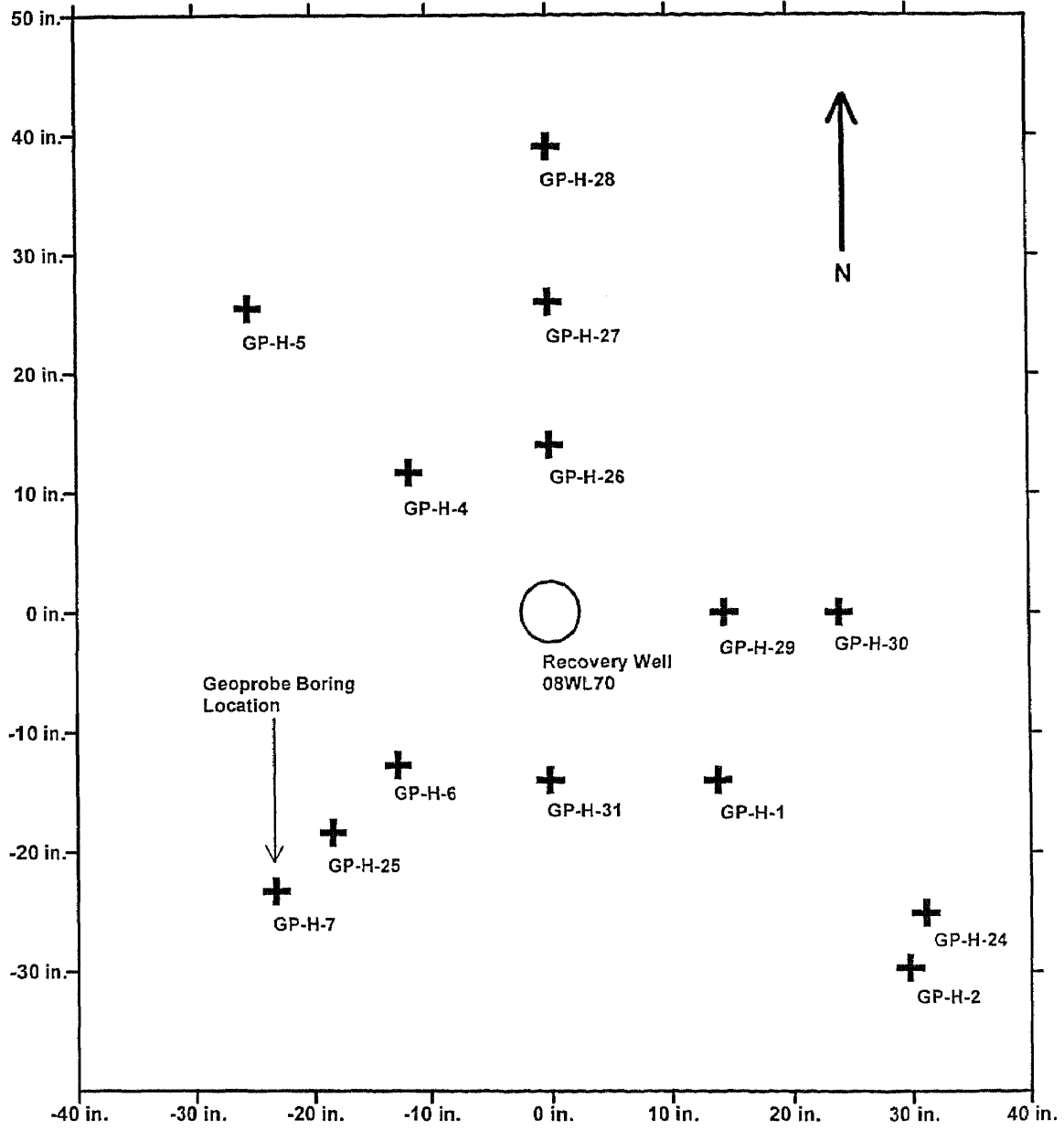


Figure 5.3 Geoprobe Boring Locations Around Recovery Well 08-WL-70 (Helical Nozzle)

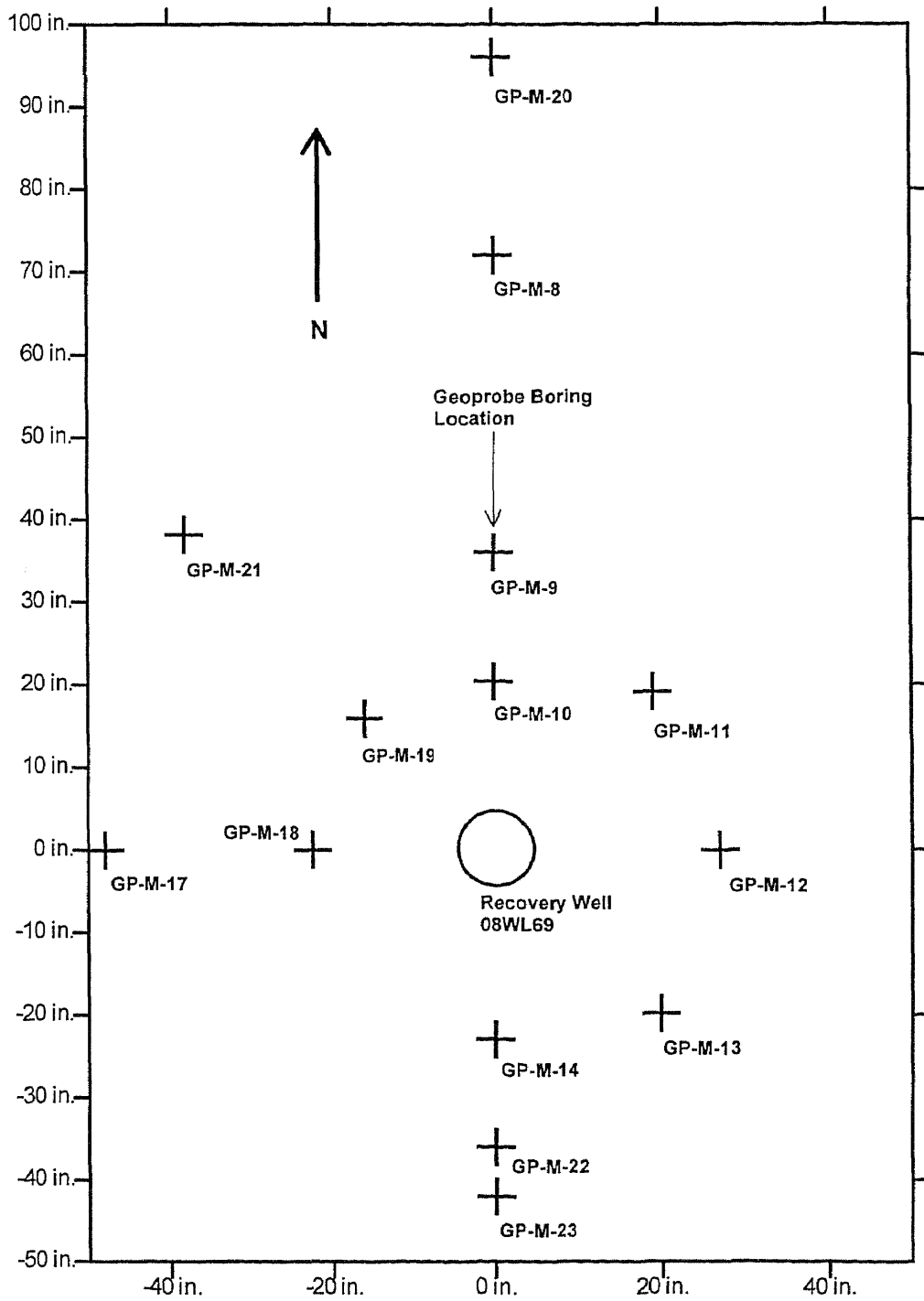


Figure 5.4 GeoProbe Boring Locations Around Recovery Well 08-WL-69 (Movable Nozzle)

sealed and shipped to the NJIT laboratory. At the laboratory, the samples were logged to record the geologic strata, as well as the presence of bead media. Of particular interest was the packing thickness, density and purity of the media lenses. The following convention was used to describe the occurrence of beads in the samples:

- Parting a layer 0 to 1/16 in. thick
- Seam a layer 1/16 to 1/2 in. thick
- Layer 1/2 to 12 in. thick
- Stratum a layer greater than 12 in. thick
- Lens lenticular shaped inclusion not extending through the entire soil boring

5.3.3.2 Geoprobe Boring Results: Results of the Geoprobe borings conducted around recovery well 08-WL-70 indicated the geology as well as the presence of discrete conductive lenses. A boring log showing both the geologic strata and media description of the beads, when present, was prepared for each geoprobe sample and is included in Appendix G. From grade to a depth of approximately 5 ft (1.7 m) bgs, the soil consisted of light brown to yellow sand. Below this sand, light brown to brown clay of moderate plasticity was encountered which also contained some organics in the form of small twigs and roots. This is believed to be backfilled material, which was placed on top of the native soil during previous construction activities. In the free product layer (between 9 to 11 ft bgs) the clay was stained black and the clay was more brittle with a lower plasticity. Below the free product layer, the soil abruptly changed to a light brown silty fine sand. Odors of free product were present in the sand below the clay stratum.

Cross sections of the geoprobe borings around Recovery Well 08-WL-70 are presented in Figures 5.5 through 5.8. These drawings are scaled and indicate the location of the geoprobe borings, sampling interval and the beads, when present. Most of the media was observed as discrete 1/8 to 1/4 in. (0.32 to 0.64 cm.) seams with few formation particles between them. Frequently bead seams occurred at the interface of the clay layer (above) and sand layer (below). Seams of beads were also noted through the both the clay layers and silty fine sand. The thickest occurrence of beads was noted in GP-H-29 at 13 ft (4.0 m) bgs, where a 3.0 to 3.5 in. (7.62 to 8.89 cm) layer of beads was observed, which was located 14.5 in. (36.8 cm) east of the recovery well.

It is noted that in two of the soil borings, GP-H-28 and GP-H-30, discrete seams of beads were observed at approximately 3.0 and 3.5 ft (0.9 and 1.07 m) bgs., respectively. The presence of media at these shallow depths indicated that the air and injected media followed the path of least resistance up through a loose zone in the backfill.

Results of the soil borings drilled around recovery well 08-WL-69 also indicate the presence of discrete conductive lenses in the subsurface. Logs of these samples are provided in Appendix G. Although recovery well 08-WL-69 was only 60 ft (18.3 m) from recovery well 08-WL-70, the geology was noticeably different in the 6 to 10 ft (1.8 to 3.0 m) zone where most of the samples were taken. The soil near 08-WL-69 mainly consisted of light brown to tan silty fine sand and brown to light brown clay. Other soil types which were observed in trace amounts, including clayey sand and organic silt.

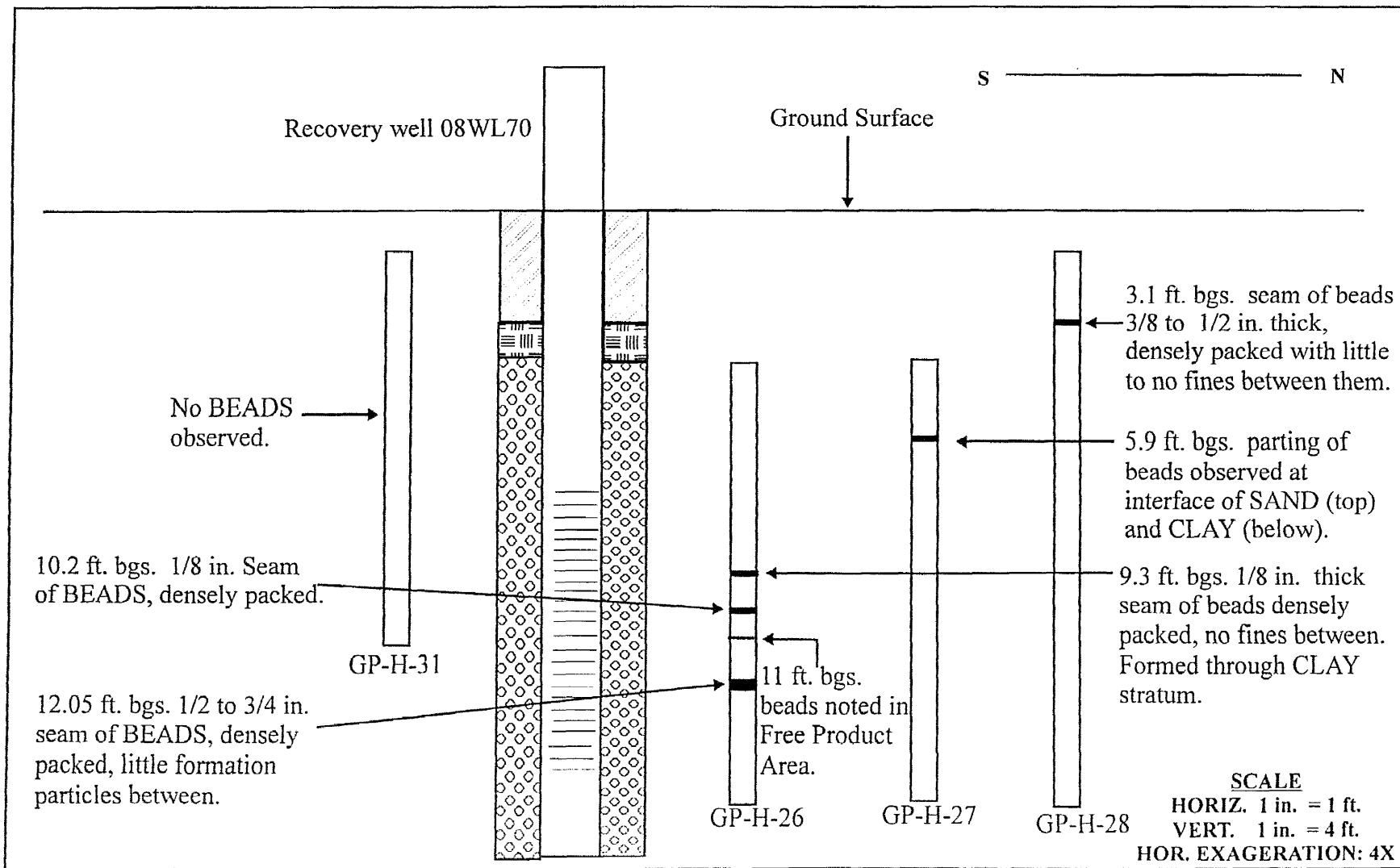


Figure 5.5 Helical Nozzle Geoprobe Borings (recovery well 08-WL-70), North/South subsurface section

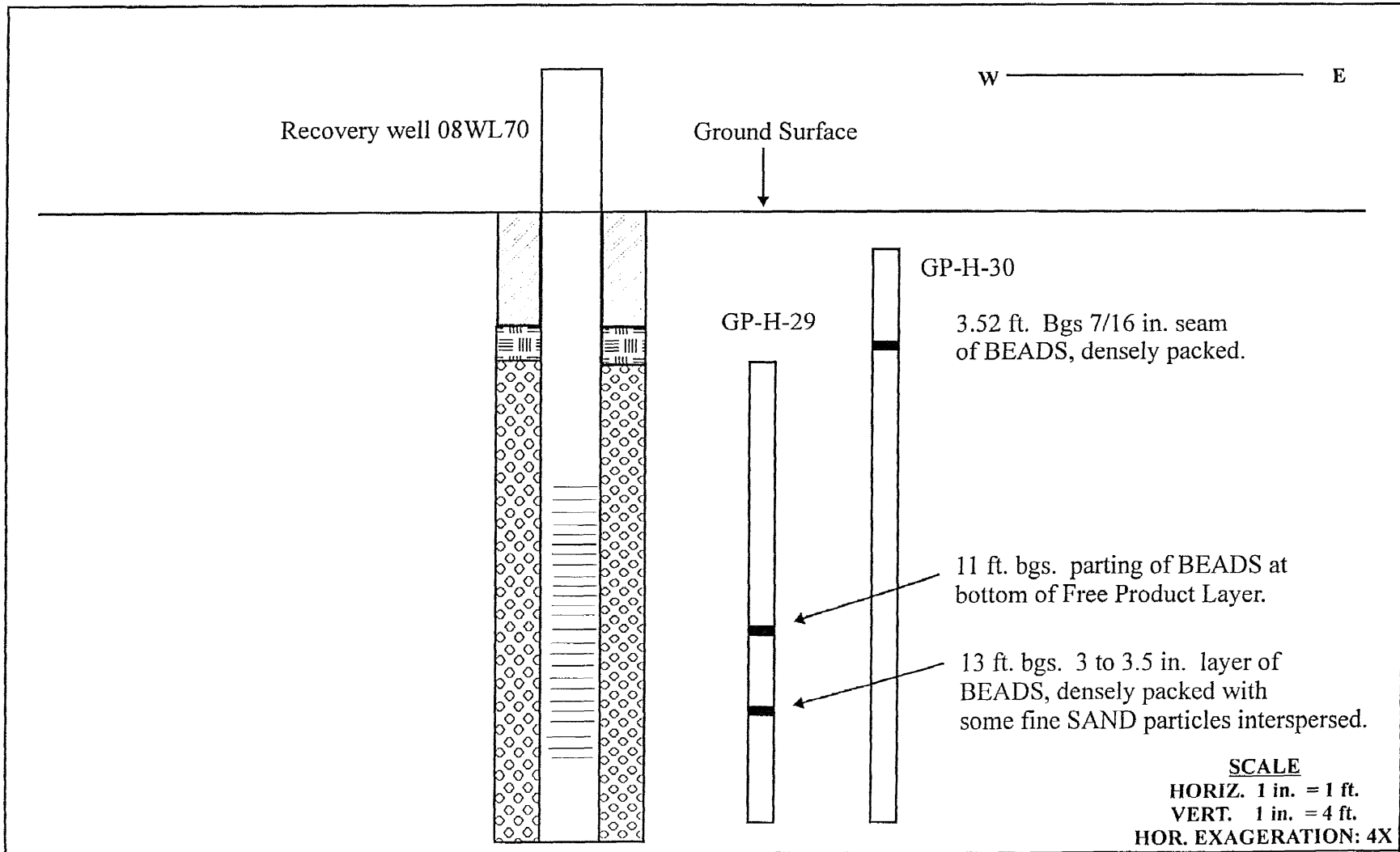


Figure 5.6 Helical Nozzle Geoprobe Borings (recovery well 08-WL-70), East/West subsurface section

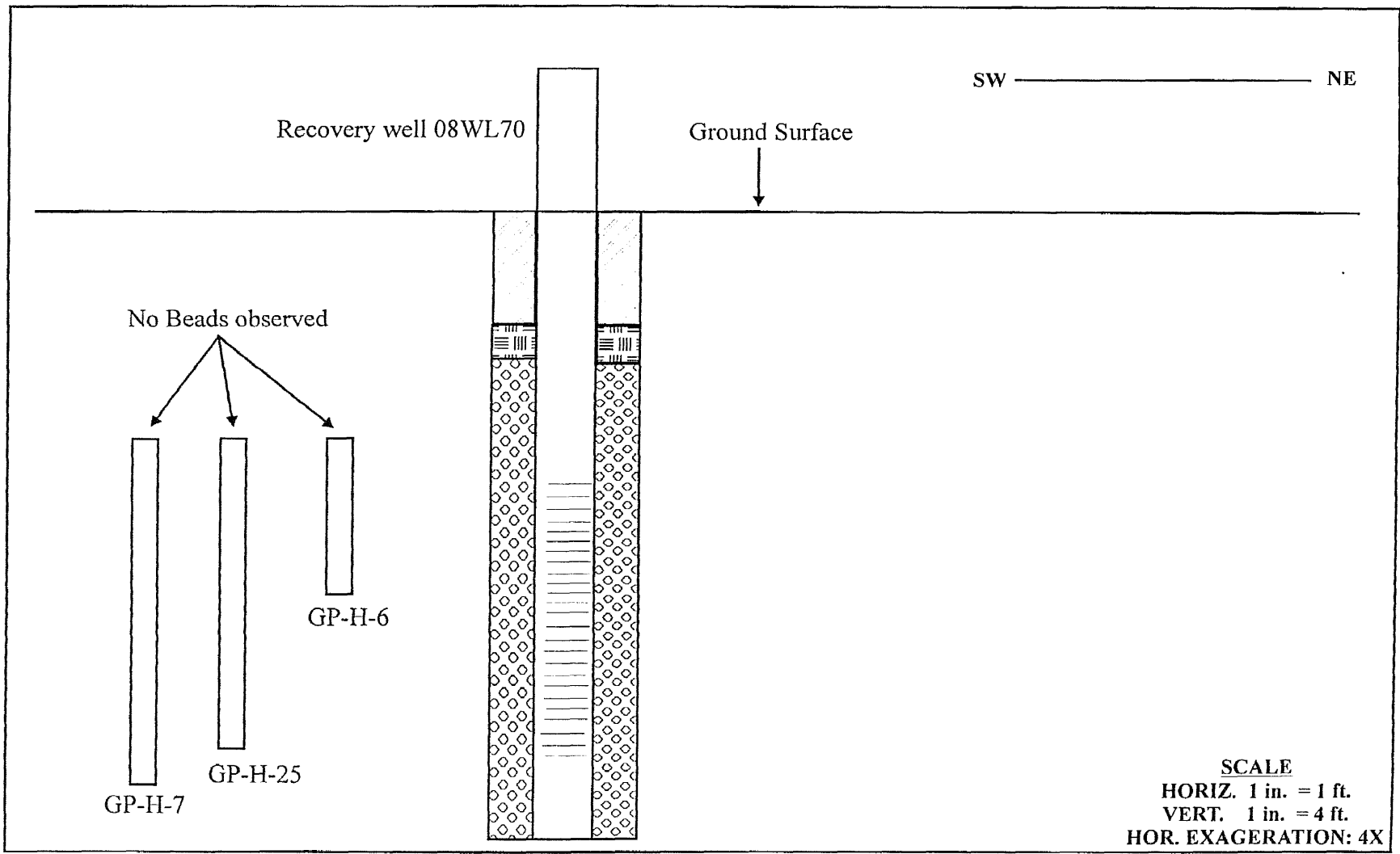


Figure 5.7 Helical Nozzle Geoprobe Borings (recovery well 08-WL-70), Southwest/Northeast subsurface section

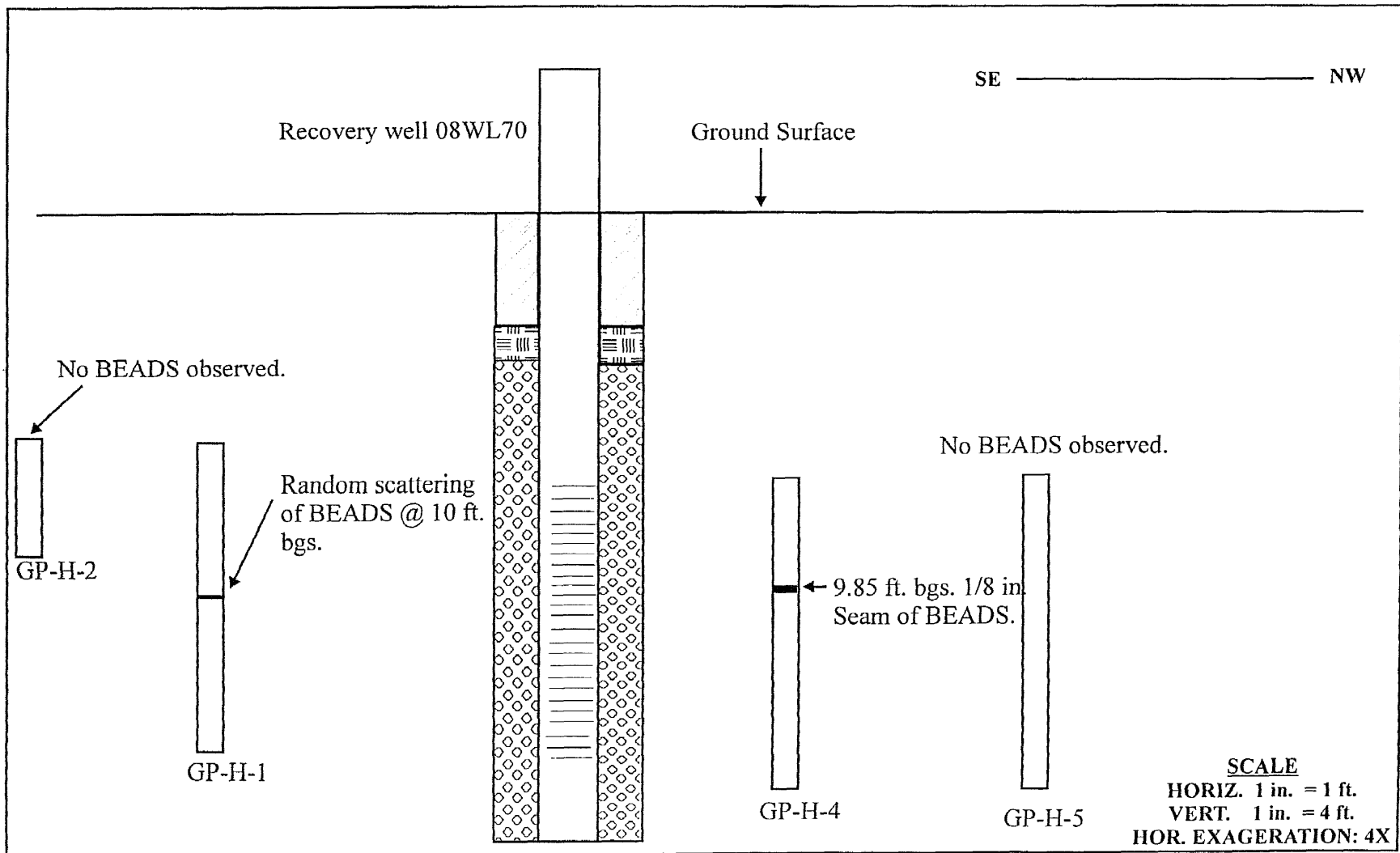


Figure 5.8 Helical Nozzle Geoprobe Borings (recovery well 08-WL-70), Southeast/Northwest subsurface section

Cross sections of the geoprobe borings around recovery well 08-WL-69 are depicted in Figures 5.9 through 5.12. As these figures indicate, beads were consistently observed 24 in. (61 cm) from recovery well 08-WL-69. A maximum influence radius of 54 in. (137.2 cm) occurred at GP-M-21, where a random scattering of beads was observed from 10.5 to 11 ft (3.2 to 3.4 m) bgs. Once again, discrete bead seams were frequently observed as at the interface between sand and clay layers, suggesting that the media traveled preferentially along strata boundaries which are often planes of weakness within the formation. At these locations, the beads were densely packed, with few formation particles between the beads, and the thickness averaged 1/8 to 1/4 in (0.32 to 0.64 cm). Occasionally, discrete seams of beads were also observed to cross both sand and clay layers. In addition to discrete seams of relatively pure media, some seams of beads were well mixed with native soil, especially in the silty fine sand layers.

5.3.4 Cost Analysis of ERWs at Field Pilot Test Site

A cost analysis was accomplished to compare the ERW concept with conventional recovery wells for the field pilot test site. The plume is estimated to cover an area of 5 acres and it contains approximately 400,000 gallons (1,514,120 liters) of free product in the depth range from 9 to 12 ft (2.7 to 3.7 m) bgs. The site consultant has estimated that if conventional recovery wells are used, the well spacing would be 15 ft (4.6 m), resulting in a total of 660 wells to recover the plume. The estimated clean-up time with conventional well is 30 years. However, if ERWs are installed at the site, it is estimated that the well spacing could be increased to 30 ft (9.1 m) resulting in 165 ERWs to treat

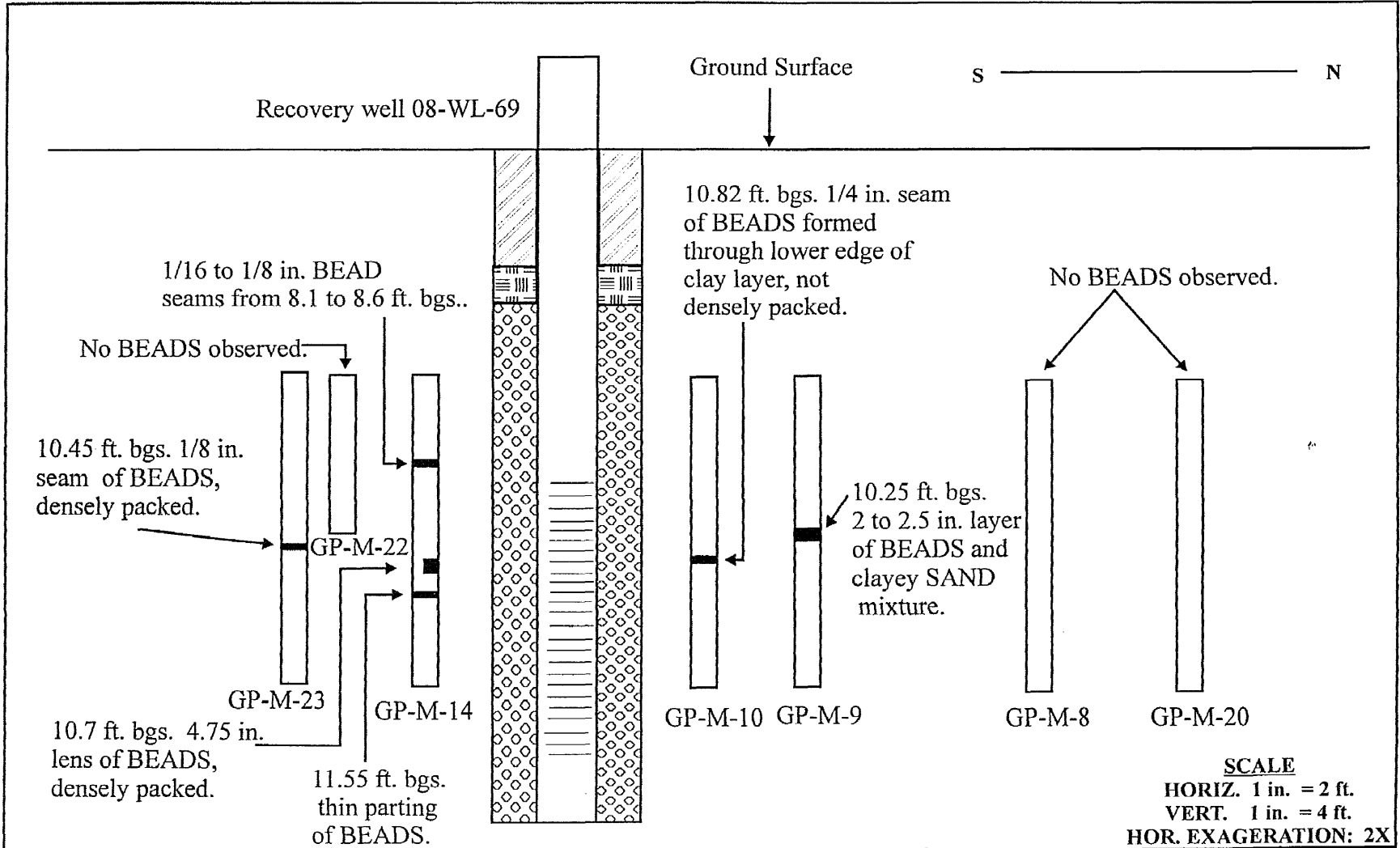


Figure 5.9 Movable Nozzle Geoprobe Borings (recovery well 08-WL-69), North/South cross section

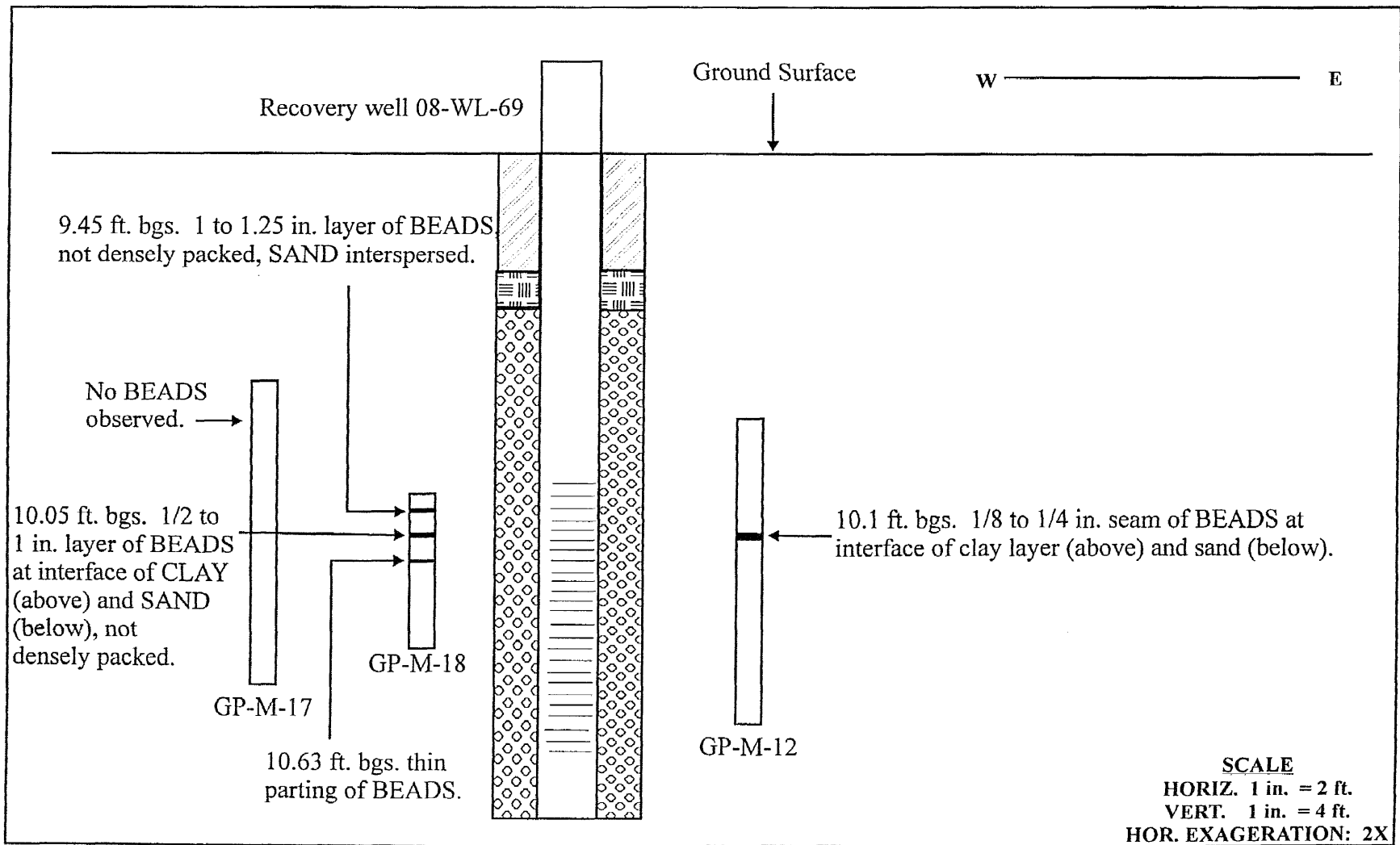


Figure 5.10 Movable Nozzle Geoprobe Borings (recovery well 08-WL-69), East/West cross section

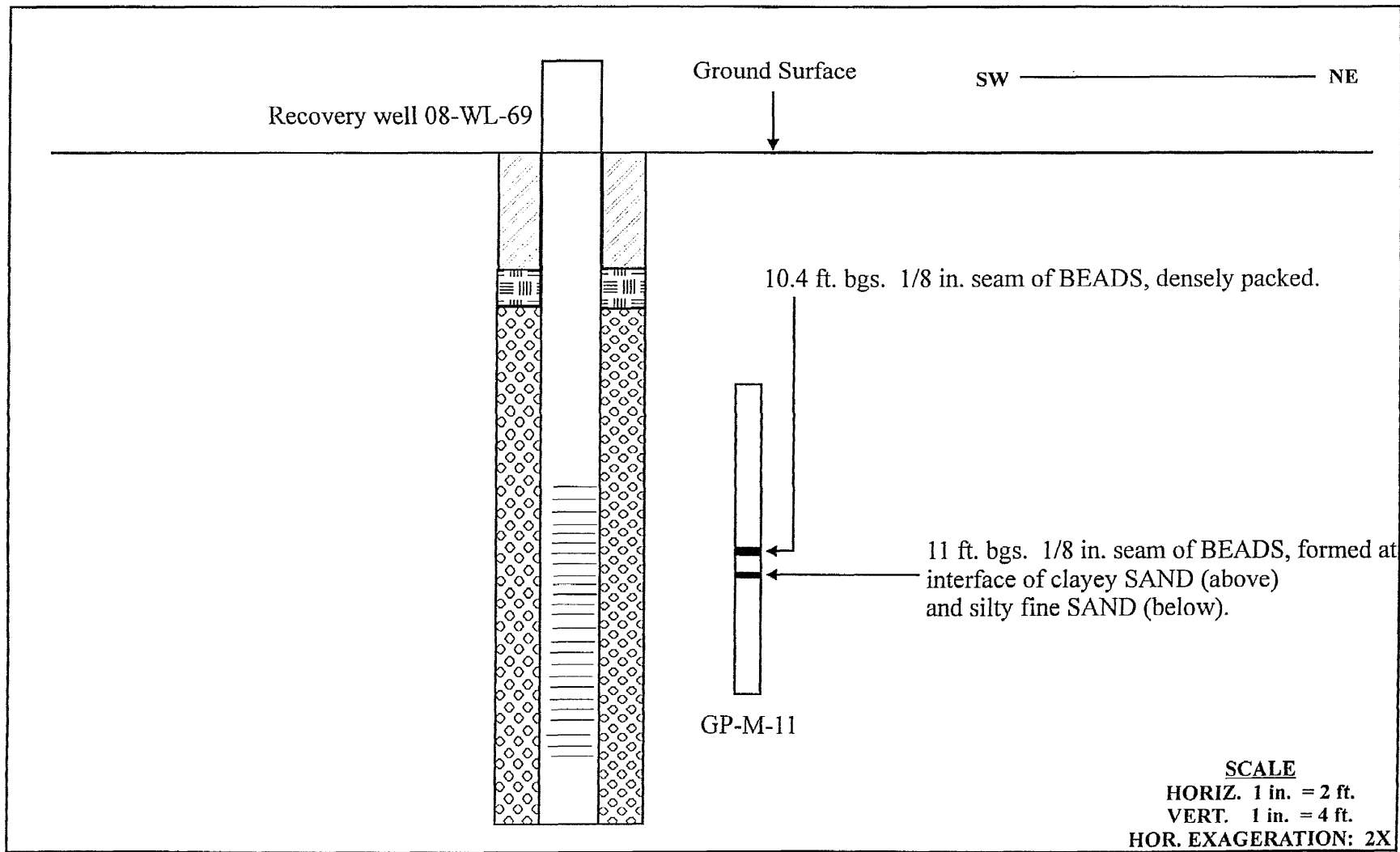


Figure 5.11 Movable Nozzle Geoprobe Borings (recovery well 08-WL-69), Southwest/Northeast cross section

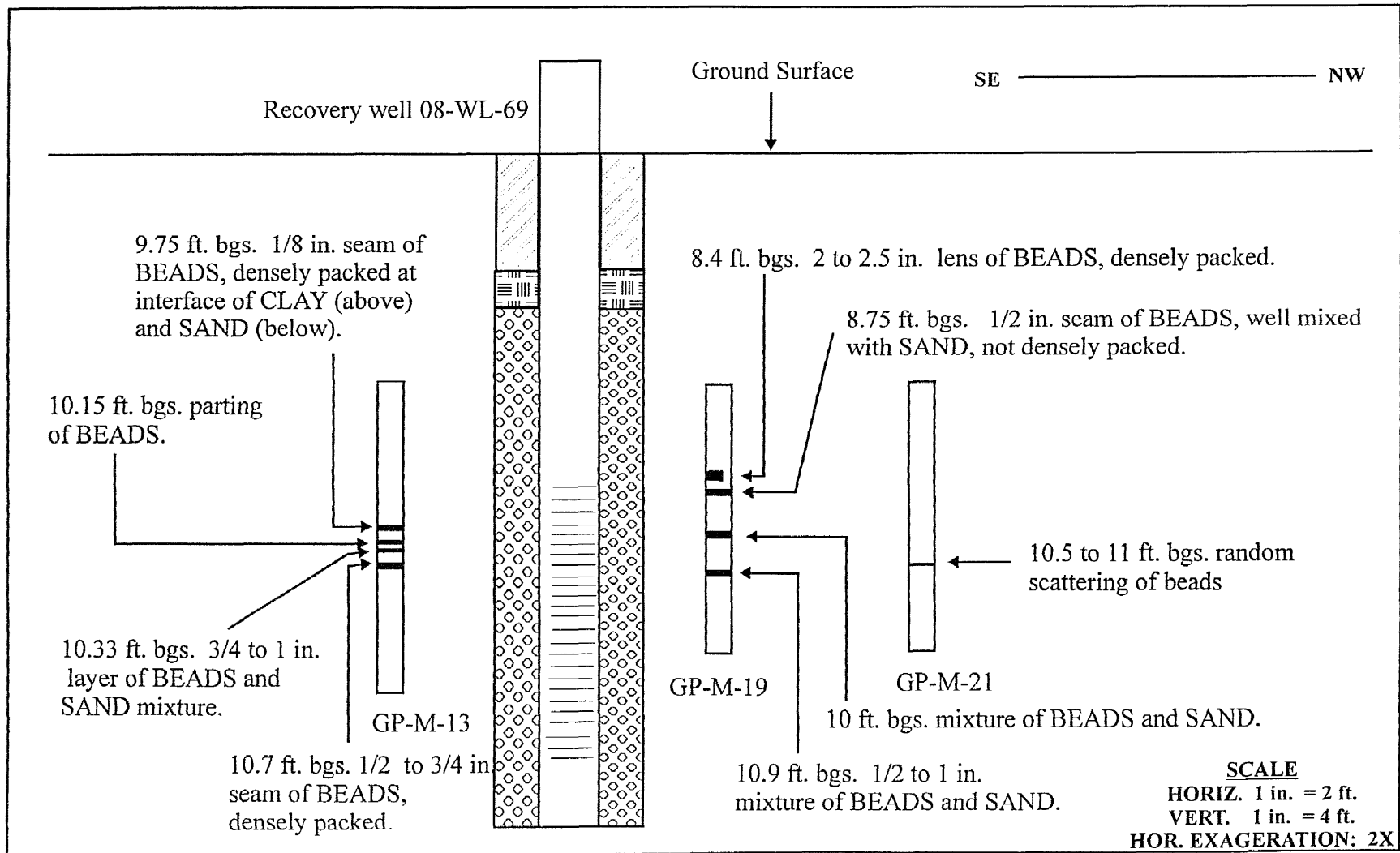


Figure 5.12 Movable Nozzle Geoprobe Borings (recovery well 08-WL-69), Southeast/Northwest cross section

the 400,000 gallon (1,514,120 liters) plume. In addition, the clean-up time would be reduced to 10 years.

A cost analysis comparing ERWs to conventional recovery wells is presented in Table 5.4. Both technologies include capital costs, design and construction oversight, labor, and operation and maintenance.

Table 5.4 Economic Cost Analysis of ERWs vs. conventional recovery wells

ERW (10 year projected Cleanup) 30 ft well spacings, 165 ERW's to treat 400,000 gallon plume.		Conventional Recovery Well (30 year Projected Cleanup) 15 ft well spacings, 660 recovery wells to treat 400,000 gallon plume	
Media Injections	\$742,500		
Recovery well installation (165)	\$1,140,000	Recovery well installation (660)	\$4,560,000
Capital Equipment	\$804,750	Capital Equipment	\$2,339,250
Engineering Design & Construction Oversight	\$513,725	Engineering Design & Construction Oversight	\$513,725
Operation and Maintenance (10 year period)**	\$1,069,900	Operation and Maintenance (30 year period)**	\$2,596,240
Replacement Cost (year 5)	\$303,700	Replacement Costs (years 5, 15, 25)	\$911,100
Estimated Cost to remediate Field Pilot Test Site using ERW technology (n=10)	\$4,574,575	Estimated Cost to remediate Field Pilot Test Site using conventional recovery wells (n=30)	= \$10,920,315
Estimated Total Cost Savings	\$6,345,740		
% Savings ERW technology vs. Conventional recovery wells =	$\frac{(\\$10,920,315 - \\$4,574,575)}{\\$10,920,315} \times 100 = 58\%$		
**Based upon i = 5% and 1999 dollars.			

CHAPTER 6

CONCLUSIONS AND RECOMMENDATIONS

This research study has evaluated the use of extended radius wells (ERWs) for enhancement of well recovery by injection of supplemental, high permeable media. The specific conclusions based upon the results of the bench scale experiments, engineering scale testing, and field pilot demonstration are summarized as follows;

6.1 Bench and Engineering Scale Conclusions

- 1) Laboratory investigations of ten different types of media have demonstrated that uniformly-graded ceramics beads are preferred for use as a conductive lens in an ERW. The ceramic beads possess high strength that enable them to withstand media degradation during the injection process. The round shape of the beads enables them to flow smoothly, and also maximizes porosity. In addition, the ceramic bead are available in a wide range of uniform sizes, which can be adapted to different geologic formations.
- 2) Bench scale injections of the ceramic beads through various nozzle types showed that nozzle geometry was more important than nozzle material. Degradational effects of galvanized pipe and sweated copper pipe were similar. However, injections using an abrupt 90 degree elbow design exhibited more degradation than the two-45 degree elbow design. These results were incorporated into the design of the 15-Port Helical Nozzle for the field demonstration.

- 3) Hydraulic conductivity testing of various sizes of ceramic beads was performed to identify the range of anticipated flow enhancement for the ERWs. Permeability tests performed on media with diameters ranging from 0.25 to 3.35 mm (0.008 to 0.01 in.) yielded hydraulic conductivity values of 0.048 to 0.320 cm/sec (0.002 to 0.01 ft/sec), respectively. For comparison, the hydraulic conductivity of the native soil at the demonstration site (silty fine sand) averaged 4.22×10^{-5} cm/sec (1.38×10^{-6} ft/sec).
- 4) Hydraulic conductivity tests were performed on various mixtures of native soil and beads. Enhancement in conductivity was not observed until the mixture contained at least 70% media. In addition to the mixture tests, the permeability of discrete columns of media placed within native soil was also measured. The hydraulic conductivity for columns measuring 0.75 and 1.0 in. (1.91 and 2.54 cm) in diameter were 0.008 and 0.015 cm/sec (2.6×10^{-4} and 5.0×10^{-4} ft/sec), respectively. This suggests strongly that densely packed media with little to no fine formation particles will achieve the greatest permeability enhancement in the ERWs.
- 5) Engineering scale testing conducted in the 20 yd³ (15.3 m³) containment vessel indicated that large quantities of media could be introduced into a geologic formation over a relatively short time interval with the PF injection process. Some discrete seams of media were formed; however, due to low compaction of the soil, frequent large air voids in the soil were formed as a result of the injections.

6.2 Field Demonstration Conclusions

- 1) Overall, the demonstration showed the ERWs were established successfully and showed enhanced recovery rates compared with conventional recovery wells. The degree of enhancement varied between each well, and was influenced by the lithology and the thickness of the free product.
- 2) Two ERWs utilizing two different nozzle designs were created by injecting the supplemental media from 9.0 to 12.7 ft (2.7 to 3.9 m) below ground surface. The nozzle designs consisted of a 15-Port Helical Nozzle and a Movable Nozzle. The observed recovery enhancements at the helical and movable nozzle locations were 225% and 325%, respectively.
- 3) A long term pumping test (85 days) on recovery well 08-WL-69 (Movable Nozzle) indicated that the free product recovery increased from 0.4 to 1.7 gpd (1.5 to 6.4 liters/day), a 325% enhancement. Recovery well 08-WL-70 (15-Port Helical Nozzle) demonstrated a 225% enhancement over a 42 day test, with an increase to 1.3 gpd (4.9 liters/day). The higher enhancements observed at recovery well 08-WL-69 (Movable Nozzle) are attributed to its closer proximity to the source area, and also to the geological differences between the two locations.
- 4) In the vicinity of recovery well 08-WL-70 (Helical Nozzle), clay backfill was placed on top of the native soil. Free product was observed in the geoprobe soil samples at the bottom of this clay stratum. Once the free product enters this clay, it becomes more difficult to recover due to its low permeability. The geology

surrounding recovery well 08-WL-69 (Movable Nozzle) consisted largely of native soil (silty fine sand), which had somewhat higher permeability.

- 5) On average, the radius of influence of the media was 2 to 3 ft (0.6 to 0.9 m), with a maximum extent of 4.5 ft (1.4 m). The average thickness of the media created within the soil was approximately 1/8 to 1/2 in. (0.32 to 1.27 cm), although seams up to 3.5 in. (8.89 cm) thick were observed. Approximately 1000 and 935 lbs. (454 and 424.5 kg) of media were injected through the Helical Nozzle and Movable Nozzle, respectively.
- 6) Both nozzle designs successfully created high permeable conductive lenses in the zone of the free product layer. The Helical Nozzle created seams that were more discrete which was attributed to the geology at that location. The Movable Nozzle was more efficient when performing the injections, as connection to individual delivery tubes was not required between each injection. From a cost perspective, each nozzle had certain advantages and disadvantages.
- 7) During media injection, maximum and residual surface heaves were monitored at three locations around each well using engineering transits. The total cumulative residual surface heave on the Helical Nozzle well casing was 1.8 in. (4.57 cm) and the total cumulative residual surface heave measured at a point located 3.8 ft (1.2 m) due north of the casing was 1.1 in. (2.79 cm). For the Movable Nozzle, the total residual surface heave was approximately 1.0 in. (2.54 cm) for a monitoring point located 4.85 ft (1.48 m) west of the casing, and the total residual surface heave of the Movable Nozzle was 0.75 in. (1.91 cm). It is noted that the total residual surface heave for each monitoring location was determined by summing

- the residual heaves from each injection. Maximum surface heaves during the injection event ranged up to 1.25 in. (3.18 cm) and averaged 0.47 in. (1.19 cm).
- 8) During the field demonstration, operational parameters were monitored including injection flow rate and pressure influence. Injections with the 15-Port Helical Nozzle injections averaged 34 sec. in duration, with an average mass input of 78 lbs. (35.4 kg) of media. For the Movable Nozzle, the injections averaged 28.5 sec. in duration with an average mass input of 67 lbs. (30.4 kg). Overall, the mass flow rate of the media varied between 70 and 183 lbs./min (31.8 and 83.1 kg/min). Pressure influence was detected at one monitor point, 5 ft (1.5 m) south of the 15-Port Helical Nozzle, and a maximum pressure of 7.4 psi (0.52 kg/cm²) was recorded. At the Movable Nozzle, pressure influences to monitor points located 10 ft (3.0 m) southwest, 15 ft (4.6 m) southeast, and 5 ft (1.5 m) north were 7.0 psi (0.49 kg/cm²), 6.3 psi (0.44 kg/cm²) and 9.0 psi (0.63 kg/cm²), respectively.
- 9) A cost benefit analysis indicated that if ERWs are installed at the field pilot test site instead of conventional recovery wells, a savings of \$6.3 million would be realized, which represents 58% savings. In addition, the estimated clean-up time would be reduced from 30 years to 10 years.

6.3 Recommendations for Future Study

The following are recommendations for future development of the ERW process:

- 1) More extensive permeability testing should be performed using different soil types (e.g., silts, silty sands, etc.) and different sizes of ceramic beads. The results of these studies could be used to develop a mathematical model for predicting

hydraulic conductivity enhancement by ERWs in a wider variety of geologic formations.

- 2) Quantitative strength testing should be performed on the ceramic beads and other screened media to better determine their physical properties.
- 3) Better compaction must be achieved in engineering scale tests to reduce the formation of large air voids during the injections. This can be accomplished by using a mechanical compactor.
- 4) Further engineering scale injections should be conducted at various flow rates and injection times followed by detailed excavations. This will allow optimization of air flows and injection time to form discrete media lenses in a controlled manner.
- 5) ERWs should be installed at additional sites to evaluate their applicability in different geologic formations.
- 6) The field pilot test have indicated that further improvements can be made to the pneumatic media injection system. These system adjustments will increase the penetration effectiveness of the conductive media lenses, and this will likely result in higher recovery rates and influence radii for future ERWs.
- 7) Further cost-benefit analyses should be undertaken to determine the economic impacts of ERWs for other site sizes and conditions.

APPENDIX A

EXTENDED RADIUS WELL VS. CONVENTIONAL 4 IN. RECOVERY WELL ENHANCEMENT CALCULATIONS

This appendix provides supporting calculations for the theoretical enhancement of an Extended Radius Well (ERW) as compared to a conventional recovery well for an unconfined aquifer of moderate permeability as described in Section 3.1.

The calculations presented in this appendix are for groundwater flow and are based on the following assumptions:

$K = 4 \times 10^{-5}$ (1.31×10^{-6})	hydraulic conductivity, cm/sec (ft/sec)
$h_{\max} = 304.8$ (10)	maximum drawdown height, cm (ft)
$h_1 = 152.4$ (5)	height #1, cm (ft)
$r_n = 10.16$ (4 in. conventional well)	effective radii of recovery well, cm
60.96 (2 ft ERW)	
91.44 (3 ft ERW)	
121.92 (4 ft ERW)	
152.40 (5 ft ERW)	

To compare the potential enhancements of an ERW, the Dupuit Forchheimer equation for unconfined aquifers was utilized;

$$Q_n = \pi K \frac{h_{\max}^2 - h_1^2}{\ln\left(\frac{r_{\max}}{r_n}\right)} \quad (2.4)$$

To compare various ERWs to a conventional 4 in. recovery well, three drawdown radii of influences, r_{max} , were selected: 304.8 cm (10 ft), 365.8 cm (12 ft) and 457.2 cm (15 ft), respectively. The results are provided below which includes groundwater flow rates in both cm^3/sec and ft^3/sec .

Comparison of Conventional Well vs. ERWs
(Unconfined Aquifer of Moderate Permeability $r_{max} = 10$ ft.)

Variables	Constants
$n = 1, 2.. 5$	
r_n	$h_{max} = 304.8$
10.16	$h1 = 152.4$
60.96	$r_{max} = 304.8$
91.44	$K = 0.00004$
121.92	
152.4	

$$Q_n = \pi \cdot K \cdot \frac{h_{max}^2 - h1^2}{\ln\left(\frac{r_{max}}{r_n}\right)}$$

r_n	Q_n		$Q_n \cdot 0.00212$
10.16	2.574	(4 in. conventional well)	$5.458 \cdot 10^{-3}$
60.96	5.44	(2 ft ERW)	0.012
91.44	7.273	(3 ft ERW)	0.015
121.92	9.556	(4 ft ERW)	0.02
152.4	12.632	(5 ft ERW)	0.027

= groundwater flow
from well, cm^3/sec

= groundwater flow
from well, ft^3/sec

Comparison of Conventional Well vs. ERWs
(Unconfined Aquifer of Moderate Permeability $r_{max} = 12$ ft.)

Variables

$n = 1, 2, \dots, 5$

r_n

10.16
60.96
91.44
121.92
152.4

$$Q_n = \pi \cdot K \cdot \frac{h_{max}^2 - h_1^2}{\ln\left(\frac{r_{max}}{r_n}\right)}$$

Constants

$h_{max} = 304.8$

$h_1 = 152.4$

$r_{max} = 365.76$

$K = 0.00004$

r_n

Q_n

10.16
60.96
91.44
121.92
152.4

2.443
4.887
6.316
7.97
10.001

(4 in. conventional well)
(2 ft ERW)
(3 ft ERW)
(4 ft ERW) = groundwater flow from well, cm³/sec
(5 ft ERW)

$Q_n \cdot 0.00212$

$5.18 \cdot 10^3$
0.01
0.013
0.017
0.021

= groundwater flow from well, ft³/sec

Comparison of Conventional Well vs. ERWs
(Unconfined Aquifer of Moderate Permeability $r_{max} = 15$ ft.)

Variables

$n = 1, 2, \dots, 5$

r_n

10.16
60.96
91.44
121.92
152.4

$$Q_n = \pi \cdot K \cdot \frac{h_{max}^2 - h_1^2}{\ln\left(\frac{r_{max}}{r_n}\right)}$$

Constants

$h_{max} = 304.8$

$h_1 = 152.4$

$r_{max} = 457.2$

$K = 0.00004$

r_n

Q_n

10.16
60.96
91.44
121.92
152.4

2.3
4.346
5.44
6.624
7.97

(4 in. conventional well)
(2 ft ERW)
(3 ft ERW) = groundwater flow from well, cm³/sec
(4 ft ERW)
(5 ft ERW)

$Q_n \cdot 0.00212$

$4.876 \cdot 10^3$
$9.213 \cdot 10^3$
0.012
0.014
0.017

= groundwater flow from well, ft³/sec

APPENDIX B

HYDRAULIC CONDUCTIVITY CALCULATIONS OF NATIVE SOIL

This appendix provides supporting hydraulic conductivity calculations of the native soil from the field demonstration as described in Section 4.1. The permeability calculations were determined by performing a falling head permeability test using an ELE K605-A combination permeameter to ASTM standards. Three tests were conducted for increased quality assurance. The calculations of the tests are provided below:

Constants

$n := 1, 2, 3$

$L := 6.5$ = length of sample
in permeameter, cm

$a := 1.77$ = area of cross section
of pipette, cm^2

$h_0 := 59.06$ = initial hydraulic head
difference across length L

Variables

$t_n :=$

2400
2415
2400

 = time, sec

$h_n :=$

45.09
44.45
44.45

 = final hydraulic
head in cm of
water

k_n

$4.084 \cdot 10^{-5}$
$4.273 \cdot 10^{-5}$
$4.3 \cdot 10^{-5}$

$$k_n := \frac{a \cdot L}{13.76 \cdot t_n} \cdot \log\left(\frac{h_0}{h_n}\right)$$

k = hydraulic conductivity of tested material
(calculations based upon laboratory
permeameter tests, expressed in cm/sec)

$$k_{\text{avg}} = 4.22 \times 10^{-5} \text{ cm/sec}$$

APPENDIX C

MEDIA SCREENING AND SELECTION FLOW AND STRENGTH TESTING RESULTS

This appendix presents data for the screening process used to select media for the conductive lens in the ERWs. Two tests were performed on each media, which included flow testing through various diameter funnels and qualitative strength testing to determine crushability of individual particles. For the funnel flow tests, the size of the media is provided, and the elapsed time for each media to pass through each funnel is also included. Three trials were performed, and observations of each test are provided. For the strength testing, a value of 1 through 5 was selected (in order of increasing strength) for each media, and comments are also provided.

Table C.1 Flow Testing Data for various Media

Media		Time (seconds)			Comments
		Funnel # 1 0.5 in. dia (12.7 mm)	Funnel # 2 0.38 in. dia. (9.5 mm)	Funnel # 3 0.25 in. dia. (6.35 mm)	
Carboceramics <i>CarboHSP</i> High Strength Ceramic Proppant Size 6/12	Trial # 1 Trial # 2 Trial # 3 Avg.	3.02 3.13 3.12 3.09	--- --- --- ---	--- --- --- ---	<u>Funnel 1</u> Media flowed well through funnel. <u>Funnels 2 & 3</u> Media did not pass through funnel.
Carboceramics <i>CarboHSP</i> High Strength Ceramic Proppant Size 12/18	Trial # 1 Trial # 2 Trial # 3 Avg.	2.21 2.11 2.10 2.14	2.79 3.10 3.09 2.99	45.52 43.95 42.99 44.15	<u>Funnel 1</u> Media flowed well through funnel. <u>Funnel 2.</u> Beads flowed smoothly but slowly. Beads formed a pile in the pan. <u>Funnel 3</u> Material got stuck frequently. Funnel had to be shaken or tapped for beads to flow.
Carboceramics <i>CarboProp</i> Int. Strength Ceramic Proppant Size 16/30	Trial # 1 Trial # 2 Trial # 3 Avg.	2.14 1.97 1.98 2.03	2.97 2.95 3.09 3.00	26.30 25.93 26.38 26.20	<u>Funnels 1&2.</u> Media flowed well. Pile in pan was formed. <u>Funnel 3.</u> Beads flowed slowly but consistently on all three trials.
Carboceramics <i>CarboLite</i> Light Strength Ceramic Proppant Size 12/18	Trial # 1 Trial # 2 Trial # 3 Avg.	2.23 2.39 2.34 2.32	3.25 3.10 3.28 3.21	56.81 62.55 59.34 59.57	<u>Funnel 1.</u> Media flowed smoothly. Pile in pan was a little flatter and spread out than the Carboprop 16/30. <u>Funnel 2.</u> Flowed consistently. Pile in pan was also flatter. <u>Funnel 3.</u> Funnel had to be shaken and/or tapped continuously to keep the beads flowing.
Carboceramics <i>CarboEconoProp</i> Light Strength Ceramic Proppant Size 12/20	Trial # 1 Trial # 2 Trial # 3 Avg.	2.00 2.11 2.24 2.12	3.17 3.17 3.15 3.16	29.81 32.20 30.22 30.74	<u>Funnels 1 & 2.</u> Flowed smoothly, formed a pile in pan. <u>Funnel 3.</u> Flowed smoothly. On trial #2 funnel had to be tapped 2X to initiate flow. Media started to pool out from point of contact but eventually formed a flat pile.

Table C.1 (Continued) Flow Testing Data for various Media

Media		Time (seconds)			Comments
		Funnel # 1 0.5 in. dia (12.7 mm)	Funnel # 2 0.38 in. dia. (9.5 mm)	Funnel # 3 0.25 in. dia. (6.35 mm)	
Carboceramics <i>CarboEconoProp</i> Light Strength Ceramic Proppant Size 20/40 CarboProp	Trial # 1	2.03	4.59	24.09	Media flowed well through all three funnels.
	Trial # 2	2.07	4.56	23.43	
	Trial # 3	2.12	4.62	23.46	
	Avg.	2.07	4.59	23.66	
Carboceramics <i>CarboEconoProp</i> Int. Strength Ceramic Proppant Size 20/40 HSP	Trial # 1	2.09	4.53	24.68	Media flowed well through all three funnels.
	Trial # 2	2.09	4.46	25.03	
	Trial # 3	2.03	4.46	25.02	
	Avg.	2.07	4.48	24.91	
Carboceramics <i>CarboEconoProp</i> Lightweight Ceramic Proppant Size 20/40 CarboLite	Trial # 1	1.96	4.31	23.15	Media flowed well through all three funnels.
	Trial # 2	2.03	4.40	22.98	
	Trial # 3	2.06	4.37	23.28	
	Avg.	2.02	4.36	23.14	
Carboceramics <i>CarboEconoProp</i> Light Strength Ceramic Proppant Size 20/40 CarboEconoProp	Trial # 1	2.12	4.53	24.81	Media flowed well through all three funnels.
	Trial # 2	2.09	4.56	24.87	
	Trial # 3	2.09	4.61	24.87	
	Avg.	2.10	4.57	24.85	
Carboceramics <i>CarboEconoProp</i> Light Strength Ceramic Proppant Size 30/50 CarboEconoProp	Trial # 1	2.00	4.12	20.84	Media flowed well through all three funnels.
	Trial # 2	1.97	4.21	20.71	
	Trial # 3	1.96	4.21	20.62	
	Avg.	1.98	4.18	20.72	

Table C.1 (Continued) Flow Testing Data for various Media

Media		Time (seconds)			Comments
		Funnel # 1 0.5 in. dia (12.7 mm)	Funnel # 2 0.38 in. dia. (9.5 mm)	Funnel # 3 0.25 in. dia. (6.35 mm)	
Carboceramics <i>CarboEconoProp</i> Int. Strength Ceramic Proppan Size 30/60 CarboProp	Trial # 1	1.81	4.25	18.12	Media flowed well through all three funnels.
	Trial # 2	1.84	4.40	18.25	
	Trial # 3	1.84	4.15	18.46	
	Avg.	1.83	4.27	18.28	
Fine Industrial Supply <i>Hardball</i> Size 8/16 **(18 ml volume only)	Trial # 1	1.10	1.43	---	<u>Funnel 1.</u> Beads flowed very fast. Since only 18 ml of sample was tested, it difficult to get a good time rep. <u>Funnel 2.</u> Same as funnel #1, but time a little longer. <u>Funnel 3.</u> Beads did not pass through funnel.
	Trial # 2	0.90	4.45	---	
	Trial # 3	0.96	1.41	---	
	Avg.	0.99	2.43	---	
Fine Industrial Supply <i>Hardball</i> Size 10/20 **(18 ml volume only)	Trial # 1	0.86	1.26	15.56	<u>Funnels 1 & 2.</u> Beads flowed too fast. <u>Funnel 3.</u> Funnel had to be shaken and/or tapped to keep beads flowing.
	Trial # 2	0.76	1.46	17.94	
	Trial # 3	0.84	1.39	15.34	
	Avg.	0.82	1.37	16.28	
Fine Industrial Supply <i>Hardball</i> Size 18/30 **(18 ml volume only)	Trial # 1	0.83	1.23	7.83	<u>Funnel 1.</u> Flows fast. Beads form a donut shape in pan with a hollow center. <u>Funnel 2.</u> Flows consistently. Forms a pile at bottom of pan. <u>Funnel 3.</u> Media flows very consistently. Forms neat pile at bottom of pan.
	Trial # 2	0.79	1.31	7.79	
	Trial # 3	0.88	1.18	7.89	
	Avg.	0.83	1.24	7.84	
Fine Industrial Supply <i>Glass Beads</i> Size 20-30 Screen (0.0331 - 0.0232 in.)	Trial # 1	2.30	2.97	21.77	<u>Funnel 1.</u> Flows easily through funnel. Forms a large "donut" in pan approx. 3.75 in. dia. hollow ctr & 1 in. dia. glass beads. <u>Funnel 2.</u> Flows easily through funnel. Also forms "donut" approx. 3 in. dia. hollow ctr & 2 in. dia. glass beads. <u>Funnel 3.</u> flows consistently. Donut w/ 1.75 in. dia ctr.
	Trial # 2	2.03	2.92	21.83	
	Trial # 3	2.04	2.93	21.71	
	Avg.	2.12	2.94	21.77	

Table C.1 (Continued) Flow Testing Data for various Media

Media		Time (seconds)			Comments
		Funnel # 1 0.5 in. dia (12.7 mm)	Funnel # 2 0.38 in. dia. (9.5 mm)	Funnel # 3 0.25 in. dia. (6.35 mm)	
Fine Industrial Supply Glass Beads Size 30-40 Screen (0.0232 - 0.0165 in.)	Trial # 1	1.80	2.50	17.51	<p><u>Funnel 1.</u> Flows easily through funnel. Forms a large "donut" in pan approx. 3.5 in. dia. hollow ctr & 1.5 in. dia. glass beads.</p> <p><u>Funnel 2.</u> Flows easily through funnel. Also forms "donut" 4 in. hollow ctr. 1.5 - 2 in. glass beads.</p> <p><u>Funnel 3.</u> Trials 1,2 formed a donut which thinned to outside.</p>
	Trial # 2	1.80	2.57	16.40	
	Trial # 3	1.84	2.72	16.72	
	Avg.	1.81	2.60	16.88	
Union Process Glass Beads Size 3mm **(29 ml volume only)	Trial # 1	1.90	2.50	---	<p><u>Funnel 1.</u> Media flows quickly.</p> <p><u>Funnel 2.</u> beads flow easily & consistentl.</p> <p><u>Funnel 3.</u> Beads did not pass through funnel.</p>
	Trial # 2	1.59	2.57	---	
	Trial # 3	1.66	2.72	---	
	Avg.	1.72	2.60	---	
Union Process Glass Beads Size 5mm **(30 ml volume only)	Trial # 1	4.57	7.53	---	<p><u>Funnel 1.</u> Trials 1&3 beads got stuck in outlet. Funnel was tapped then beads started flowing.</p> <p><u>Funnel 2.</u> Funnel had to continuously shaken in order for beads to flow.</p> <p><u>Funnel 3.</u> Beads did not pass through funnel.</p>
	Trial # 2	1.98	6.42	---	
	Trial # 3	4.23	5.02	---	
	Avg.	3.59	6.32	---	
Agasco Corp. Quartz Size #16F	Trial # 1	2.22	3.47	21.32	<p><u>Funnel 1.</u> Quartz flows smoothly; although a little slower than glass or ceramic beads. Forms a pile in pan 3.5 in. dia.</p> <p><u>Funnel 2.</u> Similar to funnel 1. Pile in pan also similar.</p> <p><u>Funnel 3.</u> Flows slowly yet continuously. Pile is similar to funnels 1 & 2.</p>
	Trial # 2	2.18	3.35	21.65	
	Trial # 3	2.37	3.29	23.09	
	Avg.	2.26	3.37	22.02	
Agasco Corp. Quartz Size #12F	Trial # 1	2.56	3.78	49.57	<p><u>Funnels 1 & 2.</u> Both trials similar. Quartz flows nicely. Forms a pile in pan.</p> <p><u>Funnel 3.</u> Flows poorly. Funnel had to be shaken continuously to keep quartz flowing.</p>
	Trial # 2	2.53	3.84	60.34	
	Trial # 3	2.46	3.77	57.84	
	Avg.	2.52	3.80	55.92	

Table C.1 (Continued) Flow Testing Data for various Media

Media		Time (seconds)			Comments
		Funnel # 1 0.5 in. dia. (12.7 mm)	Funnel # 2 0.38 in. dia. (9.5 mm)	Funnel # 3 0.25 in. dia. (6.35 mm)	
DuPont de Nemours <i>Rynite 530 Resin</i> Size 1/8 in.	Trial # 1	13.13	---	---	<u>Funnel 1.</u> Rynite does flow well at all. Material is very coarse and oval shaped. <u>Funnels 2 & 3.</u> Media does not pass through funnel.
	Trial # 2	11.80	---	---	
	Trial # 3	10.34	---	---	
	Avg.	11.76	---	---	
DuPont de Nemours <i>Delrin 500 Resin</i> Size 1/8 in.	Trial # 1	3.03	3.85	---	<u>Funnel 1.</u> Media flows well. <u>Funnels 2 & 3.</u> Media does not pass through funnel.
	Trial # 2	2.96	3.88	---	
	Trial # 3	3.04	4.02	---	
	Avg.	3.01	3.92	---	
KLLK (S. Plainfield, NJ) <i>Concrete Sand C-33</i>	Trial # 1	2.40	3.59	---	<u>Funnel 1.</u> Flowed nicely. Forms a pile in pan. <u>Funnel 2.</u> Flowed well but sometimes larger particles got stuck and funnel had to be tapped. <u>Funnel 3.</u> Sand did not pass through funnel.
	Trial # 2	2.39	5.93	---	
	Trial # 3	2.29	4.89	---	
	Avg.	2.36	4.80	---	
KLLK (S. Plainfield, NJ) <i>00 Sand Blasting Sand</i>	Trial # 1	2.00	4.79	22.75	<u>Funnels 1 & 2.</u> Flows consistently, forms a pile in pan. <u>Funnel 3.</u> The time was long but the sand flowed steadily and never stopped.
	Trial # 2	2.08	4.84	23.03	
	Trial # 3	2.03	5.02	22.81	
	Avg.	2.04	4.88	22.86	
KLLK (S. Plainfield, NJ) <i>White Mason Sand</i>	Trial # 1	2.28	5.59	---	
	Trial # 2	2.37	5.34	---	
	Trial # 3	2.28	5.39	---	
	Avg.	2.31	5.44	---	

Table C.1 (Continued) Flow Testing Data for various Media

Media		Time (seconds)			Comments
		Funnel # 1 0.5 in. dia (12.7 mm)	Funnel # 2 0.38 in. dia. (9.5 mm)	Funnel # 3 0.25 in. dia. (6.35 mm)	
The Morie Company, Inc. <i>Commercial Sand</i> Size 1	Trial # 1	2.61	3.79	---	<u>Funnels 1 & 2.</u> Flows consistently; does not form a pile in pan. <u>Funnel 3.</u> Sand does not pass through funnel.
	Trial # 2	2.65	3.96	---	
	Trial # 3	2.53	3.88	---	
	Avg.	2.60	3.88	---	
The Morie Company, Inc. <i>Commercial Sand</i> Size 2	Trial # 1	3.10	4.50	---	<u>Funnel 1.</u> Flows well. <u>Funnel 2.</u> Sand got stuck in funnel on trial #3. <u>Funnel 3.</u> Sand does not pass through funnel.
	Trial # 2	3.03	4.46	---	
	Trial # 3	3.12	6.36	---	
	Avg.	3.08	5.11	---	
The Morie Company, Inc. <i>Commercial Sand</i> 3/16 in. X 10	Trial # 1	7.22	---	---	<u>Funnel 1.</u> funnel had to be shaken continuously. <u>Funnels 2 & 3.</u> Sand does not pass through funnel.
	Trial # 2	9.59	---	---	
	Trial # 3	13.49	---	---	
	Avg.	10.10	---	---	
Esco, Inc. <i>Walnut Shell</i> Size 8/12	Trial # 1	2.89	3.80	---	<u>Funnels 1 & 2.</u> Flows well. Forms a pile in pan. <u>Funnel 3.</u> Media does not pass through funnel.
	Trial # 2	2.95	3.90	---	
	Trial # 3	2.78	3.70	---	
	Avg.	2.87	3.80	---	
Esco, Inc. <i>Corn Cob</i> Size 14/20	Trial # 1	2.97	4.20	---	<u>Funnels 1 & 2.</u> Flows well. Forms a pile in pan. <u>Funnel 3.</u> Media does not pass through funnel.
	Trial # 2	2.91	4.05	---	
	Trial # 3	2.90	4.00	---	
	Avg.	2.93	4.08	---	

Table C.1 (Continued) Flow Testing Data for various Media

Media		Time (seconds)			Comments
		Funnel # 1 0.5 in. dia (12.7 mm)	Funnel # 2 0.38 in. dia. (9.5 mm)	Funnel # 3 0.25 in. dia. (6.35 mm)	
Esco, Inc. <i>Aluminum Oxide</i> 30 Grit	Trial # 1	2.42	3.69	27.82	<u>Funnel 1 & 2.</u> Flows well. Forms a pile in pan. <u>Funnel 3.</u> Flows slowly but smoothly through funnel. Forms a pile.
	Trial # 2	2.40	3.78	28.78	
	Trial # 3	2.45	3.71	29.10	
	Avg.	2.42	3.73	28.57	
The Morie Company, Inc. <i>Commercial Sand</i> Size 3	Trial # 1	3.58	3.59	---	<u>Funnel 1.</u> Sand got stuck in funnel on trial #3. <u>Funnel 2.</u> Sand kept getting stuck. Funnel had to be shaken and/or tapped continuously to initiate flow. <u>Funnel 3.</u> Sand does not pass through funnel.
	Trial # 2	3.58	10.54	---	
	Trial # 3	5.26	9.73	---	
	Avg.	4.14	7.95	---	

Table C.2 Strength Test Data for Various Media

Media	Strength Rating (1-5)	Comments
Carboceramics <i>CarboHSP</i> High Strength Ceramic Proppant Size 6/12	5	Tested 5 beads. Could not break any of them.
Carboceramics <i>CarboHSP</i> High Strength Ceramic Proppant Size 12/18	5	Very Strong. Pulverized 1 ball using extreme force.
Carboceramics <i>CarboProp</i> Intermediate Strength Ceramic Proppant Size 16/30	4	Fairly Strong. Bead pulverizes into many pieces using fair amount of force.
Carboceramics <i>CarboLite</i> Light Strength Ceramic Proppant Size 12/18	4	Fairly Strong. About same strength as CarboProp 16/30.
Carboceramics <i>CarboEconoProp</i> Light Strength Ceramic Proppant Size 12/20	3.5	Strong material. Pulverizes a little easier than the other Carboceramics samples.
Fine Industrial Supply <i>Hardball</i> Size 8/16	5	Very strong. Could not break any of the beads.
Fine Industrial Supply <i>Hardball</i> Size 10/20	4	Strong.
Fine Industrial Supply <i>Hardball</i> Size 18/30	5	Small but very strong!

Table C.2 (Continued) Strength Test Data for Various Media

Media	Strength Rating (1-5)	Comments
Fine Industrial Supply <i>Glass Beads</i> Size 20-30 Screen	2.5	Somewhat strong but could shatter every bead with applied force.
Fine Industrial Supply <i>Glass Beads</i> Size 30-40 Screen	2.5	Same strength as smaller beads, only these are larger in size.
Union Process <i>Glass Beads</i> Size 3mm	5	Strong. Could not shatter any of the beads.
Union Process <i>Glass Beads</i> Size 5mm	5	Strong. None of the beads broke.
Agasco Corp. <i>Quartz</i> Size #16F	1	Has very little strength.
Agasco Corp. <i>Quartz</i> Size #12F	1	Poor strength.
DuPont de Nemours <i>Rynite 530 Resin</i> Size 1/8 in.	5	Nothing broke. Very strong.
DuPont de Nemours <i>Delrin 500 Resin</i> Size 1/8 in.	5	Also very strong.
KLK <i>S. Plainfield, NJ</i> <i>Concrete Sand C-33</i>	1	Poor strength and material is not uniform in size.

Table C.2 (Continued) Strength Test Data for Various Media

Media	Strength Rating (1-5)	Comments
KLK <i>S. Plainfield, NJ</i> <i>00 Sand Blasting Sand</i>	1	Poor strength.
KLK <i>S. Plainfield, NJ</i> <i>White Mason Sand</i>	1	Pulverize easily. Poor strength.
Harrison Concrete Supply <i>Concrete Sand</i>	2	Similar to KLK, but a little stronger.
The Morie Company, Inc. <i>Commercial Sand</i> Size 00	1.5	Poor Strength
The Morie Company, Inc. <i>Commercial Sand</i> Size 00N	1.5	Poor Strength
The Morie Company, Inc. <i>Commercial Sand</i> Size 0	2	
The Morie Company, Inc. <i>Commercial Sand</i> Size 1	1.5	Broke easily.
The Morie Company, Inc. <i>Commercial Sand</i> Size 2	2	Not very resistant to pressure.
The Morie Company, Inc. <i>Commercial Sand</i> Size 3	3	A little stronger than the finer Morie samples.

Table C.2 (Continued) Strength Test Data for Various Media

Media	Strength Rating (1-5)	Comments
Esco, Inc. <i>Walnut Shell</i> Size 8/12	4	Suprisingly strong
Esco, Inc. <i>Corn Cob</i> Size 14/20	3	Hard material to test. Media is not very round.
Esco, Inc. <i>Aluminum Oxide</i> 30 Grit	3	Hard material to test. Media is not rounded and the size is very small.

APPENDIX D

FILTER CALCULATION FOR MEDIA SELECTION FOR THE ERW

This appendix presents the calculation for determining the media size for the conductive lenses for the ERWs for the field pilot demonstration. The calculation was based upon filter pack design criteria, and is listed as follows:

- 1) Multiply the D_{30} of the native soil by a factor between 4 and 10 and set this equal to the D_{70} of the filter media.

$$D_{30} \text{ (native soil)} = 0.075 \text{ mm} \qquad \text{Multiplier factor} = 10$$

$$D_{30} \text{ (native soil)} \times 10 = 0.75 \text{ mm} \qquad 0.075\text{mm} \times 10 = 0.75 \text{ mm}$$

$$D_{70} \text{ (filter media)} = 0.75 \text{ mm}$$

- 2) Check the uniformity coefficient (C_u) of the filter media using the Hazen

Formula, where $C_u = D_{60}/D_{10}$.

$$C_u = 0.8 \text{ mm}/0.6 \text{ mm} = 1.33$$

- 3) Choose a filter media with a D_{70} in this range.

*Media chosen was 16/30 CarboProp (Figures 4.1, 4.2)

APPENDIX E

HYDRAULIC CONDUCTIVITY CALCULATIONS OF CERAMIC BEADS

This appendix presents the hydraulic conductivity calculations of the various sizes of ceramic beads for use as a conductive lens in an ERW. All the tests were performed using the constant head method, in accordance with ASTM standard, D 2434-68. As discussed in section 3.2.4, all testing was performed with a ELE[®] K-605A combination permeameter, with the average value of each head increment included in the calculations. For each product line, the average hydraulic conductivity value is also provided, which was the value used to compare the hydraulic conductivity values of all the ceramic beads tested (Figure 4.3). Hydraulic Conductivity calculations using both the constant head and falling head method are also provided for the combined media and soil testing using 16/30 CarboProp[®] and the native soil for the field demonstration.

Permeability Testing
CarboCeramics 16/30 CarboProp

variables

$n := 1, 2..5$

$h_n :=$ = head of water, cm

5.08
10.16
15.24
20.32
25.40

$Q_n :=$ = flowrate of
water, cm³/sec

37
62
83.3
105
127

k_n

0.207
0.174
0.155
0.147
0.142

constants

$L := 13.5$ = length of sample in permeameter, cm

$A := 31.65$ = cross sectional area
of permeameter, cm²

$t := 15$ = time, sec

$$k_n := \frac{Q_n \cdot L}{(A \cdot t \cdot h_n)}$$

k = hydraulic conductivity of tested material
(calculations based upon laboratory permeameter
tests, expressed in cm/sec)

$$k_{avg.} = 0.165 \text{ cm/sec}$$

Permeability Testing
CarboCeramics 20/40 HSP

Constants

Variables

$n = 1, 2..5$

$h_n :=$ = head of water, cm

5.08
10.16
15.24
20.32
25.40

$Q_n =$ = flowrate of
water, cm³/sec

30
68
91.7
114
132.3

k_n

0.162
0.183
0.165
0.154
0.143

$L := 13$ = length of sample in permeameter, cm

$A := 31.65$ = cross sectional area
of permeameter, cm²

$t := 15$ = time, sec

$$k_n := \frac{Q_n \cdot L}{(A \cdot t \cdot h_n)}$$

k = hydraulic conductivity of tested material
(calculations based upon laboratory
permeameter tests, expressed in cm/sec)

$$k_{avg.} = 0.161 \text{ cm/sec}$$

Permeability Testing
CarboCeramics 20/40 CarboProp

Variables		Constants						
$n = 1, 2..5$		$L = 13$	= length of sample in permeameter, cm					
$h_n =$	= head of water, cm	$A = 31.65$	= cross sectional area of permeameter, cm ²					
<table border="1" style="display: inline-table; vertical-align: top;"><tr><td>5.08</td></tr><tr><td>10.16</td></tr><tr><td>15.24</td></tr><tr><td>20.32</td></tr><tr><td>25.40</td></tr></table>	5.08	10.16	15.24	20.32	25.40	$Q_n =$	$t = 15$	= time, sec
5.08								
10.16								
15.24								
20.32								
25.40								
	= flowrate of water, cm ³ /sec							
	<table border="1" style="display: inline-table; vertical-align: top;"><tr><td>32</td></tr><tr><td>55.3</td></tr><tr><td>79.7</td></tr><tr><td>99.7</td></tr><tr><td>119.7</td></tr></table>	32	55.3	79.7	99.7	119.7		
32								
55.3								
79.7								
99.7								
119.7								
	k_n	$k_n = \frac{Q_n \cdot L}{(A \cdot t \cdot h_n)}$						
	<table border="1" style="display: inline-table; vertical-align: top;"><tr><td>0.172</td></tr><tr><td>0.149</td></tr><tr><td>0.143</td></tr><tr><td>0.134</td></tr><tr><td>0.129</td></tr></table>	0.172	0.149	0.143	0.134	0.129	$k =$ hydraulic conductivity of tested material (calculations based upon laboratory permeameter tests, expressed in cm/sec)	
0.172								
0.149								
0.143								
0.134								
0.129								
		$k_{avg.} = 0.145$ cm/sec						

Permeability Testing
CarboCeramics 20/40 CarboLite

Variables		Constants						
$n = 1, 2..5$		$L = 13$	= length of sample in permeameter, cm					
$h_n =$	= head of water, cm	$A = 31.65$	= cross sectional area of permeameter, cm ²					
<table border="1" style="display: inline-table; vertical-align: top;"><tr><td>5.08</td></tr><tr><td>10.16</td></tr><tr><td>15.24</td></tr><tr><td>20.32</td></tr><tr><td>25.40</td></tr></table>	5.08	10.16	15.24	20.32	25.40	$Q_n =$	$t = 15$	= time, sec
5.08								
10.16								
15.24								
20.32								
25.40								
	= flowrate of water, cm ³ /sec							
	<table border="1" style="display: inline-table; vertical-align: top;"><tr><td>30</td></tr><tr><td>52.3</td></tr><tr><td>77.7</td></tr><tr><td>95.3</td></tr><tr><td>114</td></tr></table>	30	52.3	77.7	95.3	114		
30								
52.3								
77.7								
95.3								
114								
	k_n	$k_n = \frac{Q_n \cdot L}{(A \cdot t \cdot h_n)}$						
	<table border="1" style="display: inline-table; vertical-align: top;"><tr><td>0.162</td></tr><tr><td>0.141</td></tr><tr><td>0.14</td></tr><tr><td>0.128</td></tr><tr><td>0.123</td></tr></table>	0.162	0.141	0.14	0.128	0.123	$k =$ hydraulic conductivity of tested material (calculations based upon laboratory permeameter tests, expressed in cm/sec)	
0.162								
0.141								
0.14								
0.128								
0.123								
		$k_{avg.} = 0.139$ cm/sec						

Permeability Testing
CarboCeramics 20/40 CarboEconoProp

Variables		Constants						
$n := 1, 2..5$		$L := 13$	= length of sample in permeameter, cm					
$h_n :=$	= head of water, cm	$A := 31.65$	= cross sectional area of permeameter, cm ²					
<table border="1" style="display: inline-table; vertical-align: middle;"><tr><td>5.08</td></tr><tr><td>10.16</td></tr><tr><td>15.24</td></tr><tr><td>20.32</td></tr><tr><td>25.40</td></tr></table>	5.08	10.16	15.24	20.32	25.40	$Q_n :=$	$t := 15$	= time, sec
5.08								
10.16								
15.24								
20.32								
25.40								
	= flowrate of water, cm ³ /sec							
<table border="1" style="display: inline-table; vertical-align: middle;"><tr><td>30</td></tr><tr><td>52</td></tr><tr><td>74.3</td></tr><tr><td>93.7</td></tr><tr><td>114</td></tr></table>	30	52	74.3	93.7	114		$k_n := \frac{Q_n \cdot L}{(A \cdot t \cdot h_n)}$	
30								
52								
74.3								
93.7								
114								
	k_n	<table border="1" style="display: inline-table; vertical-align: middle;"><tr><td>0.162</td></tr><tr><td>0.141</td></tr><tr><td>0.14</td></tr><tr><td>0.128</td></tr><tr><td>0.123</td></tr></table>	0.162	0.141	0.14	0.128	0.123	$k =$ hydraulic conductivity of tested material (calculations based upon laboratory permeameter tests, expressed in cm/sec)
0.162								
0.141								
0.14								
0.128								
0.123								
		$k_{avg.} = 0.137$ cm/sec						

Permeability Testing
CarboCeramics 30/50 CarboEconoProp

Variables		Constants						
$n := 1, 2..5$		$L := 13$	= length of sample in permeameter, cm					
$h_n :=$	= head of water, cm	$A := 31.65$	= cross sectional area of permeameter, cm ²					
<table border="1" style="display: inline-table; vertical-align: middle;"><tr><td>5.08</td></tr><tr><td>10.16</td></tr><tr><td>15.24</td></tr><tr><td>20.32</td></tr><tr><td>25.40</td></tr></table>	5.08	10.16	15.24	20.32	25.40	$Q_n :=$	$t := 15$	= time, sec
5.08								
10.16								
15.24								
20.32								
25.40								
	= flowrate of water, cm ³ /sec							
<table border="1" style="display: inline-table; vertical-align: middle;"><tr><td>20.3</td></tr><tr><td>38</td></tr><tr><td>53.7</td></tr><tr><td>72.3</td></tr><tr><td>86.3</td></tr></table>	20.3	38	53.7	72.3	86.3		$k_n := \frac{Q_n \cdot L}{(A \cdot t \cdot h_n)}$	
20.3								
38								
53.7								
72.3								
86.3								
	k_n	<table border="1" style="display: inline-table; vertical-align: middle;"><tr><td>0.109</td></tr><tr><td>0.102</td></tr><tr><td>0.096</td></tr><tr><td>0.097</td></tr><tr><td>0.093</td></tr></table>	0.109	0.102	0.096	0.097	0.093	$k =$ hydraulic conductivity of tested material (calculations based upon laboratory permeameter tests, expressed in cm/sec)
0.109								
0.102								
0.096								
0.097								
0.093								
		$k_{avg.} = 0.099$ cm/sec						

Permeability Testing
CarboCeramics 30/60 CarboProp

Variables

$n = 1, 2..5$

$h_n =$ = head of water, cm

5.08
10.16
15.24
20.32
25.40

$Q_n =$ = flowrate of
water, cm³/sec

10
17.7
26
35
42.8

k_n

0.054
0.048
0.047
0.047
0.046

k = hydraulic conductivity of tested material
(calculations based upon laboratory
permeameter tests, expressed in cm/sec)

$k_{avg.} = 0.048$ cm/sec

Constants

$L = 13$ = length of sample in permeameter, cm

$A = 31.65$ = cross sectional area
of permeameter, cm²

$t = 15$ = time, sec

$$k_n = \frac{Q_n \cdot L}{(A \cdot t \cdot h_n)}$$

Permeability Testing
CarboCeramics 12/20 CarboEconoProp

constants

variables

$n = 1, 2..5$

$h_n =$ = head of water, cm

5.08
7.62
10.16
12.70
15.24

$Q_n =$ = flowrate of
water, cm³/sec

33.3
47.8
62
77.3
90

k_n

0.179
0.172
0.167
0.167
0.162

k = hydraulic conductivity of tested material
(calculations based upon laboratory permeameter
tests, expressed in cm/sec)

$k_{avg.} = 0.169$ cm/sec

$L = 13$ = length of sample in permeameter, cm

$A = 31.65$ = cross sectional area
of permeameter, cm²

$t = 15$ = time, sec

$$k_n = \frac{Q_n \cdot L}{(A \cdot t \cdot h_n)}$$

Permeability Testing
CarboCeramics 12/18 CarboLite

constants

variables

$L := 13$ = length of sample in permeameter, cm

$n = 1, 2..5$

$A := 31.65$ = cross sectional area of permeameter, cm^2

$h_n :=$ = head of water, cm

$t := 15$ = time, sec

$Q_n :=$ = flowrate of water, cm^3/sec

5.08
7.62
10.16
12.70
15.24

36
58
76
90
103.3

k_n

0.194
0.208
0.205
0.194
0.186

$$k_n = \frac{Q_n \cdot L}{(A \cdot t \cdot h_n)}$$

k = hydraulic conductivity of tested material (calculations based upon laboratory permeameter tests, expressed in cm/sec)

$k_{avg.} = 0.197$ cm/sec

Permeability Testing
CarboCeramics 6/12 CarboHSP

constants

variables

$L := 13.5$ = length of sample in permeameter, cm

$n = 1, 2..5$

$A := 31.65$ = Cross Sectional Area of permeameter, cm^2

$h_n :=$ = head of water, cm

$t := 15$ = time, sec

$Q_n :=$ = flowrate of water, cm^3/sec

2.54
5.08
7.62
10.16
12.7

38
54
86
104
117

k_n

0.425
0.302
0.321
0.291
0.262

$$k_n = \frac{Q_n \cdot L}{(A \cdot t \cdot h_n)}$$

k = hydraulic conductivity of tested material (calculations based upon laboratory permeameter tests, expressed in cm/sec)

$k_{avg.} = 0.320$ cm/sec

Permeability Testing 80 % 16/30 CarboProp 20% Soil Mixture
Constant Head Permeability Test

Constants

Variables

$L = 13$ = length of sample in permeameter, cm

$n = 1, 2, \dots, 5$

$A = 31.65$ = cross sectional area
of permeameter, cm^2

$h_n =$ = head of water, cm

$t = 15$ = time, sec

5.08
10.16
15.24
20.32
25.40

$Q_n =$ = flowrate of
water, cm^3/sec

5
9
13
16.5
20.5

k_n

0.027
0.024
0.023
0.022
0.022

$$k_n = \frac{Q_n \cdot L}{(A \cdot t \cdot h_n)}$$

k = hydraulic conductivity of tested material
(calculations based upon laboratory
permeameter tests, expressed in cm/sec)

$k_{\text{avg.}} = 0.024 \text{ cm}/\text{sec}$

Permeability Testing 50% 16/30 CarboProp 50% Soil
Falling Head Permeability Test

Variables

Constants

$t_n =$ = time, sec

$n = 1, 2, \dots, 3$

2415
2400
2400

$h_n =$

$L = 6$ = length of sample in permeameter, cm

$h_n =$
31.45
31.12
30.48
= final hydraulic
head in cm of
water

$a = 1.77$ = area of cross section
of pipette, cm^2

$h_0 = 58.42$ = initial hydraulic head difference
across length L

k_n

$8.595 \cdot 10^{-5}$
$8.796 \cdot 10^{-5}$
$9.086 \cdot 10^{-5}$

k = hydraulic conductivity of tested material
(calculations based upon laboratory
permeameter tests, expressed in cm/sec)

$k_{\text{avg.}} = 8.83 \times 10^{-5} \text{ cm}/\text{sec}$

$$k_n = \frac{a \cdot L}{13.76 \cdot t_n} \cdot \log\left(\frac{h_0}{h_n}\right)$$

Permeability Testing 20% 16/30 CarboProp 80% Soil
Falling Head Permeability Test

Constants

Variables

$n = 1, 2, 3$

$t_n :=$ = time, sec

$L = 6$ = length of sample in permeameter, cm

2640
2640
2700

$h_n :=$

$a = 1.77$ = area of cross section of pipette, cm^2

30.48
30.48
30.48

= final hydraulic head in cm of water

$h_0 = 58.42$ = initial hydraulic head difference across length L

$$k_n = \frac{a \cdot L}{13.76 \cdot t_n} \cdot \log\left(\frac{h_0}{h_n}\right)$$

$8.26 \cdot 10^{-5}$
$8.26 \cdot 10^{-5}$
$8.077 \cdot 10^{-5}$

k = hydraulic conductivity of tested material (calculations based upon laboratory permeameter tests, expressed in cm/sec)

$k_{avg.} = 8.20 \times 10^{-5}$ cm/sec

Permeability Testing 16 % 16/30 CarboProp 84% Soil Mixture
1 in. Column of Beads
Constant Head Permeability Test

Variables

Constants

$n = 1, 2, 5$

$L = 6.5$ = length of sample in permeameter, cm

$h_n :=$ = head of water, cm

$A = 31.65$ = cross sectional area of permeameter, cm^2

$t := 15$ = time, sec

12.7
17.78
22.86
27.94
33.02

$Q_n :=$ = flowrate of water, cm^3/sec

$$k_n = \frac{Q_n \cdot L}{(A \cdot t \cdot h_n)}$$

15.3
20
25.3
28
30

k_n

0.016
0.015
0.015
0.014
0.012

k = hydraulic conductivity of tested material (calculations based upon laboratory permeameter tests, expressed in cm/sec)

$k_{avg.} = 0.014$ cm/sec

Permeability Testing 9 % 16/30 CarboProp 91% Soil Mixture
 0.75 in. Column of Beads
 Constant Head Permeability Test

Variables

$n := 1, 2..5$

$h_n :=$ head of water, cm

12.7
15.24
17.78
20.32
22.86

$Q_n :=$ flowrate of water, cm³/sec

7.5
9
10
11
12.5

k_n

$8.085 \cdot 10^{-3}$
$8.085 \cdot 10^{-3}$
$7.7 \cdot 10^{-3}$
$7.412 \cdot 10^{-3}$
$7.487 \cdot 10^{-3}$

$$k_n := \frac{Q_n \cdot L}{(A \cdot t \cdot h_n)}$$

k = hydraulic conductivity of tested material (calculations based upon laboratory permeameter tests, expressed in cm/sec)

$k_{avg.} = 7.75 \times 10^{-3}$ cm/sec

Constants

$L := 6.5$ = length of sample in permeameter, cm

$A := 31.65$ = cross sectional area of permeameter, cm²

$t := 15$ = time, sec

Permeability Testing
 Falling Head Test
 70% CarboCeramics 16/30 CarboProp
 30% Soil Mixture

Constants

$n := 1, 2..3$

$L = 6.5$ = length of sample in permeameter, cm

$a = 1.77$ = area of cross section of pipette, cm²

$h_0 = 22.75$ = initial hydraulic head difference across length L

k_n

$2.313 \cdot 10^{-4}$
$2.313 \cdot 10^{-4}$
$2.383 \cdot 10^{-4}$

k = hydraulic conductivity of tested material (calculations based upon laboratory permeameter tests, expressed in cm/sec)

$k_{avg.} = 2.34 \times 10^{-4}$ cm/sec

Variables

$t_n :=$ time, sec

1500
1500
1500

$h_n :=$

8.75
8.75
8.5

= final hydraulic head in cm of water

$$k_n := \frac{a \cdot L}{13.76 \cdot t_n} \cdot \log\left(\frac{h_0}{h_n}\right)$$

Permeability Testing
 Falling Head Test
 75% CarboCeramics 16/30 CarboProp
 25% Soil Mixture

Constants

$n = 1, 2, 3$	
$L = 6.5$	= length of sample in permeameter, cm
$a = 1.77$	= area of cross section of pipette, cm^2
$h_0 = 22.75$	= initial hydraulic head difference across length L

Variables

$t_n =$	
840	= time, sec
840	
855	
$h_n =$	
3	= final hydraulic head in cm of water
4.5	
5.25	

$$k_n = \frac{a \cdot L}{13.76 \cdot t_n} \cdot \log\left(\frac{h_0}{h_n}\right)$$

k_n

$8.758 \cdot 10^{-4}$
$7.005 \cdot 10^{-4}$
$6.228 \cdot 10^{-4}$

k = hydraulic conductivity of tested material
 (calculations based upon laboratory permeameter tests, expressed in cm/sec)

$k_{\text{avg.}} = 7.73 \times 10^{-4} \text{ cm/sec}$

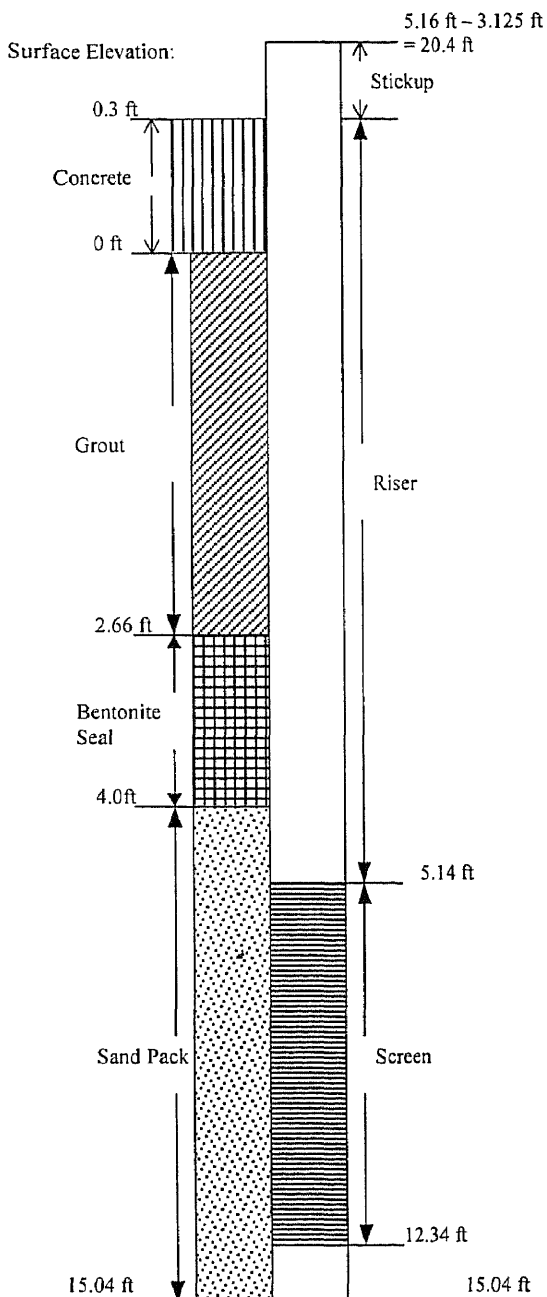
APPENDIX F

RECOVERY WELL LOGS

RECOVERY WELL 08-WL-70 CONSTRUCTION DIAGRAM

PROJECT: Field Pilot Test Site	START DATE: 4/28/98
DRILLING CONTRACTOR: M & R	FINISH DATE: 4/29/98
DRILLING EQUIPMENT: F-7	DRILLER: Doug W.
DRILLING METHOD: Filled 12 in. hole from casing	INSPECTOR: T. B.

WELL DESIGN



WELL CONSTRUCTION MATERIALS

PROTECTIVE COVER:

Manhole Prot. Casing Other _____

RISER MATERIAL: PVC 4 in.

WELL DIAMETER: 12 in.

SCREEN MATERIAL: PVC 4 in.

SCREEN SLOT SIZE: .010 .020 _____ in

SAND PACK GRADE: 0 QUAN. _____

BENTONITE TYPE: Med Chips QUAN. 50 lbs

GROUT TYPE: _____ QUAN. _____

INITIAL WATER LEVEL: 8.48 ft BGS

WATER LEVEL AT DEVELOPMENT:
11.68 - 2.04 = 9.64 ft BGS

REMARKS AND OBSERVATIONS:

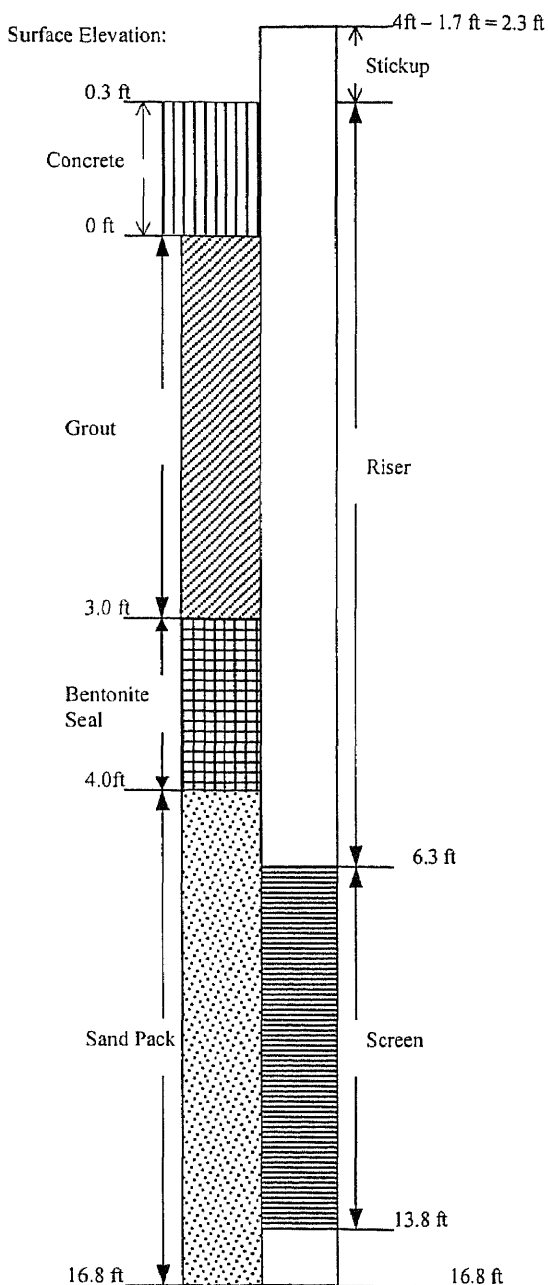
- Revert and water add to hold hole open at start
- Pulled 12 in nozzle while adding revert. Bottom was opened with rod
- Note: hole was down to 16.9 ft - 1.9 ft collapse = 15 ft deep

RECOVERY WELL 08-WL-69 CONSTRUCTION DIAGRAM

PROJECT: Field Pilot Test Site	START DATE: 4/28/98
DRILLING CONTRACTOR: M & R	FINISH DATE: 4/29/98
DRILLING EQUIPMENT: F - 7	DRILLER: Doug W.
DRILLING METHOD: Hollow Stem	INSPECTOR: T. B.

WELL DESIGN

WELL CONSTRUCTION MATERIALS



PROTECTIVE COVER:

Manhole Prot. Casing Other _____

RISER MATERIAL: PVC SCH 40

WELL DIAMETER: 8.25 in.

SCREEN MATERIAL: 0.020 PVC - 7ft

SCREEN SLOT SIZE: .010 .020 _____ in

SAND PACK GRADE: # 0 QUAN. 480 lbs

BENTONITE TYPE: Med Chips QUAN. 50 lbs

GROUT TYPE: _____ QUAN. _____

INITIAL WATER LEVEL: 9.19 ft BGS Top

WATER LEVEL AT DEVELOPMENT: 11.55 - 23 = 9.25 ft BGS

REMARKS AND OBSERVATIONS:

- Large quantities of beads found on auger
- In area of injection. Hand full of clumps.

APPENDIX G

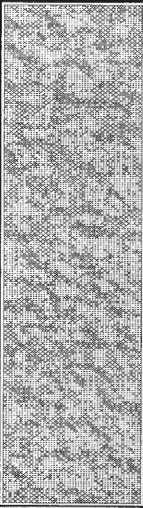

GEOPROBE BORING LOGS

This appendix provides the boring logs of the geoprobe soil sampling conducted around each ERW, as detailed in section 5.3.5.2. The borings logs conducted around the Helical Nozzle are first provided, followed by the borings logs around the Movable Nozzle. Each log gives a lithologic description of the samples, as well as an illustrative depth profile. A description of the media is provided, whenever present. General information is shown, at the top of each, including boring number, total depth, and distance from the ERW.


**RECOVERY WELL 08-WL-70
(15-PORT HELICAL NOZZLE)
GEOPROBE SOIL BORINGS**

NJIT SOIL BORING LOG

GP-H-1

PROJECT: Field Pilot Demonstration (ERW) CONTRACTOR: M&R Soil Investigations DRILLING EQUIPMENT: Geoprobe SAMPLING EQUIPMENT: 4 ft. thin acetate sleeve SHEET: 1 of 1				DISTANCE FROM WELL 08WL70: 28" SE DATE OF SAMPLING: 7/27/98 DRILLER: Bob Forshaw LOGGED BY: Michael T. Galbraith TOTAL DEPTH OF BOREHOLE: 6' - 14'		
Depth (ft)	USCS	Sample Interval	Recovery	Profile	Lithologic Description	
1					Borehole not sampled 1' - 6'.	
2						
3						
4						
5						
6	CL	6' - 10'	3.6'		Light brown to yellow silty CLAY. Hard at top. Becomes moister and a little softer at 8.6' below ground surface. Some organics such as wood chunks interspersed.	
7						
8						
9					9.5' Soil contains more SILT and less CLAY	
10					Fuel oil odors noted at bottom of sample.	
11	CL	10' - 14'	1.15'		Light brown and tan silty CLAY. Poor recovery. Fuel oil odors present	
12	SM					11.3' Gradual change from CLAY to fine silty SAND of the same color. Moist and soft. A couple of BEADS observed at top of sample, but only a few.
13						No other BEADS
14						
15						



**NJIT SOIL BORING LOG
GP-H-2**

PROJECT: Field Pilot Demonstration (ERW) CONTRACTOR: M&R Soil Investigations DRILLING EQUIPMENT: Geoprobe SAMPLING EQUIPMENT: 4 ft. thin acetate sleeve SHEET: 1 of 1				DISTANCE FROM WELL 08WL70: 42" SE DATE OF SAMPLING: 7/27/98 DRILLER: Bob Forshaw LOGGED BY: Michael T. Galbraith TOTAL DEPTH OF BOREHOLE: 6' - 9'	
Depth (ft)	USCS	Sample Interval	Recovery	Profile	Lithologic Description
1 2 3 4 5					Borehole not sampled 1' - 6'.
6 7 8	CL	6' - 9'	3		Abrupt change to light brown to brown CLAY very hard, dry, slight plasticity. extends to the bottom of the sample, except for a large chunk of wood located 7.55' to 7.75' below ground surface. NO BEADS OBSERVED.
9 10 11 12 13 14 15					


**NJIT SOIL BORING LOG
GP-H-4**

PROJECT: Field Pilot Demonstration (ERW) CONTRACTOR: M&R Soil Investigations DRILLING EQUIPMENT: Geoprobe SAMPLING EQUIPMENT: 4 ft. thin acetate sleeve SHEET: 1 of 1				DISTANCE FROM WELL 08WL70: 16.5" NW DATE OF SAMPLING: 7/27/98 DRILLER: Bob Forshaw LOGGED BY: Michael T. Galbraith TOTAL DEPTH OF BOREHOLE: 7' - 15'	
Depth (ft)	USCS	Sample Interval	Recovery	Profile	Lithologic Description
1 2 3 4 5 6					Borehole not sampled 1' -7'.
7 8 9 10 11	CL OL BEADS OL	7' - 11'	3.1'		Brown to light brown CLAY, fairly dry, firm, slight plasticity. Railroad tie chunk of wood observed 7.7' below ground surface. 9.15' Free Product layer. dark gray to black extends to bottom of sample. Soft, moderate plasticity with small roots interspersed. Strong odors. 9.85' 1/8" seam of BEADS. 9.87' Free Product layer continues.
12 13 14 15	OL SM	11' - 15'	2.92'		Same as above. 11.3' Light brown silty fine SAND. Damp, firm at top and softer at bottom of sample. Continues to bottom of sample.



**NJIT SOIL BORING LOG
GP-H-5**

PROJECT: Field Pilot Demonstration (ERW)				DISTANCE FROM WELL 08WL70: 36" NW	
CONTRACTOR: M&R Soil Investigations				DATE OF SAMPLING: 7/27/98	
DRILLING EQUIPMENT: Geoprobe				DRILLER: Bob Forshaw	
SAMPLING EQUIPMENT: 4 ft. thin acetate sleeve				LOGGED BY: Michael T. Galbraith	
SHEET: 1 of 1				TOTAL DEPTH OF BOREHOLE: 7' - 15'	
Depth (ft)	USCS	Sample Interval	Recovery	Profile	Lithologic Description
1 2 3 4 5 6					Borehole not sampled 1' -7'.
7 8 9 10 11	CL CL	7' - 11'	3.33'		7' Brown to light brown CLAY, firm, moist moderate plasticity. Organics such as twigs present. 9.7' Top of Free Product layer. Turns soil black. CLAY is brittle, softer and crumbles to the touch. Product continues to bottom of sample.
12 13 14 15	SM		2.72		Yellowish, light brown fine SAND contaminated with fuel oil, changes to light brown to gray in color at 11.3'. NO BEADS OBSERVED.


**NJIT SOIL BORING LOG
GP-H-6**

PROJECT: Field Pilot Demonstration (ERW) CONTRACTOR: M&R Soil Investigations DRILLING EQUIPMENT: Geoprobe SAMPLING EQUIPMENT: 4 ft. thin acetate sleeve SHEET: 1 of 1					DISTANCE FROM WELL 08WL70: 18" SW DATE OF SAMPLING: 7/27/98 DRILLER: Bob Forshaw LOGGED BY: Michael T. Galbraith TOTAL DEPTH OF BOREHOLE: 6' - 10'				
Depth (ft)	USCS	Sample Interval	Recovery	Profile	Lithologic Description				
1					Borehole not sampled 1' -6'.				
2									
3									
4									
5									
6	CL	6' - 10'	3.45'		Tan to yellowish tan CLAY, hard, dry low plasticity.				
7	CL				7' Large dark gray to black organic chunk of wood.				
8					7.6' Hard dry CLAY of low plasticity continues, a little darker in color, brown to light brown.				
9					Softer at bottom of sample. NO BEADS OBSERVED.				
10									
11									
12									
13									
14									
15									




**NJIT SOIL BORING LOG
GP-H-7**

PROJECT: Field Pilot Demonstration (ERW) CONTRACTOR: M&R Soil Investigations DRILLING EQUIPMENT: Geoprobe SAMPLING EQUIPMENT: 4 ft. thin acetate sleeve SHEET: 1 of 1				DISTANCE FROM WELL 08WL70: 33" SW DATE OF SAMPLING: 7/27/98 DRILLER: Bob Forshaw LOGGED BY: Michael T. Galbraith TOTAL DEPTH OF BOREHOLE: 6' - 15'	
Depth (ft)	USCS	Sample Interval	Recovery	Profile	Lithologic Description
1 2 3 4 5					Borehole not sampled 1' -6'.
6 7 8 9	SM CL	6' - 10'	2.88'		6' Light brown to yellow fine SAND. 6.3' Abrupt change to brown to light brown CLAY, fairly dry, firm, slight plasticity. Odors of Fuel Oil noted. Some organics in the form of tiny roots and small bits of wood observed. Clay turns a little darker at the bottom of the sample.
10 11 12 13 14	OL SM	10' - 15'	3.43'		10' Free Product layer, heavy odors. Dark brown to black organic CLAY with moderate plasticity. 11' Changes to a light brown silty fine SAND, firm at top, becomes softer with increasing depth. NO BEADS OBSERVED.
15					







**NJIT SOIL BORING LOG
GP-H-24**

PROJECT: Field Pilot Demonstration (ERW)				DISTANCE FROM WELL 08WL70: 44" SE	
CONTRACTOR: M&R Soil Investigations				DATE OF SAMPLING: 7/27/98	
DRILLING EQUIPMENT: Geoprobe				DRILLER: Bob Forshaw	
SAMPLING EQUIPMENT: 4 ft. thin acetate sleeve				LOGGED BY: Michael T. Galbraith	
SHEET: 1 of 1				TOTAL DEPTH OF BOREHOLE: 6' - 10'	
Depth (ft)	USCS	Sample Interval	Recovery	Profile	Lithologic Description
1					Borehole not sampled 1' -6'.
2					
3					
4					
5					
6	CL	6' - 10'	2.55'		6' Brown to tan with yellow undertones CLAY, hard, dry, low plasticity. Some organics in the form of black wood chunks (RR ties) interspersed. Extends to bottom of sample. NO BEADS OBSERVED.
7					
8					
9					
10					
11					
12					
13					
14					
15					



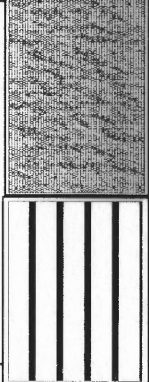

**NJIT SOIL BORING LOG
GP-H-25**

PROJECT: Field Pilot Demonstration (ERW) CONTRACTOR: M&R Soil Investigations DRILLING EQUIPMENT: Geoprobe SAMPLING EQUIPMENT: 4 ft. thin acetate sleeve SHEET: 1 of 1					DISTANCE FROM WELL 08WL70: 26" SW DATE OF SAMPLING: 7/27/98 DRILLER: Bob Forshaw LOGGED BY: Michael T. Galbraith TOTAL DEPTH OF BOREHOLE: 6' - 14'
Depth (ft)	USCS	Sample Interval	Recovery	Profile	Lithologic Description
1					Borehole not sampled 1' -6'.
2					
3					
4					
5					
6	CL	6' - 10'	3.55'		6' Tan to brown CLAY. hard,dry, low plasticity at top of sample becomes softer and darker with increasing depth. Organic material in the form of wood chunks (railroad ties ??) interspersed.
7					
8					
9					
10	CL	10' - 14'	3.7'		10' Free product layer. Dark gray to black organic CLAY. Moderate plasticity, strong odors.
11	CL				
12					
13	SM				
14					
15					

**NJIT SOIL BORING LOG
GP-H-26**

PROJECT: Field Pilot Demonstration (ERW) CONTRACTOR: M&R Soil Investigations DRILLING EQUIPMENT: Geoprobe SAMPLING EQUIPMENT: 4 ft. thin acetate sleeve SHEET: 1 of 1				DISTANCE FROM WELL 08WL70: 14" N DATE OF SAMPLING: 7/27/98 DRILLER: Bob Forshaw LOGGED BY: Michael T. Galbraith TOTAL DEPTH OF BOREHOLE: 4' - 15'	
Depth (ft)	USCS	Sample Interval	Recovery	Profile	Lithologic Description
1					Borehole not sampled 1' -4'.
2					
3					
4	SP	4' - 7'	2.19'		4' Tan to yellow with mottled grays and oranges fine SAND, moist, soft.
5					5.05' Brown to light brown yellowish CLAY, very hard, dry, low plasticity. Some organics (wood, lignite) throughout sample.
6					
7	CL	7' - 11'	3.52'		Same as above, becomes moister and lighter in color with increasing depth, extends to 9.6', odors at bot.
8					9.3' 1/8" Seam of BEADS, densely packed.
9	BEADS				9.6' Dark brown organic CLAY, low plasticity, heavy odors of Free Product.
	OL				10.2' 1/8" Seam of BEADS, densely packed.
10	BEADS				10.3' Dark brown, dark gray CLAY, medium plasticity. May be dark due to fuel oil. Organic roots interspersed.
11	OH				
	BEADS	11' -15'	3.0'		11' BEADS, Free Product, with some fines lying at top of acetate sleeve (disturbed from transport).
12	SM				11.1' Light brown, tan brown SILT.
13	BEADS				12.05' Seam of BEADS 1/2" - 3/4" thick, densely packed with little formation particles between them
14	SM				12.09' Light brown to light gray silty fine SAND with alternating layers of coarser SAND. Extends to bottom of sample.
15					

NJIT SOIL BORING LOG
GP-H-27

PROJECT: Field Pilot Demonstration (ERW) CONTRACTOR: M&R Soil Investigations DRILLING EQUIPMENT: Geoprobe SAMPLING EQUIPMENT: 4 ft. thin acetate sleeve SHEET: 1 of 1				DISTANCE FROM WELL 08WL70: 27" N DATE OF SAMPLING: 7/27/98 DRILLER: Bob Forshaw LOGGED BY: Michael T. Galbraith TOTAL DEPTH OF BOREHOLE: 4' - 15'	
Depth (ft)	USCS	Sample Interval	Recovery	Profile	Lithologic Description
1					Borehole not sampled 1' - 4'.
2					
3					
4	SM	4' - 7'	2.8'		4' Dark brown, light black FILL including Coal waste moist and soft, some fine SAND interspersed.
5	SM				4.6' Light brown/yellow fine SAND, moist.
6	BEADS CL				5.9' At interface of fine SAND (top) to CLAY (bot.) a parting of BEADS (2-3 beads thick) observed.
7	CL	7' - 11'	2.8'		5.95' Brown yellowish CLAY, hard, low plasticity.
8					Same as above.
9	OL				9.2' Abrupt change from the CLAY, to a dark gray to light brown organic CLAY. At this interface contamination is noted due to the dark color and heavy odors. Small roots and twigs observed.
10					**Scattered BEADS observed at bottom of sample, but do not exist a a lens or parting.
11	OL SM	11' - 15'	3.0'		Same as above.
12					11.2' Abrupt transition to light tan silty fine SAND, moist and soft. Odors of fuel oil present. One alternating layer of coarser SAND observed at 13.1' to 13.2'.
13					
14					
15					




**NJIT SOIL BORING LOG
GP-H-28**

PROJECT: Field Pilot Demonstration (ERW) CONTRACTOR: M&R Soil Investigations DRILLING EQUIPMENT: Geoprobe SAMPLING EQUIPMENT: 4 ft. thin acetate sleeve SHEET: 1 of 1				DISTANCE FROM WELL 08WL70: 39" N DATE OF SAMPLING: 7/27/98 DRILLER: Bob Forshaw LOGGED BY: Michael T. Galbraith TOTAL DEPTH OF BOREHOLE: 1' - 15'	
Depth (ft)	USCS	Sample Interval	Recovery	Profile	Lithologic Description
1	SM	1' - 4'	3.81'		Light brown to orange fine SAND, dry, soft.
2	SM				2.55' Black fill with lignite, and some of the same sand described above interspersed.
3	BEADS SM				3.1' Seam of BEADS 3/8"-1/2" thick, densely packed little fine sand particles between them.
4	SM	4' - 7'	3.03'		3.15' Light tan yellowish fine SAND, moist, firm.
5					Same as above, darker particles interspersed.
6	CL				5.5' Abrupt change to brown to light brown CLAY, hard, fairly dry, low plasticity. The clay continues to bottom of sample.
7	CL	7' - 11'	2.64'		7' Same as above, with chunks of railroad ties interspersed.
8					8.9' Soil turns black due to presence of Free Product.
9	OL				Organic CLAY.
10					Same as above, strong odors of product.
11	OL SM	11' - 15'	3.37'		11.4' Free Product layer ends. Light tan fine silty SAND, moist and firm, fine particles of mica also observed. Continues to bottom of sample with one seam (0.01') thick of coarser grained particles at 13.3'.
12					
13					
14					
15					






NJIT SOIL BORING LOG
GP-H-29

PROJECT: Field Pilot Demonstration (ERW) CONTRACTOR: M&R Soil Investigations DRILLING EQUIPMENT: Geoprobe SAMPLING EQUIPMENT: 4 ft. thin acetate sleeve SHEET: 1 of 1				DISTANCE FROM WELL 08WL70: 14.5" E DATE OF SAMPLING: 7/27/98 DRILLER: Bob Forshaw LOGGED BY: Michael T. Galbraith TOTAL DEPTH OF BOREHOLE: 4' - 15'	
Depth (ft)	USCS	Sample Interval	Recovery	Profile	Lithologic Description
1					Borehole not sampled 1' -4'.
2					
3					
4	SM	4' - 7'	3.43'		4' Misc. FILL black to brown in color.
5	SM				4.5' Tan to yellow fine SAND, soft, fairly dry.
6	CL				5.5' Abrupt change to tan to brown CLAY, hard, dry, low plasticity. Clay extends to bottom of sample, wood chunk at 7.35'.
7	CL	7' - 11'	3.63'		7' Same as above, weathered chunks of wood interspersed.
8					
9					
10	OL				9.85' Free Product layer begins. Many organics present in the form of twigs, small roots and decomposed wood. Strong odors present.
11	BEADS	11' - 15'	2.5'		11' Parting of BEADS at bottom of product layer.
12	SM				11.1' Abrupt change to light brown silty fine SAND with some clay of the same color, clay has moderate plasticity.
13	BEADS				13' Thick layer of BEADS observed 3" - 3.5" thick. BEADS are densely packed with some finer particles from the formation interspersed.
14	SM				13.3' Gray silty fine SAND, extends to bottom of sample.
15					

NJIT SOIL BORING LOG
GP-H-30

PROJECT: Field Pilot Demonstration (ERW) CONTRACTOR: M&R Soil Investigations DRILLING EQUIPMENT: Geoprobe SAMPLING EQUIPMENT: 4 ft. thin acetate sleeve SHEET: 1 of 1				DISTANCE FROM WELL 08WL70: 24" E DATE OF SAMPLING: 7/27/98 DRILLER: Bob Forshaw LOGGED BY: Michael T. Galbraith TOTAL DEPTH OF BOREHOLE: 1' - 15'	
Depth (ft)	USCS	Sample Interval	Recovery	Profile	Lithologic Description
1	SM	1' - 4'	3.8'		1' Light brown to yellow SAND, changes to black fill containing lignite and organics at 2.5'.
2	SM				2.8' Light brown, yellow to orange fine SAND, dry.
3	BEADS SM				3.52' Seam of BEADS 7/16" densely packed. 3.57' Brown fine SAND.
4	SM	4' - 7'	2.9'		Same as above.
5	CL				5.2' Abrupt change to brown, tan yellowish CLAY, hard, dry, low plasticity. Some dark organics in the form of twigs and roots present.
6					
7					No sample obtained from 7' - 11'.
8					
9					
10					
11	SM	11' - 15'	2.83'		11' Gray to brown fine SAND, soft and moist.
12	SM				11.2' Soil is stained black due to presence of Free Product.
13	SM				11.65' Gray very fine silty SAND, firm and moist, with clay mixed interspersed.
14					13' At 13' the soil is coarser grained with little to no fines. The sand is the same color, soft, but still a fine sand.
15					

**NJIT SOIL BORING LOG
GP-H-31**

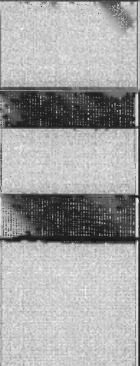

PROJECT: Field Pilot Demonstration (ERW) CONTRACTOR: M&R Soil Investigations DRILLING EQUIPMENT: Geoprobe SAMPLING EQUIPMENT: 4 ft. thin acetate sleeve SHEET: 1 of 1				DISTANCE FROM WELL 08WL70: 14" E DATE OF SAMPLING: 7/27/98 DRILLER: Bob Forshaw LOGGED BY: Michael T. Galbraith TOTAL DEPTH OF BOREHOLE: 1' - 11'	
Depth (ft)	USCS	Sample Interval	Recovery	Profile	Lithologic Description
1	SM	1' - 4'	3.32'		Light gray concrete.
2					1.23' Light brown/yellow fine SAND, soft and moist, at 2' becomes coarser grained and well graded.
3	SM				2.4' Abrupt change to black fill with lignite.
4	SM	4' - 7'	3.0'		3.5' Abrupt change to light brown to tan fine SAND.
5					Same as above.
6	CL				5.65' Abrupt change to brown to tan to yellow tan CLAY, very hard, dry, low plasticity.
7	CL	7' - 11'	3.6'		7' Same as above, some organics in the form of wood chunks and twigs observed.
8					9.55' Light brown, tan fine SAND.
9	SM				9.9' Soil stained black due to presence of Free Product, organic CLAY. Slight plasticity,
10	OL				strong odors. NO BEADS OBSERVED.
11					
12					
13					
14					
15					

**RECOVERY WELL 08-WL-69
(MOVABLE NOZZLE)
GEOPROBE SOIL BORINGS**

**NJIT SOIL BORING LOG
GP-M-8**

PROJECT: Field Pilot Demonstration (ERW) CONTRACTOR: M&R Soil Investigations DRILLING EQUIPMENT: Geoprobe SAMPLING EQUIPMENT: 4 ft. thin acetate sleeve SHEET: 1 of 1					DISTANCE FROM WELL 08WL69: 72" N DATE OF SAMPLING: 7/23/98 DRILLER: Jeramiah Poley LOGGED BY: Michael T. Galbraith TOTAL DEPTH OF BOREHOLE: 6' - 14'				
Depth (ft)	USCS	Sample Interval	Recovery	Profile	Lithologic Description				
1					Borehole not sampled 1' - 6'.				
2									
3									
4									
5									
6	SM	6' - 10'	1.55'		Yellow to light brown fine SAND.				
7	CL				7' Brown to light brown CLAY, hard, dry, low plasticity.				
8									
9									
10	SM	10' - 14'	2.0'		Light brown to tan silty fine SAND, mica particles present. Poor recovery due to collapse of ballast rocks near surface. Entire representative sample consisted of tan silty fine SAND.				
11									
12									
13					NO BEADS OBSERVED.				
14									
15									




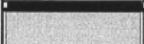

**NJIT SOIL BORING LOG
GP-M-9**

PROJECT: Field Pilot Demonstration (ERW) CONTRACTOR: M&R Soil Investigations DRIL 2 SAMPLING EQUIPMENT: 4 ft. thin acetate sleeve SHEET: 1 of 1				DISTANCE FROM WELL 08WL69: 36" N DATE OF SAMPLING: 7/23/98 DRILLER: Jeramiah Poley LOGGED BY: Michael T. Galbraith TOTAL DEPTH OF BOREHOLE: 6' - 14'	
Depth (ft)	USCS	Sample Interval	Recovery	Profile	Lithologic Description
1 2 3 4 5					Borehole not sampled 1' - 6'.
6 7 8 9	SM/CL	6' - 10'	1.65'		6' Poor recovery. Brown to tan silty fine SAND interspersed with CLAY seams of the same color.
10 11 12 13	SM/CL BEADS/ SM SM	10' - 14'	3.2'		Same as above. 10.25' 2" - 2.5" layer of approx. 50/50 mixture of BEADS and clayey SAND. 10.45' Tan to light gray silty fine SAND, with a parting of BEADS (3-4 BEADS thick) at 10.9'. 11.7' Brown to light brown fine silty SAND, extends to bottom of sample with occasional CLAY seams dispersed.
14 15					









**NJIT SOIL BORING LOG
GP-M-10**

PROJECT: Field Pilot Demonstration (ERW) CONTRACTOR: M&R Soil Investigations DRILLING EQUIPMENT: Geoprobe SAMPLING EQUIPMENT: 4 ft. thin acetate sleeve SHEET: 1 of 1				DISTANCE FROM WELL 08WL69: 20.4" N DATE OF SAMPLING: 7/23/98 DRILLER: Jeramiah Poley LOGGED BY: Michael T. Galbraith TOTAL DEPTH OF BOREHOLE: 6' - 14'	
Depth (ft)	USCS	Sample Interval	Recovery	Profile	Lithologic Description
1					Borehole not sampled 1' - 6'.
2					
3					
4					
5					
6	SC	6' - 10'	2.9'		6' Tan to light brown clayey fine SAND, firm, moist. Trace small gravels present.
7	OL				6.9' Brown to dark brown organic clayey SILT, soft, low plasticity. Gradual change to more silt with increasing depth. Odors present.
8	SM				7.8' Yellow tan silty fine SAND, firm, extends to bottom of sample. Gasoline ?? odors present.
9					
10	SM	10' - 14'	3.12'		10' Trace of BEADS at top of sample, scattered. Light brown to tan silty fine SAND.
11	CL				10.65' Light brown layer of CLAY, firm, moist, high plasticity.
12	BEADS				10.82' 1/4" Seam of BEADS formed through the lower edge of the CLAY layer, not densely packed. CLAY and fine SAND particles well mixed together.
13	SM/CL				10.83' Abrupt transition to light brown to light gray fine silty SAND. Turns to light brown to brown with increasing depth. Occasional CLAY seams of same color noted. CLAY seams soft, moist, high plasticity.
14					
15					

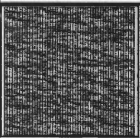
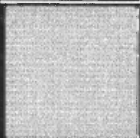
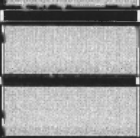
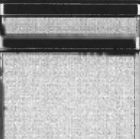
**NJIT SOIL BORING LOG
GP-M-11**

PROJECT: Field Pilot Demonstration (ERW) CONTRACTOR: M&R Soil Investigations DRILLING EQUIPMENT: Geoprobe SAMPLING EQUIPMENT: 4 ft. thin acetate sleeve SHEET: 1 of 1					DISTANCE FROM WELL 08WL69: 27" NE DATE OF SAMPLING: 7/23/98 DRILLER: Jeramiah Poley LOGGED BY: Michael T. Galbraith TOTAL DEPTH OF BOREHOLE: 6' - 14'				
Depth (ft)	USCS	Sample Interval	Recovery	Profile	Lithologic Description				
1					Borehole not sampled 1' - 6'.				
2									
3									
4									
5									
6	CL	6' - 10'	2.23'		6' Brown silty CLAY, dry hard. Becomes moister with increasing depth.				
7	SM				7.2' Light brown fine silty SAND, hard, moist. Odors noted at bottom of sample.				
8									
9									
10	SC	10' - 14'	3.1'		10' Light brown to orange clayey fine SAND, moist, firm, fair plasticity, extends to 11.0'.				
11	BEADS				10.4' Seam of BEADS 1/8" thick observed, densely packed, few formation particles packed within. Seam was formed through the clayey SAND.				
12	SM				11' 1/8" Seam of BEADS, formed at interface of clayey SAND (above) and fine silty SAND (below).				
13					11.05' Light brown silty fine SAND with mica particles present, firm, moist. CLAY layer dark brown observed at 11.7' - 11.9'.				
14									
15									



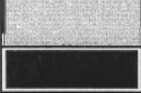





NJIT SOIL BORING LOG
GP-M-12

PROJECT: Field Pilot Demonstration (ERW) CONTRACTOR: M&R Soil Investigations DRILLING EQUIPMENT: Geoprobe SAMPLING EQUIPMENT: 4 ft. thin acetate sleeve SHEET: 1 of 1				DISTANCE FROM WELL 08WL69: 27" E DATE OF SAMPLING: 7/23/98 DRILLER: Jeramiah Poley LOGGED BY: Michael T. Galbraith TOTAL DEPTH OF BOREHOLE: 7' - 15'	
Depth (ft)	USCS	Sample Interval	Recovery	Profile	Lithologic Description
1					Borehole not sampled 1' - 7'.
2					
3					
4					
5					
6					
7	CL	7' - 11'	3.1'		7' Brown CLAY, fill ??, firm, low plasticity.
8	SM				7.5' Light brown silty fine SAND, occasional CLAY layers interspersed.
9	CL				9.2' Light yellow brown CLAY, firm, wet, high plasticity (appears natural).
10	BEADS				10.1' At interface of CLAY layer (above) to clayey fine SAND (below), a seam of BEADS 1/8" - 1/4", densely packed.
11	SM	11' - 15'	3.1'		10.15' Light brown to tan clayey fine SAND, firm to soft, moist.
12	SM/CL				11' Light brown to brown silty fine SAND, mica particles present.
13	SM				11.3' Stratified brown CLAY then light brown seams 1/16" - 1/8" silty fine SAND.
14					11.9' Light brown to brown silty fine SAND, mica particles present. Odors noted.
15					


**NJIT SOIL BORING LOG
GP-M-13**

PROJECT: Field Pilot Demonstration (ERW) CONTRACTOR: M&R Soil Investigations DRILLING EQUIPMENT: Geoprobe SAMPLING EQUIPMENT: 4 ft. thin acetate sleeve SHEET: 1 of 1				DISTANCE FROM WELL 08WL69: 28" SE DATE OF SAMPLING: 7/23/98 DRILLER: Jeramiah Poley LOGGED BY: Michael T. Galbraith TOTAL DEPTH OF BOREHOLE: 6' - 13'	
Depth (ft)	USCS	Sample Interval	Recovery	Profile	Lithologic Description
1					Borehole not sampled 1' - 6'.
2					6' Brown to tan sandy CLAY. Organics in the form of small roots and twigs interspersed.
3					7.5' Tan to light yellow silty fine SAND (extends to bottom of sample).
4					Same as above.
5					9.1' Light brown to orange CLAY, wet, soft, high plasticity.
6	CL	6' - 9'	2.3'		9.25' 1/8" seam of BEADS at interface of CLAY layer (above) to silty fine SAND (below), densely packed, little fine formation particles between them.
7					
8	SM				9.27' Light brown silty fine SAND, wet, firm 9.7' 1" light brown to brown CLAY layer, wet, soft, high plasticity.
9	SM/CL BEADS	9' - 13'	2.42'		9.75' Parting of BEADS observed at CLAY (above) to SAND (below) interface. Large wooden twig present here, BEADS packed around it.
10	SM/CL SM				9.8' Light brown silty fine SAND, extends to bottom.
11					10' 1.25" brown CLAY layer, wet, soft, plastic.
12					10.15' 1" - 1.25" layer of BEADS, densely packed. 10.25' Light brown silty fine SAND. 10.33' 3/4"-1" layer of 50/50 mixture of BEADS and SAND.
13					10.4 Stratified brown CLAY and light brown silty fine SAND.
14					10.7' 1/2" - 3/4" seam of BEADS, densely packed.
15					10.75' Light Brown silty fine SAND.


**NJIT SOIL BORING LOG
GP-M-14**

PROJECT: Field Pilot Demonstration (ERW) CONTRACTOR: M&R Soil Investigations DRILLING EQUIPMENT: Geoprobe SAMPLING EQUIPMENT: 4 ft. thin acetate sleeve SHEET: 1 of 1					DISTANCE FROM WELL 08WL69: 23" S DATE OF SAMPLING: 7/23/98 DRILLER: Jeramiah Poley LOGGED BY: Michael T. Galbraith TOTAL DEPTH OF BOREHOLE: 6' - 14'				
Depth (ft)	USCS	Sample Interval	Recovery	Profile	Lithologic Description				
1					Borehole not sampled 1' - 6'.				
2									
3									
4									
5									
6	CL	6' - 10'	3.0'		6' Light brown to brown CLAY, fairly dry and firm, low plasticity. Some wood chunks interspersed.				
7	SM				7' Brown silty SAND. Becomes lighter, wet, firm, changes to a tan silty fine SAND at 7.8'.				
8	BEADS SM				8.1' 1/16" - 1/8" seams of BEADS observed from 8.1' - 8.6'. Seams are primarily horizontal with some vertical connections between them, densely packed, little to no fines between them.				
9					8.6' Tan silty fine SAND, moist, firm. Strong odors.				
10	SM/CL BEADS	10' - 14'	2.0'		10' Light brown fine silty SAND and alternating layers of highly plastic CLAY of the same color, some patches of orange.				
11	SM/CL SM				10.7' Lens of BEADS 4 3/4" long, densely packed, little to no fines between them. Other half of the sample tube, light brown silty SAND.				
12					11.1' Light brown to brown fine silty SAND with occasional seams of brown plastic CLAY.				
13					11.55' Thin parting of BEADS, 2 - 3 BEADS thick.				
14					11.56' Light brown fine silty fine SAND, mica particles present.				
15									


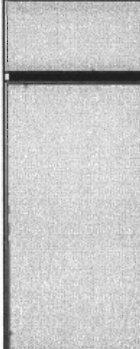
NJIT SOIL BORING LOG
GP-M-17

PROJECT: Field Pilot Demonstration (ERW) CONTRACTOR: M&R Soil Investigations DRILLING EQUIPMENT: Geoprobe SAMPLING EQUIPMENT: 4 ft. thin acetate sleeve SHEET: 1 of 1				DISTANCE FROM WELL 08WL69: 48" W DATE OF SAMPLING: 7/23/98 DRILLER: Jeramiah Poley LOGGED BY: Michael T. Galbraith TOTAL DEPTH OF BOREHOLE: 6' - 14'		
Depth (ft)	USCS	Sample Interval	Recovery	Profile	Lithologic Description	
1					Borehole not sampled 1' - 6'.	
2						
3						
4						
5						
6	SM/CL	6' - 10'	2.9'		6' Tan, light brown to brown fine SAND with some interspersed CLAY of the same color.	
7						
8	SM					8.3' Abrupt change to tan to light orange silty fine SAND.
9						
10	SM	10' - 14'	2.75'			10' Same as above.
11	SM					10.85' Same as above, becomes very wet with water visible, soft, light brown CLAY interspersed.
12						
13						NO BEADS OBSERVED.
14						
15						



**NJIT SOIL BORING LOG
GP-M-18**

PROJECT: Field Pilot Demonstration (ERW)				DISTANCE FROM WELL 08WL69: 22.5" W	
CONTRACTOR: M&R Soil Investigations				DATE OF SAMPLING: 7/23/98	
DRILLING EQUIPMENT: Geoprobe				DRILLER: Jeramiah Poley	
SAMPLING EQUIPMENT: 4 ft. thin acetate sleeve				LOGGED BY: Michael T. Galbraith	
SHEET: 1 of 1				TOTAL DEPTH OF BOREHOLE: 9' - 13.'	
Depth (ft)	USCS	Sample Interval	Recovery	Profile	Lithologic Description
1					Borehole not sampled 1' - 9'.
2					
3					
4					
5					
6					
7					
8					
9	SM/CL	9' - 13'	2.81'		9' Tan to light orange silty fine SAND with alternating CLAY seams of the same color.
10	SM				9.45' 1" – 1.25" layer of BEADS, not densely packed, silty fine SAND well mixed in.
11	SM				9.55' Light brown to orange silty fine SAND. Fine particles of mica present. 3/4" CLAY seam at bottom.
12					10.05' 1/2" – 1" layer of BEADS below the CLAY seam and above the silty fine SAND. BEADS not densely packed, with fines well mixed.
13					10.15' Tan to light gray silty fine SAND, with parting of BEADS (1 - 2 BEADS thick) present at
14					10.63'. SAND extends to bottom of sample.
15					

**NJIT SOIL BORING LOG
GP-M-19**

PROJECT: Field Pilot Demonstration (ERW)				DISTANCE FROM WELL 08WL69: 22.5" NW	
CONTRACTOR: M&R Soil Investigations				DATE OF SAMPLING: 7/23/98	
DRILLING EQUIPMENT: Geoprobe				DRILLER: Jeramiah Poley	
SAMPLING EQUIPMENT: 4 ft. thin acetate sleeve				LOGGED BY: Michael T. Galbraith	
SHEET: 1 of 1				TOTAL DEPTH OF BOREHOLE: 6' - 14'	
Depth (ft)	USCS	Sample Interval	Recovery	Profile	Lithologic Description
1 2 3 4 5					Borehole not sampled 1' - 6'.
6 7 8 9	CL SM BEADS SM	6' - 10'	3.0'		Light brown to brown CLAY, low plasticity, initially hard, becomes softer with increasing depth. Plasticity increases with increasing depth. 7.9' tan to light orange silty fine SAND, firm, moist. 8.4' 2" – 2.5" Lens of BEADS, densely packed, with fines between the BEADS. Strong odors. 8.6' Tan silty fine SAND. 8.75' 1/2" seam of BEADS, well mixed with SAND,
10 11 12 13	BEADS SM	10' - 14'	2.9		not densely packed. 8.8' Tan silty fine SAND, trace of BEADS at bottom of sample. 10' 50/50 mixture of BEADS and silty fine SAND. 10.25' Light brown silty fine SAND, mica particles present, occasional CLAY seams. 10.9' Seam 1/2" – 1" of BEADS observed. 50/50 mixture of BEADS and SAND.
14 15					11.1' Light brown silty fine SAND, mica present.

NJIT SOIL BORING LOG
GP-M-20




PROJECT: Field Pilot Demonstration (ERW)				DISTANCE FROM WELL 08WL69: 96" N		
CONTRACTOR: M&R Soil Investigations				DATE OF SAMPLING: 7/24/98		
DRILLING EQUIPMENT: Geoprobe				DRILLER: Jeramiah Poley		
SAMPLING EQUIPMENT: 4 ft. thin acetate sleeve				LOGGED BY: Michael T. Galbraith		
SHEET: 1 of 1				TOTAL DEPTH OF BOREHOLE: 6' - 14'		
Depth	USCS	Sample Interval	Recovery	Profile	Lithologic Description	
1					Borehole not sampled 1' - 6'.	
2						
3						
4						
5						
6	CL	6' - 10'	2.8'		6' Light brown to brown CLAY, hard, dry, low plasticity. Some tan patches interspersed. Some organics in the form of decomposed wooden chunks present. CLAY extends to bottom, becomes a little moister and softer at bottom of sample.	
7						
8						
9						
10	CL	10' - 14'	3.5'		10' Same as above.	
11	CL SM					10.45' Light brown to gray 2" CLAY layer. 10.6' Light brown to brown silty fine SAND. Brown CLAY layer observed at 11.3' - 11.4'.
12						NO BEADS OBSERVED.
13						
14						
15						

**NJIT SOIL BORING LOG
GP-M-21**


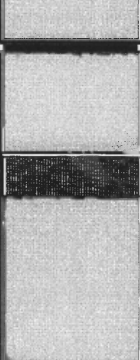
PROJECT: Field Pilot Demonstration (ERW) CONTRACTOR: M&R Soil Investigations DRILLING EQUIPMENT: Geoprobe SAMPLING EQUIPMENT: 4 ft. thin acetate sleeve SHEET: 1 of 1				DISTANCE FROM WELL 08WL69: 54" NW DATE OF SAMPLING: 7/23/98 DRILLER: Jeramiah Poley LOGGED BY: Michael T. Galbraith TOTAL DEPTH OF BOREHOLE: 6' - 14'	
Depth (ft)	USCS	Sample Interval	Recovery	Profile	Lithologic Description
1					Borehole not sampled 1' - 6'.
2					
3					
4					
5					
6	SM	6' - 10'	3.0'		6' Tan to yellow fine SAND, soft, moist.
7					6.2' Brown to tan silty CLAY, hard, low plasticity
8					7' Yellow to tan silty fine SAND, wet and firm. Soil becomes darker with increasing depth. Some organics in the form of wood twigs interspersed.
9					Odors noted at bottom of sample.
10	SM	10' - 14'	2.2'		10' Same as above, mica particles present. Random scattering of BEADS between 10.5' - 11', although not in any appreciable quantity. Odors detected at top of sample.
11					
12					
13					
14					
15					

NJIT SOIL BORING LOG

GP-M-22

PROJECT: Field Pilot Demonstration (ERW)				DISTANCE FROM WELL 08WL69: 36" S	
CONTRACTOR: M&R Soil Investigations				DATE OF SAMPLING: 7/24/98	
DRILLING EQUIPMENT: Geoprobe				DRILLER: Jeramiah Poley	
SAMPLING EQUIPMENT: 4 ft. thin acetate sleeve				LOGGED BY: Michael T. Galbraith	
SHEET: 1 of 1				TOTAL DEPTH OF BOREHOLE: 6' - 10'	
Depth (ft)	USCS	Sample Interval	Recovery	Profile	Lithologic Description
1					Borehole not sampled 1' - 6'.
2					
3					
4					
5					
6	MH	6' - 10'	1.33'		6' Brown fine sandy SILT with decomposed organics interspersed, very wet and soft.
7	SM				6.6' Tan to yellow with mottled gray fine SAND, firm and moist.
8	MH				6.9' Brown fine sandy SILT with decomposed organics interspersed, very wet and soft.
9					NO BEADS OBSERVED.
10					
11					
12					
13					
14					
15					

NJIT SOIL BORING LOG

PROJECT: Field Pilot Demonstration (ERW) LOCATION: CONTRACTOR: M&R Soil Investigations DRILLING EQUIPMENT: Geoprobe SAMPLING EQUIPMENT: 4 ft. thin acetate sleeve SHEET: 1 of 1					BORING NO: GP-M-23 DISTANCE FROM WELL 08WL69: 42" S DATE OF SAMPLING: 7/23/98 DRILLER: Jeramiah Poley LOGGED BY: Michael T. Galbraith TOTAL DEPTH OF BOREHOLE: 6' - 14'
Depth (ft)	USCS	Sample Interval	Recovery	Profile	Lithologic Description
1					Borehole not sampled 1' - 6'.
2					
3					
4					
5					
6	CL	6' - 10'	2.92'		6' Brown CLAY, dry, hard, low plasticity. Some organics in the form of large wood chunks and small roots interspersed. 7' Tan to yellow fine silty SAND. Occasional thin seams of brownish orange CLAY, extends to bottom of sample.
10	SM BEADS	10' - 14'	2.3'		10' Light brown fine silty SAND. 10.3' Yellowish tan CLAY, moist, low plasticity. 10.45' Seam of densely packed BEADS 1/8" thick observed at interface of CLAY (above) and SAND (below). 10.47' Light brown silty fine SAND with one seam of brown CLAY at 10.8'. 11.2' Brown CLAY layer 5" thick observed. Thin seams of light brown silty CLAY between.
14					11.7' Light brown fine silty SAND, mica particles present. Extends to bottom of sample.
15					

REFERENCES

- ASTM (American Society for Testing and Materials). 1993. "Standard Test Method for Flow Rate of Metal Powders", *Annual Book of ASTM Standards*. Volume 02.05, Philadelphia, PA.
- Driscoll, F.G. 1986. *Groundwater and Wells*. Johnson Division, St. Paul, MN.
- Fernandez, H.J. 1997. *An Investigation Into the Feasibility of Utilizing Pneumatic Ultrasonic Devices Coupled with Pneumatic Fracturing in Enhancing Removal of Volatile Organic Compounds from Soils*. M.S. Thesis, Department of Civil and Environmental Engineering, New Jersey Institute of Technology, Newark, NJ.
- Fetter, C.W. 1994. *Applied Hydrogeology*. Macmillan College Publishing Company, New York, NY.
- Fitzgerald, C.D. 1993. *Integration of Pneumatic Fracturing to Enhance In Situ Bioremediation*, M.S. Thesis, Department of Civil and Environmental Engineering, New Jersey Institute of Technology, Newark, NJ.
- Hall, H.A. 1995. *Investigation Into Fracture Behavior and Longevity of Pneumatically Fractured Fine-grained Formations*. M.S. Thesis, Department of Civil and Environmental Engineering, New Jersey Institute of Technology, Newark, NJ.
- Hall, H.A. (in progress). *Volume Change Effects on Discrete Fractures in Fine-Grained Soil Formations*., Ph.D. Dissertation, Department of Civil and Environmental Engineering, New Jersey Institute of Technology, Newark, NJ.
- HSMRC (Hazardous Substance Management Research Center), Accutech Remedial Systems, Inc., Battelle Memorial Institute, and Battelle Pacific Northwest Laboratories. 1994. "Pneumatic Fracturing Demonstration, Tinker Air Force Base, Oklahoma City, Oklahoma." U.S. Department of Energy Office of Research, U.S. Air Force, and U.S. Environmental Protection Agency Northeast Hazardous Waste Research Center.
- King, T.C. 1993. *Mechanism of Pneumatic Fracturing*. M.S. Thesis, Department of Civil and Environmental Engineering, New Jersey Institute of Technology, Newark, NJ.
- Leonards, G.A. 1962. *Foundation Engineering*, Chapter 3 "Dewatering" Mansur, C.I. and Kaufman, R.I.. McGraw Hill, New York, NY.

- Lin, C.Y. 1998. *An Investigation of the Effects of Sonic Frequency of the Removal of Volatile Organic Compounds from Soils using a Siren-Pneumatic Fracturing Coupled Technique*. M.S. Thesis, Department of Civil and Environmental Engineering, New Jersey Institute of Technology, Newark, NJ.
- McGonigal, S.T., 1995 *Integration of Pneumatic Fracturing and In Situ Vitriification in Coarse Grained Soils*. M.S. Thesis, Department of Civil and Environmental Engineering, New Jersey Institute of Technology, Newark, NJ.
- Nautiyal, D. 1994. *Fluid Flow Modeling for Pneumatically Fractured Formations*. M.S. Thesis, Department of Civil and Environmental Engineering, New Jersey Institute of Technology, Newark, NJ.
- Papanicolaou, P. 1989. *Laboratory Model Studies of Pneumatic Fracturing of Soils to Remove Volatile Organic Compounds*. M.S. Thesis, Department of Civil and Environmental Engineering, New Jersey Institute of Technology, Newark, NJ.
- Puppala, S. 1998. *Pneumatic Fracture Propagation and Particulate Transport in Geologic Formations*. Ph.D. Dissertation, Department of Civil and Environmental Engineering, New Jersey Institute of Technology, Newark, NJ.
- Rahman, A.M. 1994. *Integration of Surfactants and Time Release Nutrients with Pneumatic Fracturing Process*. M.S. Thesis, Department of Civil and Environmental Engineering, New Jersey Institute of Technology, Newark, NJ.
- Schuring, J., Chan, P. 1992. *Removal of Contaminants from the Vadose Zone by Pneumatic Fracturing*. U.S. Geological Survey, Department of the Interior, U.S.G.S. Award 14-08-001-G1739. New Jersey Institute of Technology, Newark, NJ.
- Schuring, J., Jurka, V., and Chan, P. 1991. "Pneumatic Fracturing of a Clay Formation to Enhance Removal of VOCs," *Proceedings of the Fourteenth Annual Madison Waste Conference*, University of Wisconsin, Madison, WI.
- Sielski, B.M. 1999 *Development of a Computer Model and Expert System for Pneumatic Fracturing of Geologic Formations*. Ph.D. Dissertation, Department of Civil and Environmental Engineering, New Jersey Institute of Technology, Newark, NJ.
- Shah, N.P. 1991. *Study of Pneumatic Fracturing to Enhance Vapor Extraction of the Vadose Zone*, M.S. Thesis, Department of Civil and Environmental Engineering, New Jersey Institute of Technology, Newark, NJ.
- Spitz and Moreno 1996. *A Practical Guide to Groundwater and Solute Transport Modeling*. John Wiley and Sons, Inc., New York, NY.

- Taylor, D.W., 1948. *Fundamentals of Soil Mechanics*. John Wiley and Sons, Inc., New York, NY.
- U.S. Environmental Protection Agency. 1993. "Accutech Pneumatic Fracturing Extraction and Hot Gas Injection, Phase I, Applications Analysis Report." EPA/540/AR-93/509, Superfund Innovative Technology Evaluation, Risk Reduction Engineering Laboratory, Office of Research and Development, Cincinnati, OH.
- U.S. Environmental Protection Agency. 1995. "Integrating Pneumatic Fracturing and Bioremediation for the In Situ Treatment of Contaminated Soil." Prepared by Rutgers, The State University of New Jersey and New Jersey Institute of Technology for U.S. EPA-ORD, Releases Control Branch (MS-106), Edison, NJ.
- Vukovic, M. and Soro, A. 1992. Determination of Hydraulic Conductivity of Porous Media from Grain Size Composition. Water Resources Publications, Littleton, Colorado.